UTRECHT UNIVERSITY

Optimal decarbonization of ammonia production in the Netherlands

MILP-based Modeling and Analysis of a Multi-Energy System

MASTER'S THESIS – MASTER ENERGY SCIENCE

May 15, 2023

Utrecht University

Makrakis Charidimos (8139969)
c.makrakis@students.uu.nl
makrakis.ch@gmail.com

Supervisor: Julia Tiggeloven

1st assessor: Dr. Matteo Gazzani

2nd assessor: Prof. dr. André Faaij

Master Thesis Energy Science (GEO4-2510)

Abstract

This study investigates the decarbonization of ammonia production in the Netherlands, which currently accounts for roughly a quarter of the country's chemical sector emissions. The primary objective is to determine the most cost-effective production route for decarbonizing the Dutch ammonia industry while taking into account site limitations.

The study begins with a comprehensive literature review, providing an overview of various production technologies for ammonia. Among the alternatives considered, conventional steam methane reforming (SMR) with carbon capture and storage (CCUS), electrified SMR (eSMR) with CCUS and proton exchange membrane (PEM) electrolyzers emerge as the most promising low-carbon routes for ammonia production.

To evaluate the viability of these processes, the study collects and standardizes techno-economic data, including information on auxiliary systems. A multi-energy systems (MES) approach combined with mixed-integer linear programming (MILP) optimization is employed to analyze ammonia production at two specific sites: Sluiskil and Chemelot.

The research explores four distinct cases to assess the feasibility, capacity, and associated costs of the alternative routes for decarbonizing ammonia production. The first two cases assume unlimited availability of current grid electricity and an imaginary future low-carbon grid electricity, respectively. The third case incorporates the impact of renewable energy resources (RES), such as offshore wind (OSW) and solar photovoltaic (PV), while considering limitations in grid electricity imports. The fourth case further incorporates the expansion of electricity networks to examine how the geographical location of ammonia production sites affects decarbonization efforts.

The findings indicate that SMR-based ammonia with CCUS can potentially eliminate up to 84% of current emissions. However, achieving further reductions relies on reducing the carbon intensity of the Dutch electricity grid. Further decarbonization of ammonia production becomes feasible through eSMR-based and PEM-based production, but it requires substantial amounts of OSW, PV, hydrogen storage (HOS), and electric battery storage (BAT). Moreover, the study highlights the influence of electricity networks on ammonia production and reveals that the Sluiskil site holds a substantial comparative advantage over the Chemelot site in terms of costs.

The average cost of ammonia in the Netherlands for an 84% reduction in emissions is estimated at 300 €/ton$_{NH3}$, with an average abatement cost of 32.4 €/ton$_{CO2}$. For complete emission reductions, the cost rises to 1671 €/ton$_{NH3}$ and 858 €/ton$_{CO2}$. Notably, the data underscore the challenges associated with decarbonizing the final 1% of emissions due to the limited availability of renewable energy resources during specific periods of the year. An 88% increase in ammonia price and a corresponding 123% increase in abatement costs would be necessary.

The study acknowledges several limitations that future research should address. These include the exclusion of dynamics related to ammonia storage, insufficient consideration of flexibility parameters for certain technologies, reliance on eSMR with a low technological readiness level (TRL), absence of a conventional plant with a high carbon capture rate, assumption of unlimited available area for technology deployment, disregard for excess electricity and heat sales and assumption of constant gas prices, among others.

In conclusion, this study provides valuable insights into the decarbonization of ammonia production in the Netherlands. It emphasizes the need for policy interventions such as the development of CO2 transport and offshore storage, funding for eSMR research and support for renewable electricity to facilitate a sustainable and low-carbon ammonia industry.
Wordcount: 17318

Στή γιαγιά μου Θεανώ...

Nomenclature

Abbreviations

AEAS Absorbent Enhanced Ammonia Synthesis

ASU Air Separation Unit

AT R Autothermal Reforming

BAT Best Available Technology

BAT Electricity Storage

BG Biomass Gasification

BOW F Borssele Offshore Wind Farm

CAPEX Capital Expenditures

CCUS Carbon Capture, Utilisation, and Storage

CEPCI Chemical Engineering Plant Cost Index

Chemelot OCI Nitrogen Ammonia Plant

DEA Danish Energy Agency

EJ Exajoule

ELOFF Offshore electricity transmission

ELON Onshore electricity transmission

*ERA*5 European Environment Agency

eSMR Electrified steam methane reforming

eSMRCCS Electrified steam methane reforming with CCS

FOM Fixed Operations Costs

GHG Greenhouse Gas

GJ Gigajoule

HABER Stand-alone Haber Bosch plant

HBP Haber-Bosch Process

HOS Hydrogen Storage

HT High Temperature

IEA International Energy Agency

IEAGHG IEA Greenhouse Gas RD Programme

IRENA International Renewable Energy Agency

KBR Conventional steam methane reforming ammonia plant

KBRCCS Conventional steam methane reforming ammonia plant with CCS

KNMI Royal Netherlands Meteorological Institute

LAC Linde Ammonia Concept

LHV Lower Heating Value

MES Multi-Energy Systems

MILP Mixed-Integer Linear Programming

MP Methane Pyrolysis

Mt Million Tonnes

NG Natural Gas

OSW Offshore Wind

PBL Environmental Assessment Agency

PEM Polymer Electrolyte Membrane

PEME PEM Electrolyzers

PSA Pressure Swing Adsorption

PtL Power to Liquids

PV Solar Photovoltaics

Sluiskil Yara Sluiskil B.V Ammonia Plant

SMR Steam Methane Reforming

SOLAR Goeree-Overflakkee Solar Park

SSAS Solid State Ammonia Synthesis

TNO Netherlands Organisation for Applied Scientific Research

ton metric tonne

T PD Tons Per Day

T RL Technology Readiness Level

T SO Transmission System Operators

UNFCCC United Nations Framework on Climate Change Convention

VOM Variable Operations Costs

WGS Water-Gas Shift

Contents

1 Introduction

Ammonia is one of the seven basic chemicals out of which most other chemical products are produced [1]. Approximately 80% of ammonia production is used for nitrogen-based fertilizers such as urea and ammonium nitrate, which are essential to feed about half of the world's population [1], [2]. In addition, ammonia is vital in the production of a diverse range of goods, including explosives, plastics, textiles and pharmaceuticals. Ammonia is widely used as a cleaning agent and refrigerant in various industrial processes. [1], [3]. Recently, ammonia has gained interest as a potential zero-carbon fuel for the transportation sector, particularly for the maritime industry, and as a seasonal energy storage for power generation [1], [3], [4].

In 2020, the worldwide production of ammonia amounted to 183 million tonnes (Mton), making it the second most produced substance by mass, after sulfuric acid. This production required 2% (8.6 EJ) of the total global energy consumption and resulted in emitting 1.3% (450 Mton) of the total global greenhouse gas emissions [1], [3]. Since the ratification of the United Nations Framework on Climate Change Convention (UNFCCC) by most nations, limiting greenhouse gas (GHG) emissions has become a global priority [5]. However, ammonia production is very GHG intensive and with the expected significant increase in demand for ammonia in the future, the decarbonization of the sector is critical [1], [3]. Figure 1 below presents ammonia production's energy and emission intensity in context.

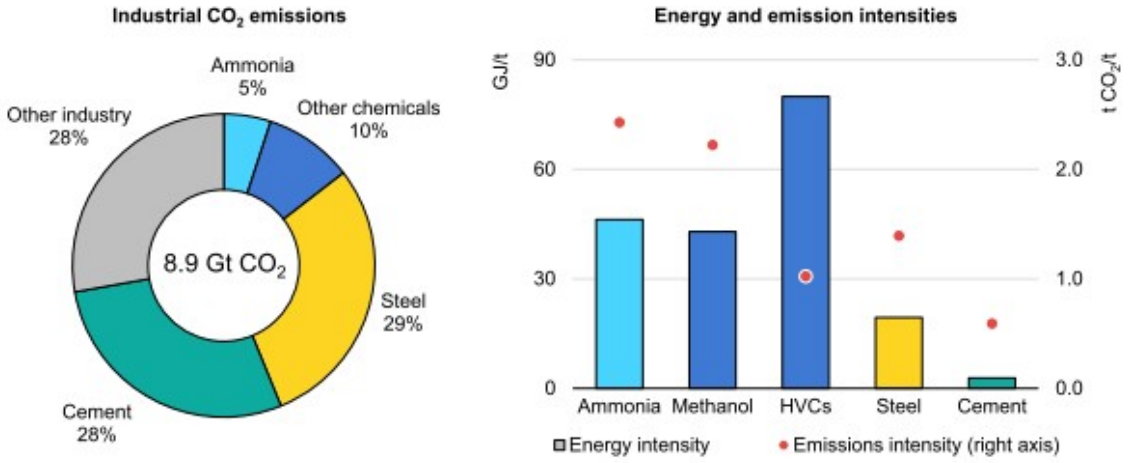

Figure 1: Share of ammonia production to industrial CO_2 emissions along with energy and emissions intensity in 2020. HVCs are the high value chemicals ethylene, propylene, benzene, toluene and mixed xylenes. [3].

Over 90% of current global ammonia production uses the Haber-Bosch process (HBP), developed in the 1910s. This process involves nitrogen and hydrogen reacting with catalysts under high pressure and medium temperature [6]. While nitrogen is sourced from the air, almost all of the hydrogen utilized in ammonia production currently comes from fossil fuel feedstocks, which also generate the process heat required [3]. Natural gas (NG) provides 70% of the energy required for ammonia production worldwide, with coal provides another 26% mainly in China due to relative expensive NG imports [3]. Many decarbonization routes exist, with varying level of TRL and color codes are typically assigned to these routes according to their emissions intensity as shown in Figure 2 below [1], [3], [7].

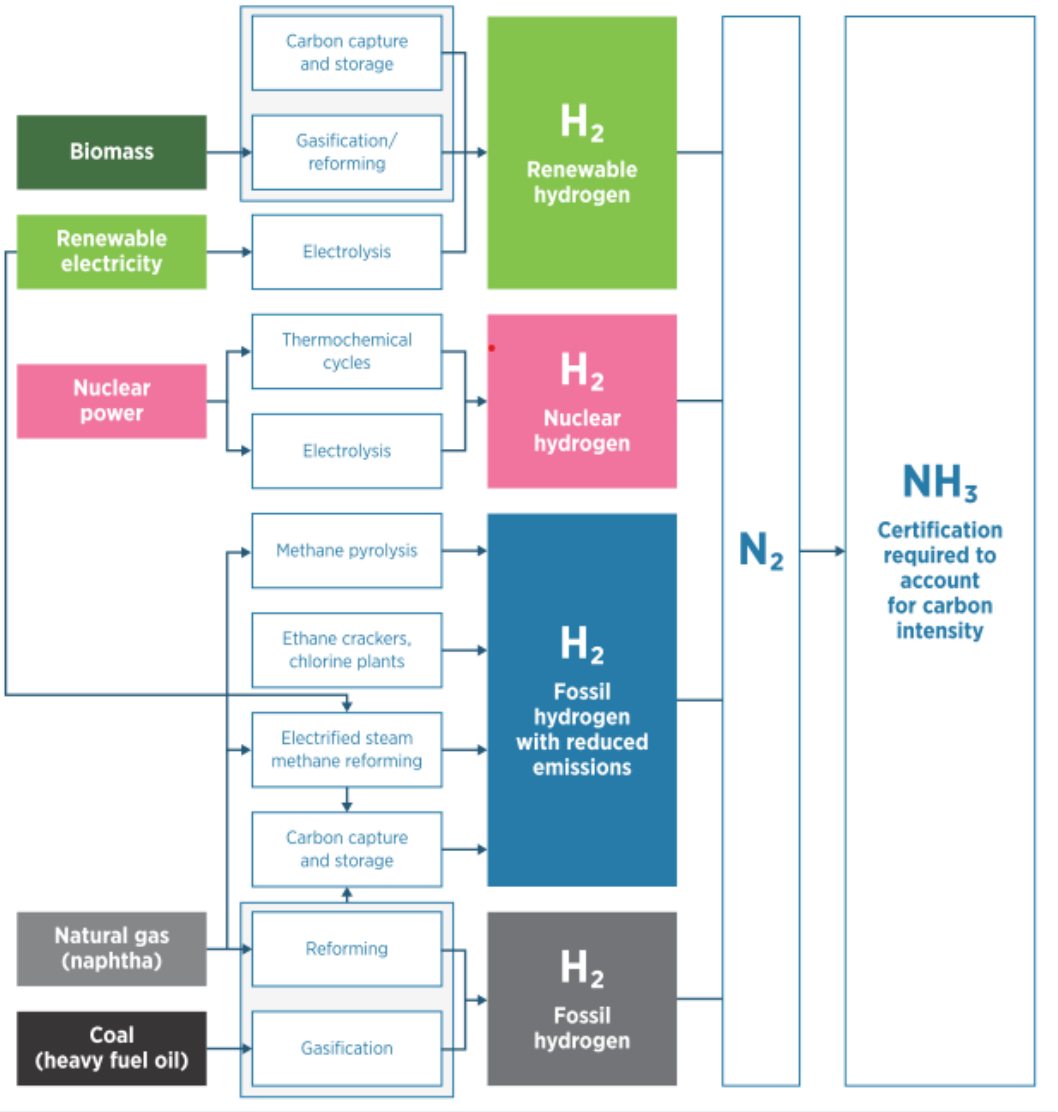

Figure 2: Various feedstocks and routes for ammonia production. Grey ammonia made with fossil-based hydrogen, blue ammonia made with fossil-based hydrogen but with reduced emissions, pink ammonia made produced with nuclear-based hydrogen and green ammonia utilizing renewable electricity or biomass. [1].

Researchers have extensively studied the ammonia production process, analyzing various aspects such as reaction kinetics, catalysts, energy efficiency and environmental impacts. Appl's work provides a comprehensive and detailed explanation of ammonia production processes and production plants, while Rahump et al.'s work is a recent source of information on the topic. [8]–[12]. Del Pozo & Cloete model and compare different conventional SMR and alternative ammonia producing configurations including electrolyzers [13]. Arora et al. and Andersson & Lundgren have conducted techno-economic assessments of Biomass Gasification (BG) as a potential method for producing low CO_2 ammonia [14], [15]. Wismann et al. describe an experimental design for the eSMR which can potentially disrupt the technology while Zhao et al. review the recent advances in electrochemical ammonia synthesis [16], [17]. Other studies have examined CCUS related technologies. Byun et al., for instance, explored the decarbonization of ammonia production through the integration of supercritical CO_2 Allam cycle [18]. Oni et al. conducted a comparison of technologies related to blue hydrogen, while Zhang et al. and

Tuna et al. compared green non-fossil based processes [19]–[21]. Rouwenhorst et al. provide a general review of many of these technologies [22]. Regarding the Netherlands, the two major Dutch producers agree that they will be able to produce green ammonia from electricity in the near future, but at present, it is not economically feasible [23].

In the past, different parts of the energy system were traditionally kept separate both during planning and operation. However, the most effective decarbonization technology for a given region depends on numerous factors, such as the availability of feedstocks, local weather patterns, renewable energy potential, demand profiles, geological features, energy carrier networks and social acceptance, among others. Therefore, in order to affordably decarbonize the ammonia sector, it is important to take into account the interactions between various parts of the energy sector. A MES approach can be used to optimally integrate different sectors at varying levels, resulting in better spatial deployment of technologies, improved efficiency, and increased flexibility [24]. Although such complex systems are challenging to develop and operate due to the large number of variables and parameters involved, MILP is an optimization framework that can effectively replicate such systems with limited computational work [25].

Gabrielli et al. utilized MILP optimization to evaluate fuel cells and electrolyzers within a MES framework [25]. In their study, they also mention various other works that have utilized the MILP framework for modeling energy systems. Regarding ammonia, Palys & Daoutidis utilized MILP optimization to investigate the use of hydrogen and ammonia for energy storage in different cities in the United States. They concluded that ammonia is generally the more economically favorable energy storage option, and that combining it with hydrogen can further reduce costs [26]. Finally, Lazouski et al. utilized a MILP model to conclude that fully electrochemical ammonia production can achieve ammonia costs of 761 to 845 €/ton_{NH3} in Texas [27].

The existing ammonia production facilities in the Netherlands are outdated and relatively inefficient compared to the best available technologies (BAT) [3], [23]. Maintaining these facilities under current high NG prices is challenging, and as a result, producers are scaling down production [28]. Decarbonizing production would not only be economically beneficial, but also significantly reduce Dutch CO_2 emissions (approximately 3.5% in 2017) [23]. Although options for decarbonizing Dutch ammonia production have been proposed, they have not been examined in detail [23], [29]. To date, there has been no comprehensive study examining the decarbonization of ammonia production in the Netherlands using a MES modeling framework with MILP optimization. This study aims to fill this gap in the literature.

1.1 Research Questions

The main research question that will be addressed in this study is:

What is the cost-optimal production route to decarbonize the Dutch ammonia industry, taking into account site limitations?

To achieve this goal, the following sub-questions are created:

To begin with, it is necessary to identify the most promising alternative low-carbon routes of producing ammonia and the adaptations required to decarbonize current technologies. Techno-economic data, as well as information on auxiliary operations, are collected for these technologies. A literature review is performed to address the first question:

I What alternative ammonia production routes with low CO_2 emissions are available?

Subsequently, the MES approach is used to analyze the Yara Sluiskil B.V Ammonia Plant in Zeeland (referred to as Sluiskil). This analysis considers a constant demand for ammonia that must be met by the plant, with unrestricted inflow of nNG and electricity. The MILP optimization algorithm is used to answer the second question:

II What is the feasibility and capacity of alternative routes for decarbonizing ammonia production and what are the associated costs, assuming unlimited availability of electricity and gas imports?

The offshore wind potential that currently exists close to the Sluiskil plant, namely the Borssele Offshore Wind Farm (referred to as BOWF) and the proposed solar park in the island of Goeree-Overflakkee (reffered to as SOLAR), are expected to create synergies both for reducing costs and GHG emissions when linked to ammonia production. Hourly weather data and grid constraints are incorporated in the optimization to address the third question:

III What is the impact of solar and offshore wind availability on the overall decarbonization strategy?

The model takes into account the impact of geographical characteristics on the optimal decarbonization path for the ammonia industry, including factors such as electricity transmission lines and CO_2 transportation. The analysis includes the OCI Nitrogen Ammonia Plant in Limburg (referred to as Chemelot), and compares the this site with Sluiskil. The overall goal is to answer the fourth question:

IV How does the geographical location of ammonia production sites impact the industry's decarbonization?

1.2 Thesis Outline

The subsequent section focuses on ammonia production, covering both conventional and innovative technologies. The methodology section explains the research design, system description and study cases considered in the thesis. Next, the optimization framework and modeling techniques are discussed in detail. Results are presented for the different case scenarios, highlighting the outcomes of each. The discussion section acknowledges limitations, discuss the findings, proposes future research and gives policy considerations. The thesis concludes with a summary of the findings.

2 Ammonia Production

This chapter covers different methods of ammonia synthesis and production, including conventional and innovative technologies. It covers steam methane reforming, compression, the ammonia synthesis loop, electric reforming, electrolysis hydrogen, solid state synthesis and air separation units. The chapter also provides information on current Dutch production of ammonia.

2.1 Conventional Ammonia Synthesis

By 1908, a Norwegian plant was using cheap available hydroelectricity to produce ammonia via the "electric arc process", yielding 77 tons per day (TPD_{NH3}) with a high specific electricity consumption of about 216 GJ/ton_{NH3} (unless otherwise specified, all intensities are reported in terms of lower heating value (LHV)) [8]. The "cyanamide process" began commercial production of ammonia in 1910 with an energy consumption of 190 GJ/ton_{NH3} and was still in use after the 2nd World War [8]. Fritz Haber's ammonia equilibrium experiments in the 1900s identified high pressure and recycling as essential for commercial ammonia synthesis [8]. The first Haber-Bosch plant (HABER) was constructed in Oppau in 1913, consuming roughly 100 GJ/ton_{NH3} [8], [30].

The current industrial process for ammonia production typically involves the following steps: [8]:

- H_2/N_2 make-up gas production
- Compression
- Ammonia synthesis

2.1.1 Steam Methane Reforming

Any feedstock that contains carbon will experience a reaction in accordance with either or both of the reactions 1 and 2 below [8], [12].

$$CH_x + H_2O \rightleftharpoons CO + H_2 + \frac{x}{2}H_2 \quad \Delta H > 0 \tag{1}$$

$$CH_x + \frac{1}{2}O_2 \rightleftharpoons CO + \frac{x}{2}H_2 \quad \Delta H < 0 \tag{2}$$

Equation 1 depicts the process of steam reforming, where light hydrocarbons (maximum C_{11}) react with steam over a catalyst. Nevertheless, all carbon-containing feedstocks can undergo a non-catalytic reaction with oxygen, described in Equation 2, also known as partial oxidation. A small amount of steam is also used there for process reasons, resulting in a simultaneous steam reforming reaction [8], [12]. Both reactions produce a "syngas" containing hydrogen and carbon monoxide in varying ratios. It is worth noting that the composition of the raw gas is significantly affected by the feedstock and the method employed [8].

This study focuses solely on NG as a fossil fuel feedstock due to its lower energy requirement, reduced plant investment costs and global prevalence. [3], [8], [9]. In fact, the theoretical maximum yield for hydrogen production with steam reforming is attained by using methane as

feedstock [8]. Since NG is mainly composed of methane, the SMR reaction is given in Equation 3 below. This reaction is endothermic and therefore requires process heat. In modern SMR plants, this process heat originates both by burning excess NG and from excess heat from the reactions that follow [8], [12].

$$CH_4 + H_2O \rightleftharpoons CO + 3H_2 \quad \Delta H = +206\ \text{kJ/mol} \tag{3}$$

The syngas produced from reforming is then reacted with additional steam to convert carbon monoxide to carbon dioxide and generate more hydrogen [8]. This "Water-Gas Shift" (WGS) reaction shown in Equation 4 is exothermic and the catalysts used require cooling that in modern plants is provided by recovering waste heat to produce steam.

$$CO + H_2O \rightleftharpoons CO_2 + H_2 \quad \Delta H_{298} = -41\ \text{kJ/mol} \tag{4}$$

After hydrogen has been produced, carbon dioxide and leftover carbon monoxide must be eliminated since they are not only a wasteful ballast but also poisonous to the catalyst that produces ammonia later on [8]. The removal of CO_2 involves the use of either physical or chemical solvents, depending on the partial pressure of the gas. The extracted CO_2 can then be released, sold or stored underground. Roughly half of the CO_2 directly produced through the use of fossil fuel feedstocks is used for urea manufacturing [3]. To meet the purity requirements of the HBP catalysts, the hydrogen gas is subjected to further purification. The residual CO and water are typically removed through additional processes, such as methanation and molecular sieve absorption. [8].

2.1.2 Compression

It is necessary to compress the make-up gas produced to the high pressures required by the HBP [8], [22]. Reciprocal compressors were employed to compress the synthesis gas to the level of the synthesis loop up until the 1960s, but were eventually replaced with horizontally balanced compressors, whose cylinders are arranged in parallel on both sides of a shared crankshaft [8]. Gas turbines are also being used or are proposed for new designs [9]. It is best to employ steam turbine drives since enough steam can be produced from the waste-heat and because driving compressors, pumps, and blowers requires a significant amount of mechanical energy. Direct steam turbine drive was utilized to its fullest capacity, not only for large equipment like synthesis gas, process air and refrigeration, but even for comparatively small pumps and blowers. The end result was a complicated steam system. Even after replacing the smaller turbines with electric motors, the steam system remains a complex system in modern ammonia plants. [9]. To illustrate the significance of the subject, turbines and compressors in a modern ammonia plant consume 6.5 GJ out of a total 29.3 GJ/ton_{NH3} and amount to roughly 60% of the total losses [9]. Finding catalysts that operate the HBP at the lower syngas generation pressure could save up to 1 GJ/ton_{NH3} [22]. Even the NG inlet pressure can have significant impact to the overall energy intensity.

2.1.3 Ammonia Synthesis Loop

To produce ammonia, the make-up gas of a stoichiometric ratio of 1:3 N_2 to H_2 must be prepared and fed into a converter with an iron catalyst [8]. Recently other catalysts like ruthenium

are also used. This make-up gas must be completely free of catalyst poisons such as water and CO_2 [8]. The exothermic reaction of ammonia synthesis is shown in Equation 5 below.

$$N_2 + 3H_2 \longrightarrow 2NH_3 \quad \Delta H_{298} = -92.44; \text{kJ/mol} \tag{5}$$

Due to the unfavorable thermodynamic equilibrium, only partial (25%-35%) conversion is achieved during each pass through the catalyst and therefore ammonia is separated by condensation and the unreacted gases are recycled back to the converter [8]. With higher pressure, the position of equilibrium moves to the right and while plants operating from 80 bar up to 400 bar exist, most plants today are designed for pressures ranging from 150 to 250 bar [8]. Many different configurations of the ammonia synthesis loop exist depending on manufacturer and operator's needs [8], [9], [12], [31]. The product has a typical purity of 99.5% [32]. A simplified version of the entire procedure, from hydrogen production with SMR to ammonia separation, is shown in Figure 3 below.

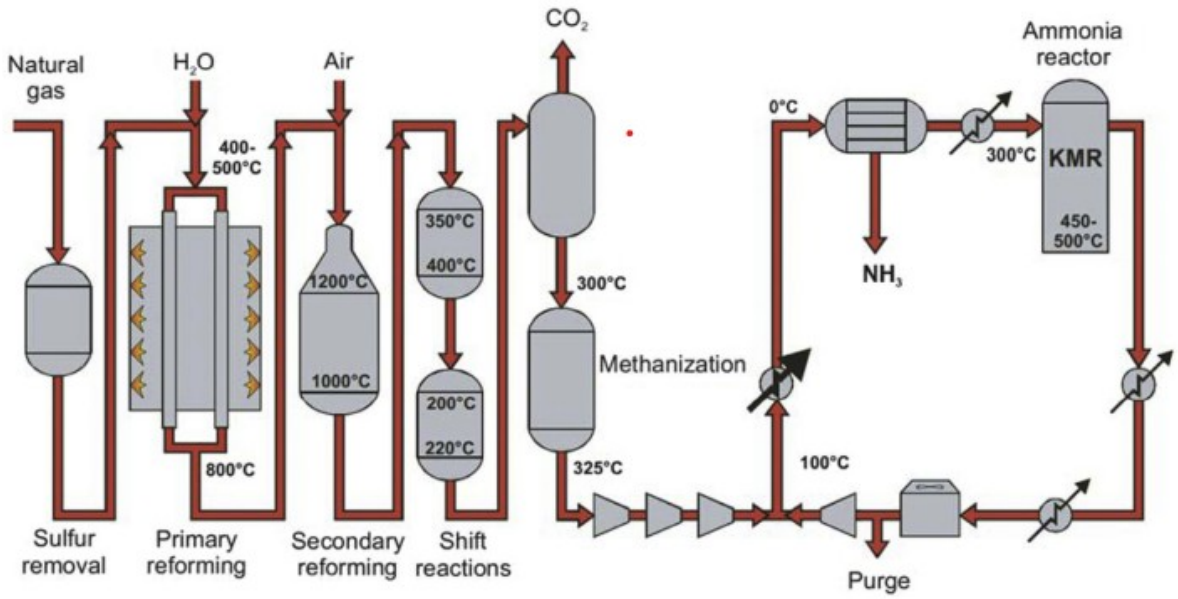

Figure 3: A simple diagram of the conventional two-step reforming ammonia synthesis [22].

2.1.4 Conventional Plants

Even though the HBP serves as the basis for designing all ammonia plants, designers use different methods of preparing and purifying syngas, as well as different separation configurations [8], [11]. The hydrogen production and purification method that is utilized in modern ammonia plants, can serve to categorize them into first- and second-generation plants [11], [33].

In first generation plants, the prevalent method for producing the synthesis gas from NG is the two-step reforming process that involves an air-blown secondary reformer [34]. As the reformer furnace and flue gas duct comprised approximately 25% of the total plant cost, and tubular steam reformers do not scale well, contemporary approaches minimized the primary reformer's size by transferring some of its duty to the secondary reformer [10], [34]. Additionally, with two-step reforming, productivity is increased, nitrogen is obtained from air without the need

of an ASU, methane slip is lessened, catalyst and tubes lifetime is increased and reductions in maintenance costs are achieved [8], [35]. There are also disadvantages like the introduction of excess air which while it decreases the duty and temperature of the primary reformer, it also requires more energy to compress the process air. Excess nitrogen should also be removed often with a cryogenic purification unit before compressing and adding the gas mixture to the synthesis loop [8].

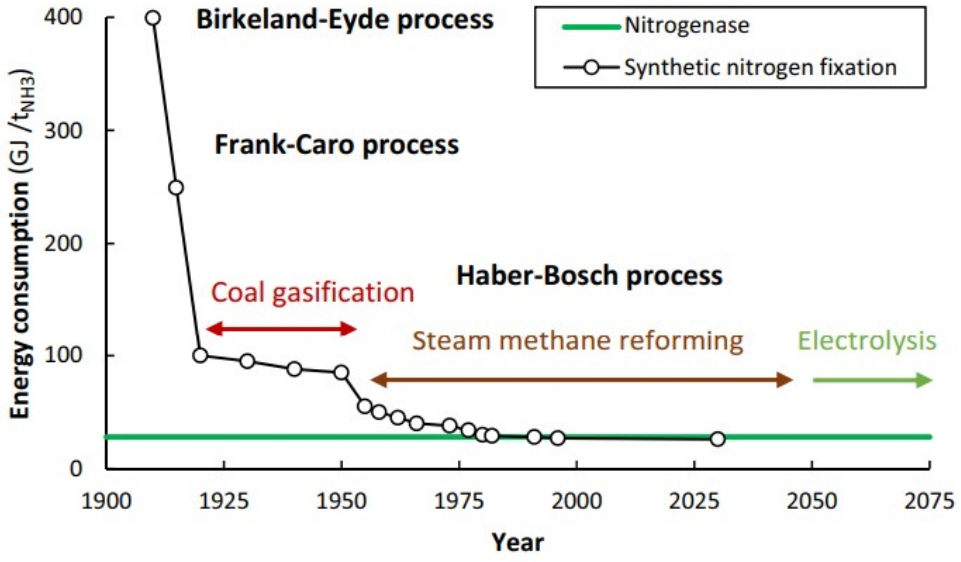

Figure 4: Historical energy consumption for ammonia production [22].

Figure 4 above shows how energy consumption of ammonia production has been decreasing over the past century with technological advancements. Efficiency improvement measures such as those proposed decades ago have indeed materialized in new plants bringing energy consumption to less than 28 GJ/ ton_{NH3} [3], [36]. Efficiency advances are decelerating since the overall ammonia plant is reaching the thermodynamic minimum energy intensity of 20.9 GJ/ton_{NH3} [3]. Nonetheless, today's goal is to achieve the highest possible level of heat recovery while simultaneously minimizing the investment necessary for the total synthesis loop [8], [9]. Utilizing more waste heat in the plant or exporting it to potential buyers is a way of increasing efficiency even more [8]. Although there has been close to no patents related to improving methods for preparing catalysts in large-scale reactors in recent years, there remains a steady stream of publications in scientific journals focused on discovering efficient reforming catalysts [35]. For example, the use of ruthenium based catalysts is promising but at the same time very expensive [8]. The most efficient ammonia plant today releases 1.6 ton_{CO2}/ton_{NH3} while the world average sits at 2.9 ton_{CO2}/ton_{NH3} [7]. The global average energy intensity is 51 GJ/ton_{NH3} while the BAT has 28 GJ/ton_{NH3} [3].

Plant capacity has also increased rapidly with newer plants output capacity up to 3300 (revamped to 3670) TPD_{NH3} as shown in Figure 5 [31], [37]. What's more, studies show that single train plants to more than 4000-5000 TPD_{NH3} often called "Megammonia Plants", are fully viable and in fact advertised [9], [38]–[41]. Kellogg Brown and Roots (KBR) offers single train ammonia plants up to 6000 TPD_{NH3} and claims an energy consumption of 26.3 GJ/ton_{NH3} [39].

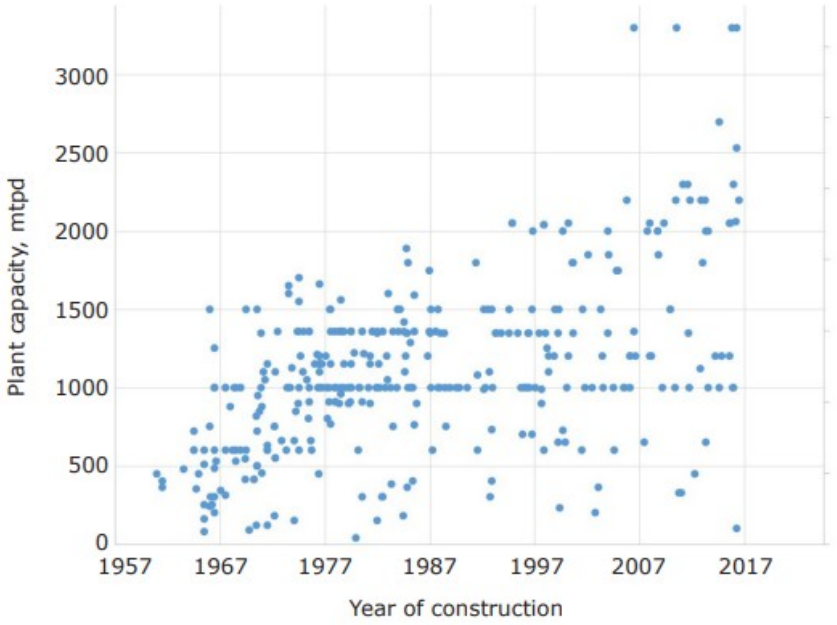

Figure 5: Capacity of plants installed over the years [37].

The primary licensers of traditional ammonia plants that create hydrogen through the process of reforming fossil fuels are the KBR, Haldor Topsoe, Lurgi, Linde, ThyssenKrupp, and Casale [11], [33]. One of the ammonia plant configurations that is most frequently utilized is provided by KBR [31]. The majority of the ammonia facilities that KBR has lately developed employ their "Purifier" method depicted in Figure 6 with a low intensity primary reformer, a liquid N_2 wash purifier, a proprietary waste-heat boiler design, a unitized chiller, and a horizontal ammonia synthesis loop [33].

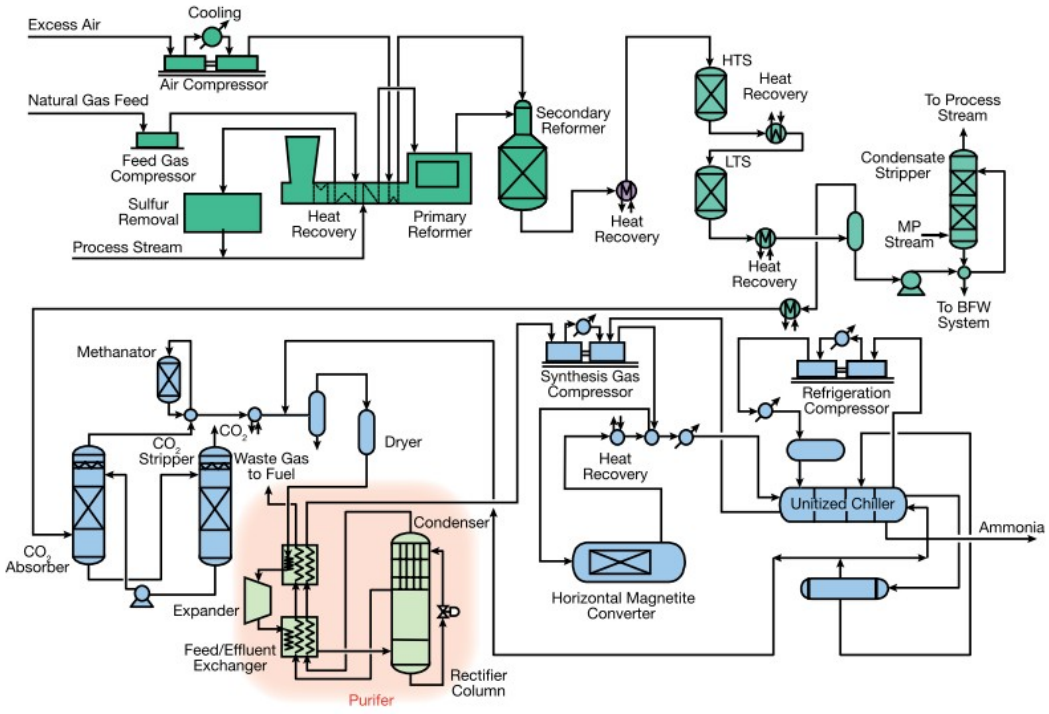

Figure 6: The KBR Purifier modern ammonia plant arrangement [33].

In second-generation technology, the secondary reformer is removed, while theCO_2 removal and methanation phases are substituted with pressure swing adsorption (PSA) devices [11]. Pure nitrogen is provided by an air separation unit (ASU) which can be greatly simplified if no oxygen production is required [11], [13]. This so called “Linde Ammonia Concept“ (LAC) is an established technology, offered by Linde with capacities up to 1750TPD_{NH3} [33]. The main advantages of this technology is high purity of the make-up gas, low compression costs and minimal hydrogen loss that otherwise takes place in methanation or in the synthesis loop purge [11], [13]. The energy consumption of the LAC plant should be similar to the KBR Purifier plant [9], [13]. A simplistic diagram of the differences between the two generations is shown in Figure 7 below.

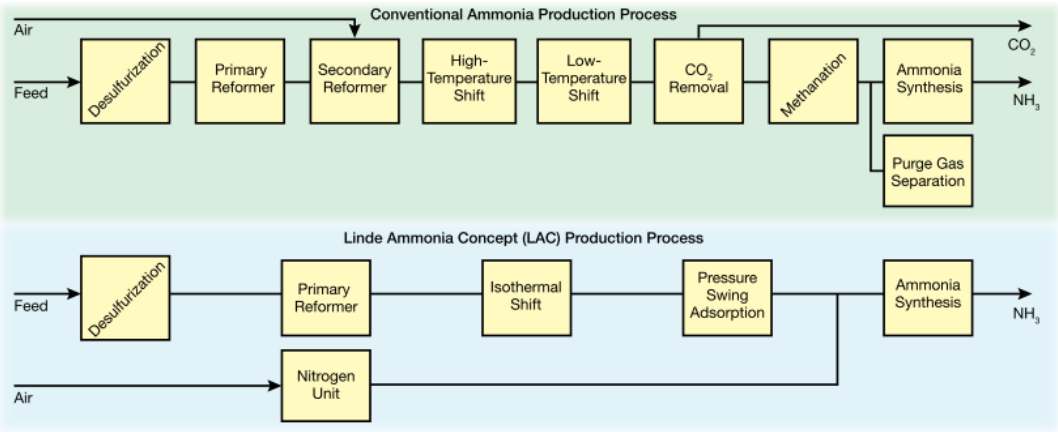

Figure 7: Simplified comparison between the conventional modern ammonia plant and the LAC plant [33].

Ammonia plants are incredibly complex and delicate systems [8], [9]. Determining the ideal synthesis pressure is a challenging task, as the answer heavily relies on optimization factors like feedstock cost, discount rate and location specifications [8], [9]. The refrigeration of the synthesis loop is significantly impacted by the temperature of the air and water in the vicinity of the plant, with even a minor increase in water temperature by 10oC potentially resulting in an additional 0.7 GJ/ton_{NH3} in total energy consumption [9], [12]. Even the specifications of the feedstock input can profoundly alter the specifications of the plants [8], [9].

The plants described can have several configurations according to the needs of the operator [9], [31]. Other companies provide different types of plants and configurations [9], [33]. A widely discussed hybrid method called Autothermal Reforming (ATR) is possible, combining traditional steam reforming with partial oxidation [34], [42], [43]. These plants are largely used for methanol production today. They are possibly competitive with two step reforming at very high capacities due to increased thermal conversion and decreased operating expenses although this is uncertain [34], [42], [43]. However, they require an ASU. Due to sparse data and resource limitations, they were not further explored.

2.2 Electric Steam Methane Reforming

A novel method for producing syngas was recently put out by Wismann et al., who suggested operating the conventional SMR utilizing electric heating rather than the traditional co-firing with methane to keep the endothermic reforming reaction going [16]. Through the potential usage of renewable electricity, this strategy not only uses less NG overall, but is also more effective due to

higher conversion rates. Additionally, compared to existing reformers, the design is potentially 100 times smaller, which lowers the overall material and area requirements [16]. Despite the fact that this specific reactor may not be very productive and scalable, it is anticipated that eSMR technology can reduce CO_2 emissions by 20% to 50% [44]. Similarly, Renda et al. experimented with a silicon carbide/kanthal structure for heating the nickel catalyst while Ambrosetti et al. investigated the direct electrification of a structured catalyst [44], [45]. In Figure 8 below, a schematic comparison of SMR and eSMR reformers is shown.

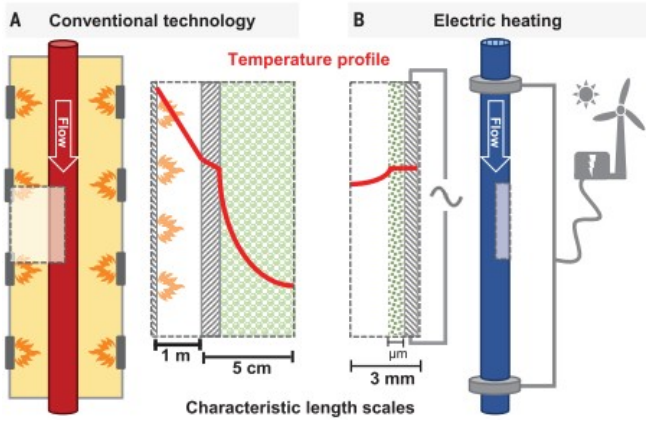

Figure 8: A schematic comparison between SMR and eSMR reformers [16].

This innovative alternative to SMR substantially increases electricity demand due to employing electrically heated reformers but results in a notable decrease in direct emissions from the facility [46]. Demonstration projects are required to fill critical knowledge gaps that will enable the implementation of this emerging technology. These projects will help to address uncertainties related to technology and economics and increase the TRL. Haldor Topsoe, the main proponent of the technology, planned to install a pilot project in 2021, set to become fully operational in early 2022, with the aim of elevating the design to TRL7 or TRL8 [46], [47]. It remains unclear whether any other organizations are actively engaged in developing a similar technology [46]. With the exception of the reformer, the majority of the crucial equipment used in the process, including hydrogen purification and WGS, remains unaltered [46].

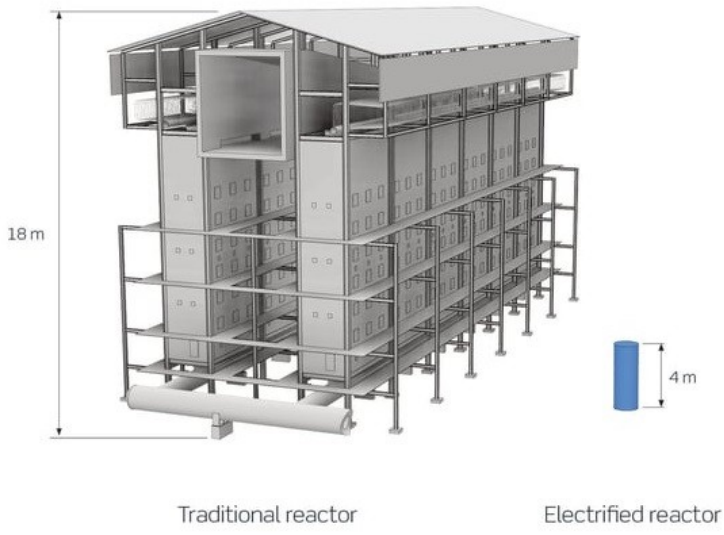

Figure 9: A comparison between SMR and eSMR reformer size [47].

2.3 Electrolysis Hydrogen

The second most popular way of producing hydrogen is water electrolysis [48]. Water electrolysis is the electrochemical conversion of water to hydrogen and oxygen with the purpose of producing high purity hydrogen. Equation 6 gives the net reaction, which is strongly endothermic and necessitates either heat or electrical energy (or the combination of both) [22].

$$2H_2O \longrightarrow 2H_2 + O_2 \quad \Delta H_{298} = 285.8 \text{ kJ/mol} \tag{6}$$

There are three main types of electrolyzers that are mainly produced nowadays [48]. Alkaline electrolyzers is a proven technology that has been used to produce hydrogen at large scale for over a century but system efficiency is typically lower [22], [48]. Proton exchange membrane electrolyzers (PEME), operating at slightly elevated temperatures (50°C to 95°C) are commercialized but there is still room for more improvements. The disadvantage of PEME is the high capital costs since they use noble metals due to the corrosive acidic conditions at the membrane [22], [48]. Solid oxide electrolyzer cells (SOEC) use steam as opposed to liquid water, and therefore requires less electrical energy [22]. A further potential advantage of this technology is that it may be able to also produce nitrogen along with hydrogen [22]. However, it is still in the early stages of commercialisation and require more development before being scaled up into industrial systems [48]. Combining electrolysis with SMR has been suggested as beneficial [22]. ATR with SOEC might be particularly complementing.

When in "hot standby", all commercial systems have load responses in the seconds range which is great for coupling with intermittent renewable electricity sources [22]. Nonetheless, PEME is the only technology that can ramp up quickly when in "cold standby" [22]. Moreover, PEME often have greater current densities and efficiency when compared to alkaline electrolyzers [48]. A PEME cell is shown in Figure 10 below. Repeating cells connected electrically in series and reactant water/product gas connected in parallel make up a PEME stack [48].

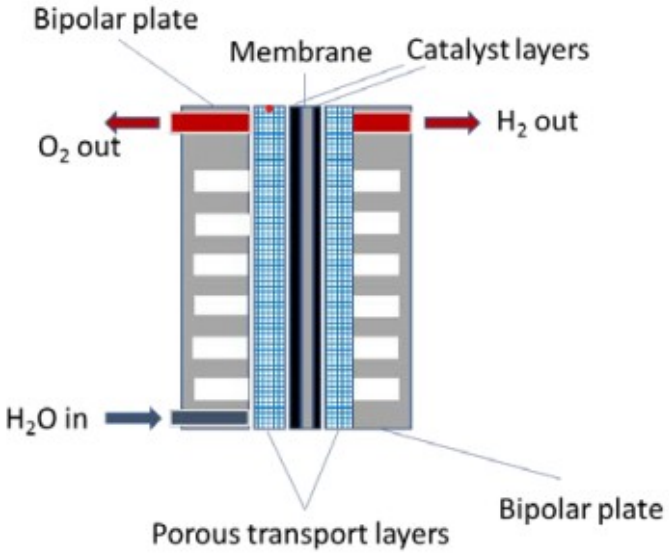

Figure 10: A diagram of a PEME cell [48].

PEME stacks share many elements with PEM fuel cell stacks and numerous techno-economic studies have shown that significant cost reductions are attainable when producing them at scale

[48]. Improvements in power density as well as reductions in membrane and power electronics costs are expected to have great impact on PEME costs [48]. Beyond stack investment costs, electricity prices play a crucial role in determining the price of hydrogen produced and therefore efficiency increases are essential [48]. Electrolyzers and fuel cells typically necessitate the use of nickel or platinum group metals; PEME specifically rely on iridium, a metal whose global production expansion is challenging [49]. However, ongoing innovation is already lessening the dependency on these materials [49]. Out of roughly 290 MW of installed electrolyzers globaly in 2020, only 89 MW were PEME, with the largest plant having a capacity of 20 MW [50]. The total world manufacturing capacity for all electrolyser technologies in 2022 globally was 11 GW_e [49].

2.4 Solid State Ammonia Synthesis

One of the many electrochemical pathways for ammonia production is solid state ammonia synthesis (SSAS), which can directly produce ammonia with a solid electrolyte. This technology demands only pure nitrogen and water (or hydrogen) as input while also requiring no high pressure [51]. It involves two porous electrodes separated by a solid electrolyte acting as a gas barrier while allowing ions to pass [51]. Figure 11 below depicts a SSAS cell and the related reactions are shown in Equations 7, 8 and 9 below [52]:

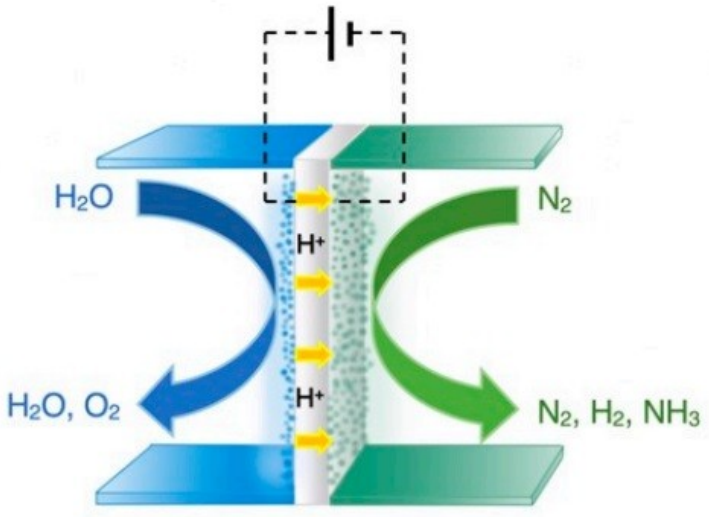

Figure 11: Diagram of a solid state cell conducting H+ and producing ammonia from nitrogen and water (steam) [52].

$$Anode: 3\,H_2O \longrightarrow 6H^+ + 6\,e^- + \frac{3}{2}O_2 \tag{7}$$

$$Cathode: N_2 + 6H^+ + 6\,e^- \longrightarrow 2NH_3 \tag{8}$$

$$Overall: N_2 + 3H_2O \rightleftharpoons 2NH_3 + \frac{3}{2}O_2 \tag{9}$$

SSAS carries great potential since there are predictions for electrochemical paths of ammonia production saving more than 20% of the energy consumption as compared to HBP [53]. Moreover, such devices could be tailored to specific requirements and they can have simplified scalability due to stacking. However, despite many experiments and encouraging progress, ammonia synthesis rate and faraday efficiency is very low. In fact, formation rates of best results are roughly two orders of magnitude worse than what is considered industrially viable [51], [53]. Jiao & Xu estimated the energy intensity of this route at roughly 311 GJ/ton_{NH3} or more than an order of mangitude the current state of the art SMR based HBP [54]. Besides, there are also durability issues. The main barrier is the performance of electrodes while substantial improvements are also needed to catalyst and electrolyte materials [51], [53].

2.4.1 Air Separation Unit

In SMR based ammonia production, air is usually required during hydrogen production in the secondary reformer. Nitrogen is isolated from air by reacting oxygen with hydrogen [9], [22], [32]. However, if hydrogen is produced via electrolysis, or for plants like the LAC, then nitrogen must also be produced typically from air with an ASU. The only viable technology at the large scale required for ammonia production is cryogenic air separation which represents approximately 90% of all commercial nitrogen production [55], [56]. To produce pure nitrogen, air must go through a series of processes to remove impurities and separate its components [55]. First, the air is compressed and cooled to eliminate any water vapor and the resulting dry air stream then undergoes purification to remove contaminants [55]. To further reduce impurities, the air is cooled using waste oxygen and purified nitrogen from the distillation column. The air is then cooled again at the dew point of air and is distilled into its components using a single distillation column[55]. Figure 12 provides a simple diagram of a cryogenic ASU.

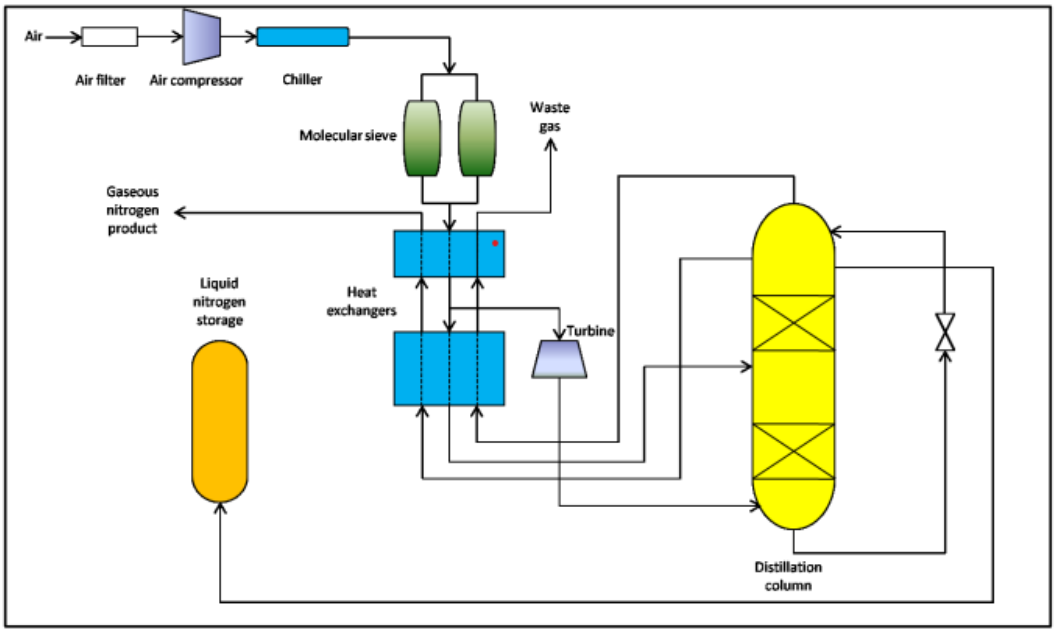

Figure 12: A diagram of an air separation unit [55].

A plethora of techno-economic data on ASUs that do not necessarily fully agree, along with CAPEX equations, can be found in the works cited [13], [22], [55], [57]–[59]

2.4.2 Other Innovative Technologies

Other technologies will be briefly mentioned here. Absorbent Enhanced Ammonia Synthesis (AEAS) is an alternative proposed process that works by extracting ammonia from the unreacted nitrogen and hydrogen using absorption instead of condensation [60]. It operates under lower pressure conditions, and may be competitive with the conventional HBP but only for less than 150 TPD_{NH3} capacities due to scaling issues [60]. Therefore, it may be a suitable technology for small-scale, decentralized operations. Plasma catalysis is a method that has recently been attracting interest due to its potential for quick response to sporadic renewable electricity [61], [62]. Rouwenhorst and Lefferts, after analysing a "best-case" scnario, conclude that even under the most favorable circumstances, plasma-catalytic ammonia synthesis is not a viable alternative to the conventional process [61]. It is nonetheless an interesting alternative for other chemical industries. On the other hand, according to the work of King et al., "dielectric barrier discharge (DBD) plasma steam methane reforming" is competitive to SMR for very low electricity prices [63].

2.5 Current Dutch Production

According to TNO and PBL, the total production of ammonia in the Netherlands for 2017 by the two major sites at Sluiskil and Chemelot, was estimated to be 2743 $kton_{NH3}$ [23]. They also provide estimates for energy consumption and CO_2 emissions. It is worth noting that the data for Sluiskil are given separately for each of the three distinct plants, whereas the data for Chemelot are provided as the combined total for the two plants in operation. Lastly, it is reported that a large amount of ammonia, CO_2 and steam produced by the plants is used locally for urea manufacturing. According to another study conducted by TNO, the quantity of hydrogen required for ammonia production in the Netherlands in 2019 was estimated to be 480 $kton_{H2}$, which translates to roughly similar ammonia amount [64]. In the proximity of the Sluiskil plant, roughly 30 km to the east, there is also the Belgian ammonia plant of Antwerp built in 1991 and has capacity of 752 $kton_{NH3}$ [38], [65]. The plant data are gathered are summarized in the Table 1 below.

Table 1: Current (as of 2017) ammonia production data [23].

	Sluiskil	Chemelot	Total	Unit
Operating hours	8000	8000		hours
Construction Year	1973,1983,1988	1971,1983		
Capacity	1819	1184	3003	kton/yr
Production	1662	1081	2743	kton/yr
NG Input	56.3	38.1	94	PJ
Weighted AV Efficiency	30.3	31.7	30.9	GJ/ton_{NH3}
GHG Emissions	3.2	2.2	5.4	$MtCO_2eq$
Steam Output	6.5	4.2	10.7	PJ
Electricity Input	0.5	0.3	0.8	PJ
Local Ammonia Use	1047	511	1558	kton/yr
Local CO_2 Use	0.9	0.4	1.3	Mton
Local Steam Demand	2.6	1.1	3.7	PJ

3 Methodology

This chapter describes the scope and research design of a study on decarbonizing the ammonia industry in the Netherlands. It includes details on the MILP optimization model used, the set of technologies, assumptions and constraints, data collection process, and the cases designed and analyzed to address the research questions. The study aims to determine the optimal decarbonizing technology deployments and their potential impact on ammonia prices and CO_2 abatement costs.

3.1 Research Design and Scope

This study aims to investigate the decarbonization of the ammonia industry in the Netherlands including integration of renewable energy resources. To achieve this, a MILP optimization model is developed and implemented in MATLAB R2020a. The optimizations are solved by using the Gurobi Optimizer v10.0.1rc0 software with academic licence on an Intel(R) Core(TM) i7-13700KF CPU with 24 threads and 32 GB if installed RAM. The relative MIP gap is set at 1%. The details of the model formulation are provided in the following chapter.

The analysis begins with the Sluiskil site, followed by the Chemelot site and eventually linking the entire system to explore existing synergies and interactions. The sensitivity analysis is performed only on the Sluiskil site due to computational time limitations. The research is twofold: first, to determine the optimal decarbonizing technologies, their capacity utilization and their decarbonization potential; and second, to examine the resulting ammonia price and CO_2 abatement costs at varying levels of decarbonization. Figure 13 below shows the geographic locations of the nodes considered in this study.

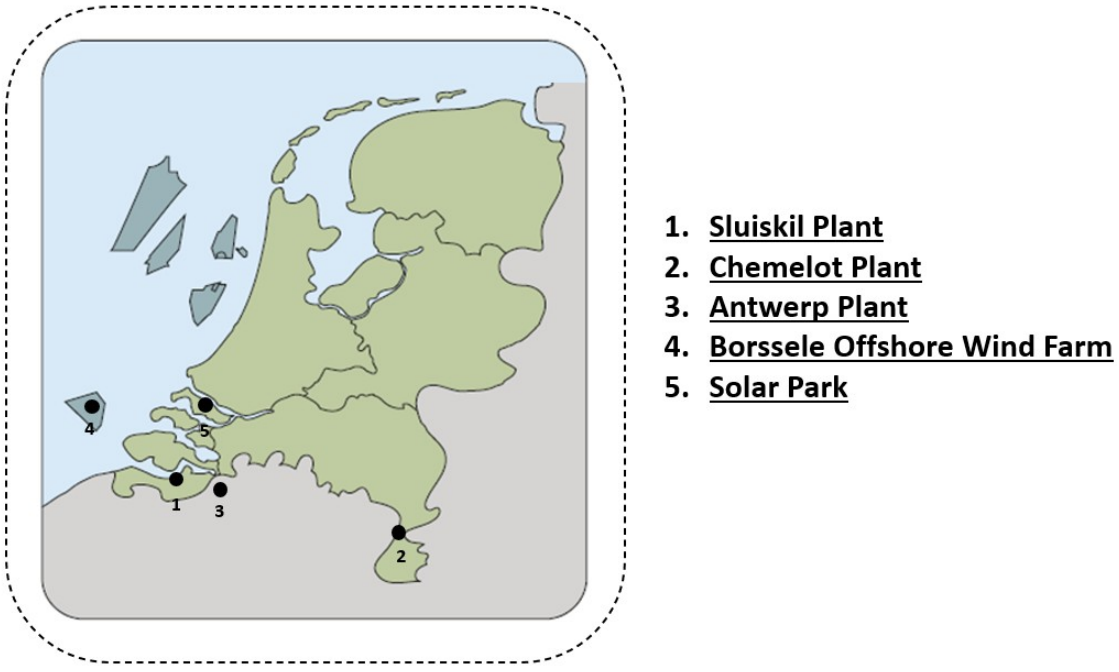

Figure 13: A map of the Netherlands indicating the nodes considered in this study. The Antwerp site is also included since it could potentially play a role in the system, although it was not analyzed due to time constraints.

In this work, the effect of location on optimal decarbonization strategy for ammonia production is also investigated, taking into account the availability of renewable resources and CO_2 geological storage formations located at varying distances from the nodes. As a result, the transmission of electricity and transportation of CO_2 are also considered in the analysis. The energy carriers that are included in the MES are natural gas, electricity, hydrogen, ammonia, nitrogen, and CO_2. However, it should be noted that while transportation of CO_2 is considered, the optimal capacity of pipelines is not calculated to decrease computational complexity. Distances between the nodes used in this study are given in the Appendix (Table 32).

3.2 System description and boundaries

The set of technologies used and the system description and boundaries are provided below.

3.2.1 Set of Technologies

The future of ammonia production technologies is uncertain, with different forecasts and expectations from various sources. If governments commit to the Paris agreement or even more ambitious climate targets, a mix of electrolyzers and SMR with CCUS is expected to dominate ammonia production by 2050, according to the IEA [3]. However, the International Renewable Energy Agency (IRENA) predicts that renewable ammonia from electrolyzers and biomass gasification (BG) will be dominant with only a small amount of SMR with CCUS by 2050 [1]. The innovative eSMR process has also been identified as having great potential for reducing emissions and could be deployed in the future [1], [3], [16]. Both IEA and IRENA agree that BG will see limited deployment due to high costs and limited availability of feedstock therefore it is not included in the set of technologies. Nevertheless, it could be used for carbon removal with CCUS and contribute significantly to decarbonization [1], [3]. PBL and TNO in the Netherlands, report on all of these technologies as well as SSAS. However, SSAS are not included in the optimization as they are not considered technologically mature for use in industrial ammonia production for the foreseeable future as explained in the previous chapter [23].

The optimization can choose between the set of ammonia producing technologies listed below, hence four different routes for ammonia production. Regarding storage, there is the choice of storing electricity in lithium-ion batteries and tanks for hydrogen storage. For the transportation of the carriers, onshore and offshore electricity cables as well as CO_2 pipelines may be used. The transmission lines are decided and expanded by the optimization.

The technologies and networks chosen to be examined and optimally deployed by the model are:

- Conventional steam methane reforming ammonia plant (KBR)
- Conventional steam methane reforming ammonia plant with CCS (KBRCCS)
- Electrified steam methane reforming with CCS (eSMRCCS)
- PEM electrolyzers (PEME)
- Stand-alone Haber Bosch plant (HABER)
- Air separation unit (ASU)
- Hydrogen Storage (HOS)
- Li-ion electricity storage (BAT)

- Offshore wind (OSW)
- Solar photovoltaics (PV)

- Onshore electricity transmission (ELON)
- Offshore electricity transmission (ELOFF)

Beyond these technologies, calculations for CO_2 transmission and storage as well as hydrogen compression are included but not optimally chosen. A diagram of the ammonia production model system is shown in Figure 14 below.

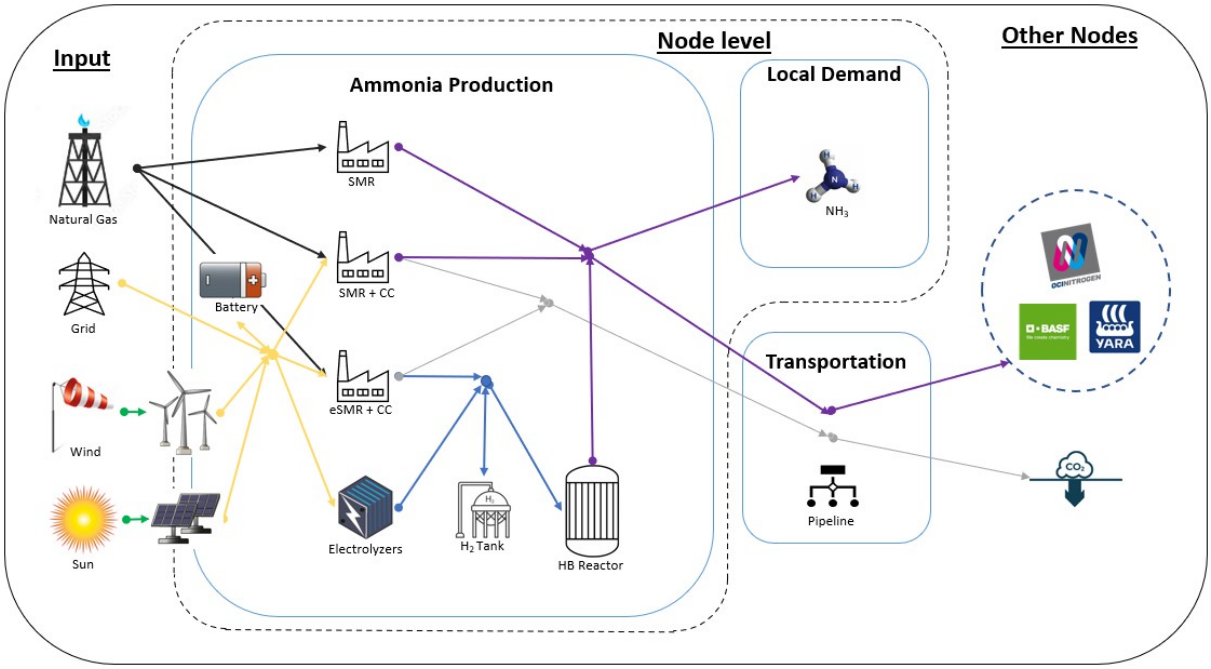

Figure 14: Graphic representation of an ammonia production node of the multi-energy system. Includes energy carrier input and demand as well as production methods, storage systems and distribution technologies. The renewable resources are also depicted.

3.2.2 Assumptions and Constraints

The optimization model has constraints related to technology, geography and networks. Technological constraints include maximum capacities, minimum operation and technology specific efficiencies. There are no limitations regarding flexibility such as ramping rates or efficiency losses at part load operation. The geographical location of each node determines which technologies can be deployed, as shown in Table 2. It is assumed that the ammonia-producing nodes are located at the same sites where ammonia is currently produced, as there is already demand for ammonia from activities such as urea manufacturing. Regarding networks, it is assumed that ELOFF can be used only between the Sluiskil and BOWF node while the rest can be connected with ELON.

Table 2: Available technologies at the four nodes of the investigated MES. The set of technologies changes depending on the case investigated. BOSW can be linked to Sluiskil only with offshore electricity transmission while the rest of nodes can be linked with onshore.

Sluiskil	Chemelot	BOWF	SOLAR
KBR	KBR	OSW	PV
KBRCCS	KBRCCS		
eSMRCCS	eSMRCCS		
PEME	PEME		
HABER	HABER		
ASU	ASU		
HOS	HOS		
BAT	BAT		

The model does not impose any constraints on the available space for deploying the technologies. This means that there is no limit on the maximum size allowed for HOS, BAT, OSW, PV, ELON, and ELOFF technologies. While space is also not a constraint for other technologies, they have maximum capacity and can only be deployed once in their specified nodes, unless otherwise specified. The eSMRCCS technology can be deployed twice.

Ammonia demand is considered constant throughout the examined year and same as the estimated production at each site today, disregarding potential changes in ammonia demand. Furthermore, the optimization model assumes that any excess production of carriers can be freely exported outside of the system. Finally, although in the Netherlands, around 28.1% of the CO_2 produced by ammonia plants is captured and used for urea manufacturing, this factor is not considered in the model [23]. The reasoning behind this is that the CO_2 will eventually be emitted to the atmosphere after fertilizers are applied, and that other CO_2 producers could potentially provide the same CO_2. In any case, what happens after the production of ammonia is beyond the scope of the study.

3.3 Study cases

To address the research questions, several cases were designed and analyzed in this study.

3.3.1 Case 1 - Base Grid Profile without RES

In this case, the analysis specifically targets the Sluiskil demand node, responsible for producing approximately 4453 TPD_{NH3}. This accounts for approximately two-thirds of the total Dutch ammonia production. All technologies are used except for the renewable electricity producing ones, OSW and PV. There is no electricity or gas limit on imports and no networks need to be build as a copperplate approach is assumed. Costs of transporting and storing CO_2 are still calculated. The electricity prices and CO_2 rates are set to the base profile.

3.3.2 Case 2 - Test Grid Profile without RES

In this case, everything is the same as in Case 1 with the exception of the electricity profile used. The electricity grid now operates under the test profile that incorporates greater price variability and includes periods of zero emissions.

3.3.3 Case 3 - Including RES

Beyond the Sluiskil node, these optimization runs include the BOWF and SOLAR nodes. As a result, renewable electricity resources like OSW and PV power are incorporated into the system. Moreover, while the system can still obtain electricity from the grid, imports are limited to 24 MW to simulate current grid capacity. To ensure that the simulation does not rely heavily on grid electricity, electricity prices are assumed to be ten times higher than the base price. Despite this, some grid electricity is still permitted to mitigate potential infeasibilities or extreme scenarios in the optimization process. No networks are built as in Case 1 and 2.

To assess the feasibility of using different energy storage setups and potentially speed up computations, the system is run three times with varying configurations of storage technologies. The first run involves only HOS, the second run involves only BAT, and the third run involves both storage technologies. This approach allows for an assessment of the extent to which one storage technology can be eliminated while still achieving satisfactory results.

3.3.4 Case 4 - Including Networks

To assess the impact of networks on the system, at first the case uses the same nodes as Case 3, but with the added complexity of incorporating electricity networks into the optimization process. The optimization algorithm has the option to select between submarine transmission to the BOWF, onshore transmission to the solar node, or a combination of both. Subsequently, the Sluiskil node is exchanged with the Chemelot node (with a demand of roughly 2962 TPD_{NH3}) to obtain results for this node as well.

Ammonia production at the Chemelot site is expected to necessitate further investments in transmission line infrastructure and should have higher electricity losses due to the greater distance to the RES nodes. Furthermore, the expenses associated with transmitting CO_2 for storage purposes ought to also experience an increase. Therefore, the Chemelot node is also being tested for the Sluiskil's production capacity to investigate geographic influence.

3.4 Data collection

The data collection process for this study began with a comprehensive literature review on ammonia production, followed by gathering techno-economic parameters for the selected technologies. Additionally, relevant techno-economic parameters for transportation and storage technologies related to ammonia, hydrogen and CO_2 were collected. Scientific literature was the primary source of information, although some data were obtained from technology datasheets and corporate reports. Estimates of ammonia demand were based primarily on data from TNO and PBL. Distances between the nodes were approximated using Google Maps and increased by 10% to account for variations due to geographic features. Finally, attempts were made to communicate with experts in the field via email. Although there was limited success, some information on the eSMRCCS technology was obtained.

3.4.1 Weather

To obtain weather data such as wind, solar irradiance and temperature, the Royal Netherlands Meteorological Institute (KNMI) and European Environment Agency (ERA5) were accessed.

The SOLAR node where PV are permitted to be built is located on the island of Goeree-

Overflakkee. Hourly data on solar irradiance and temperature at 1.5 meters for the year 2021 were obtained from the KNMI meteorological station in Wilhelminadorp, located approximately 37 kilometers southwest of the island [66]. The solar irradiance data have a precision of 1 J/cm^2, while the temperature data have a precision of 0.1°C. Data on average wind speed at 100 meters for 2022 at the BOWF node were obtained from ERA5 (latitude: 51.7°N, longitude: 3°E) [67]. The average hourly values of the physical properties used are shown in Table 3.

Table 3: Average of the yearly weather data used.

Average Hourly Temperature	10.9	oC
Average Hourly Irradiance	45.8	J/cm2
Average Hourly Wind Speed	8.9	m/s

3.4.2 Electricity and Gas Imports

Two grid electricity profiles are used in this work:

Base Profile. - The base profile for electricity prices is based on the day-ahead prices in the Netherlands for 2019, as provided by ENTSO-E [68]. To calculate theCO_2 emission rates for this profile, the hourly generation data from ENTSO-E was used, along with the emission factors from CE Delft [69]. Figure 15 illustrates the price and carbon intensity of electricity over the year for the base profile.

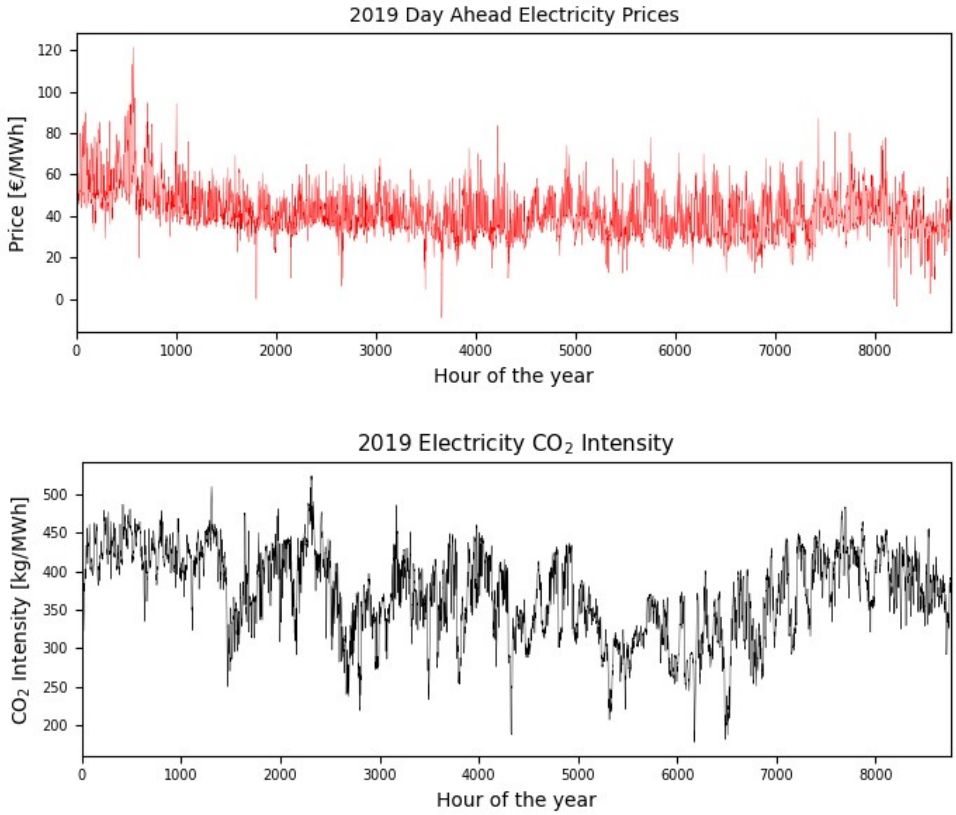

Figure 15: Grid electricity price and carbon intensity for the (2019) base profile.

Test Profile. The test profile is a simulated profile with higher average price and higher standard deviation. Moreover, there are many periods where grid emissions are zero. This profile is a speculative example and not grounded in real data or sources. It is used to test how the overall system could respond to future electricity grid with no emissions at certain periods of time. Figure 16 illustrates the price and carbon intensity of electricity over the year for the new profile.

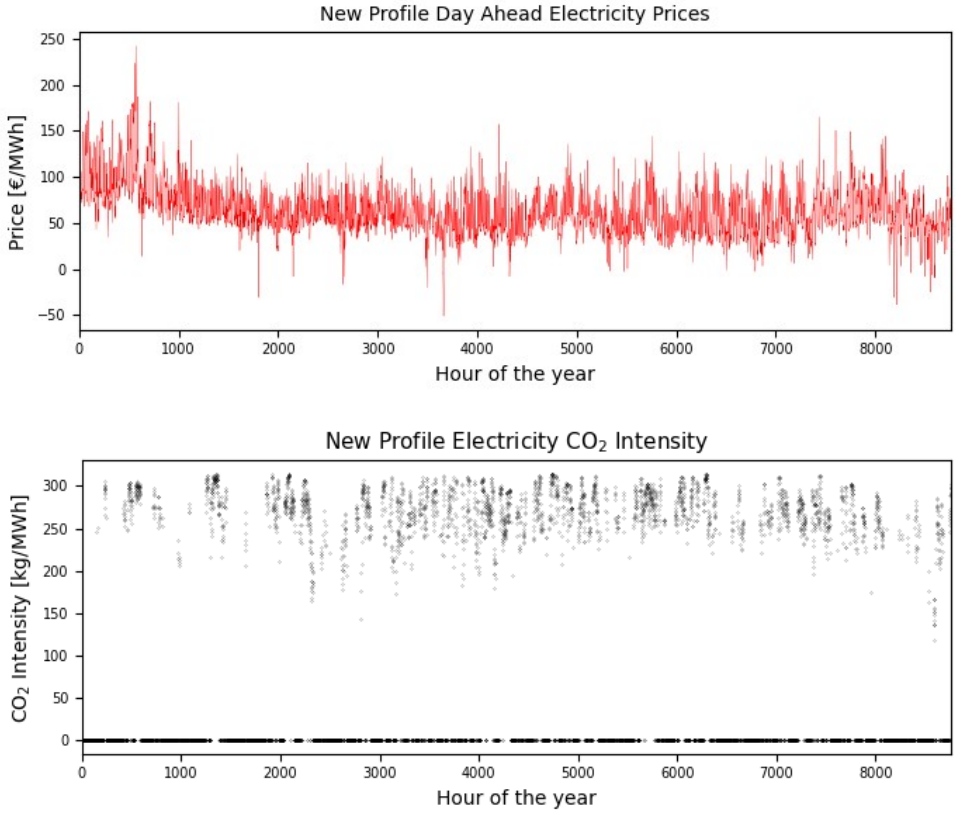

Figure 16: Grid electricity price and carbon intensity for the test profile.

Statistics for the electricity profiles used are given in Table 4 below.

Table 4: Statistics of the electricity profiles used in this work.

	Base Profile	Test Profile	Unit
Price Average	41.2	61.8	€/MWh
Price SD	11.3	25.4	€/MWh
Price Minimum	-9	-51.2	€/MWh
Price Maximum	121.5	242.4	€/MWh
CO_2 rate Average	371.6	90.9	kg_{CO2}/MWh
CO_2 rate SD	56.2	129.1	kg_{CO2}/MWh
CO_2 rate Minimum	177.7	0	kg_{CO2}/MWh
CO_2 rate Maximum	524.2	314.2	kg_{CO2}/MWh

Depending on scenario investigated, there is either no limit on the amount of electricity that can be imported to the ammonia production nodes or the imports are capped at 24 MW. This

limit is based on additional electricity that can be handled currently by the grid on Chemelot node without expanding the grid [23].

For both electricity profiles, the gas price is assumed as 16.45 € MWh_{NG}. This is based on the average of the bi-annual prices for the Netherlands in 2019 as given by EUROSTAT for consumers of more than 4 PJ [70]. There is no limitation on the amount of NG that can be imported.

4 Optimization Framework

This chapter describes the optimization framework used as well as the modeling approach for all technologies. How H_2 compression and CO_2 transmission and storage were taken into account are also discussed.

4.1 Optimization Framework

To fulfil the main research question of this study, that is, to find the optimal cost-wise decarbonization of the Dutch ammonia industry, a MES modelling and assessment is performed. The MES model includes a substantial set of different available technologies and the optimization problem requires a MILP framework which can accept both linear and discrete variables.

In this study, the modelling framework that is selected is described by Gabrielli et al. and utilizes the "Energy Hubs" method by Geidl & Andersson [71], [72]. In this modelling context, the problem is mathematically formulated as an MILP with total costs (or total CO_2 emissions) being the objective functions that need to be optimally minimized. Mathematically, the the problem can be generally formulated as depicted in Equations 10.

$$\begin{aligned} &\min_{w,v}(\mathbf{c}^T\mathbf{v}+\mathbf{d}^T\mathbf{w}) \\ &s.t. \\ &\mathbf{A}\mathbf{v}+\mathbf{B}\mathbf{w}=\mathbf{b} \\ &\mathbf{v}\geq\mathbf{0}\in\mathbb{R}^{N_v},\mathbf{w}\in\{0,1\}^{N_w} \end{aligned} \tag{10}$$

where:

c = the cost vectors related to continuous variables **v**
d = the cost vectors related to binary decision variables **w**
A, B = the corresponding constraint matrices
b = the constraint known-term
N_v = the dimension of **v**
N_w = the dimension of **w**

Given the 365-day time horizon, which equates to 8760 timeslices, the computationally intensive simulation is accelerated using the "two-stage time averaging algorithm" proposed by Weimann and Gazzani [73]. The algorithm solves the model in two stages: The first stage involves averaging the input data over several hours K_{st} and solving the model with reduced resolution. In the second stage, the model is solved at full temporal resolution, using technology and network sizes from the first stage as a lower bound. In this work, $K_{st} = 6$ and the storage technologies are not fixed in the 2nd stage.

For input, the optimization process depends on hourly energy carrier demand, which is considered constant at 979 MW and 637 MW of ammonia for the Sluiskil and Chemelot nodes respectively. Moreover, the model incorporates hourly weather data, grid electricity prices, grid emission intensity and gas prices as its input variables. Furthermore, a set of technologies and a set of networks along with their assosiated performance and cost parameters are provided.

The objective functions along with other variables are subjected to certain constraints and by running the algorithm, technology choices, capacities of technology deployment and temporal management of these technologies are automatically calculated.

There are two kind of constraints, the “performance of conversion and storage technologies“ and the “MES energy balances“ constaints. Among the former, of most importance is the size constraint. The size of each technology $i \in$M must fall within a range of minimum and maximum values as shown in Equation 11.

$$S_i^{min} a_i \leq S_i \leq S_i^{max} a_i \tag{11}$$

where:

S_i = the size of the technology (Depends on technology)
a_i = binary variable which indicates if technology is deployed (0 or 1)

The energy balance constraint is straightforward. For every energy carrier $j \in$N, the total amount of power that is imported and generated during each time step of the horizon must be equal to the total amount of power that is exported and used as formulated in Equation 12.

$$\sum_{i \in M} (U_{j,i,t} + P_{j,i,t} - V_{j,i,t}) - F_{j,i,t}) - L_{j,t} = 0 \tag{12}$$

where:

N = the set of available carriers (kWh)
M = the set of available technologies (kWh)
U = the imported energy (kWh)
P = the generated energy (kWh)
V = the exported energy (kWh)
F = the absorbed energy (kWh)
L = the energy required by the demand (kWh)

The main goal of the optimization problem is to minimize the total annual costs. The total annual costs are calculated by adding up all the contributions as given by Equation 13.

$$C_{tot} = C_{CAPEX} + C_{FOM} + C_{VOM} + C_{Imp} - C_{Exp} + C_{CO2} + C_{CO2,TS} \tag{13}$$

where:

C_{tot} = the total system cost (€)
C_{CAPEX} = the total investment costs for all technologies (€)
C_{FOM} = the total fixed costs for all technologies (€)
C_{VOM} = the total variable costs for all technologies (€)
C_{Imp} = the cost of imports (€)
C_{Exp} = the benefit of exports (€)
C_{CO2} = the cost of CO_2 emissions (€)
$C_{CO2,TS}$ = the cost of transmitting and storing captured CO_2 (€)

Additionally, the optimization can be configured to minimize the overall total annualCO_2 emissions. The toal annual emissions are determined by adding up the individual contributions of imported carrier and direct emissions by all technologies in accordance with Equation 14. It is noted that the total annual emissions may also be used as an upper constraint for the optimization.

$$e = \sum_{j \in N} \sum_{i \in M} \sum_{t=1}^{T} e_{j,t} U_{j,i,t} + e_{dir,i} \quad \Delta t \tag{14}$$

where:

$e_{j,t}$ = the specific CO_2 emission of carrier j
$e_{dir,i}$ = the direct CO_2 emissions

It should be highlighted that except if otherwise stated, in this work, the specific emissions of NG are considered as 0 kg_{CO2}/kg_{NG} since instead, the direct emissions of each technologies are used. For electricity, the specific emissions have been explained in Section 3.4.2.

A similar study by Weimann et al. uses the same framework to optimally assess hydrogen production in a "wind-dominated zero-emission energy system" [74]. More in depth details about the framework may be found in the works of Gabrielli et al. [25], [71].

4.2 Modelling

This subsection explains how the technologies in the MES have been modelled.

4.2.1 Inflation Adjustment

Cost data used in this research were gathered from various sources over the past decade. To ensure consistency, all prices were corrected for inflation using the Chemical Engineering Plant Cost Index (CEPCI) and converted to $€_{2021}$, unless otherwise noted. The conversion was performed using Equation 15. Additionally, all values originally in $ were converted to € to maintain uniformity throughout the analysis.

$$C_{2021} = C_{original} \times \frac{CEPCI_{2021}}{CEPCI_{original}} \times X_{rate} \tag{15}$$

where:

C_{2021} = the cost currently (€$_{2021}$)
$C_{original}$ = the cost at the year it was provided by source (€$_{original}$ or \$$_{original}$)
$CEPCI_{2020}$ = the CEPCI value in 2021 (–)
$CEPCI_{original}$ = the CEPCI value in the year the cost was provided (–)
X_{rate} = The exchange rate (1 if $CEPCI_{original}$ in € or 0.845 if $CEPCI_{original}$ in \$)

A table with the CEPCI values used for the inflation correction is provided in the Appendix (Table 31).

4.2.2 Scaling

Typically, data for CAPEX, FOM, and VOM are only available for specific production capacities. For other capacities, a rule of thumb is to use scaling to take into account the "economies of scale" [9]. This is achieved using Equation 16 below.

$$C_E = C_B \times \left(\frac{Q}{Q_B}\right)^M \tag{16}$$

where:

C_E = the plant cost with capacity of Q (€)
C_B = the plant cost with base capacity of Q_B (€)
Q = the plant capacity (same as in Q_B)
Q_B = the plant base capacity (same as in Q)
M = the scaling factor (–)

The FOM costs are given to the model as a percentage of investment costs and therefore do not require scaling. For VOM, cost scaling is not taken into account.

4.3 Linear Approximation

Accounting for system dynamics and changes in conversion performance with size and operation load is important, but computationally challenging [25]. While piecewise approximations have been tested and are a viable alternative, they were found to be too complex for the MES under investigation. To deal with this challenge, a linear approximation with continuous variables is used.

Since generally small plants are not expected to be built, to increase the accuracy of the linear approximations of the power functions, the linear approximation was performed with the use of the least squares method to find the best-fit line from an arbitrary minimum of 1000TPD_{NH3} – eq to the maximum of 4500 TPD_{NH3} – eq. For this, the Microsoft Excel function "LINEST" was used for data every 100 TPD_{NH3} in the range specified. A relevant example for the HABER plant CAPEX is shown in Figure 17.

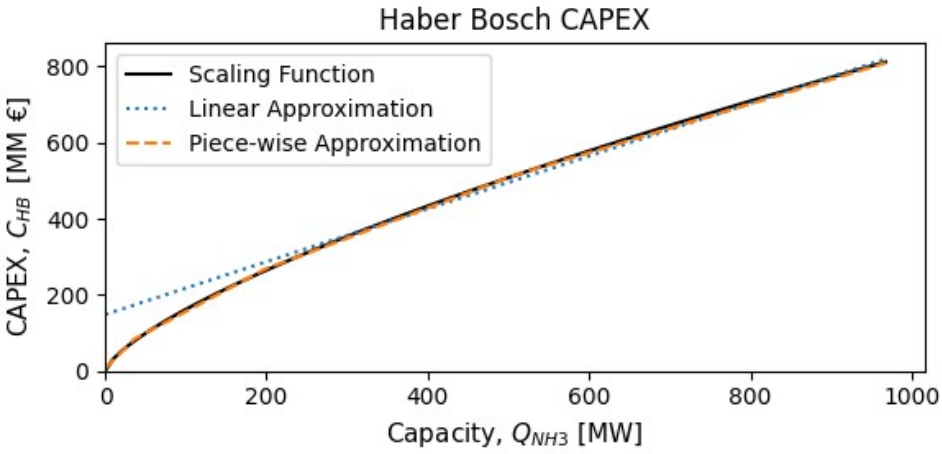

Figure 17: The HABER plant's CAPEX scaling function and the linear approximation assumed in the study. A piecewise (4 breaking points) approximation is also depicted to illustrate potential modifications for the model.

4.4 Primary technologies

To model these plants, first base data were gathered such as capacity, CAPEX, FOM, VOM, efficiencies, direct emissions etc. As explained, once the information is collected and units are standardized, all monetary figures are adjusted to reflect $€_{2021}$ using the CEPCI index. Subsequently, the base data are scaled for different capacities and a linear approximation is determined.

The maximum capacity of the plants is 4500 TPD_{NH3} plus 5% to conveniently be able to fulfil the demand of the Sluiskil node. Although this value is beyond the capacity of existing ammonia plants, it is well inside the range of plant capacities that are feasible as well as being advertised [9], [38], [39].

Table 5: Techno-economic data for the KBR and KBRCCS designs [13]. Although it is common for the fertilizer industry to utilize the captured CO_2 from the purification stage in ammonia production for urea production, in this work, all captured CO_2 is assumed to be vented for KBR.

	KBR	KBRCCS	Unit
Energy Balance			
NG In	989.9	989.9	MW
NH3 product	648.4	648.4	MW
Net Power	13.62	-1.34	MW
CO_2			
Captured	0.00	46.73	kg/s
Flue gas	9.51	9.51	kg/s
Vented	46.93	0.20	kg/s
Economic			
Capacity	3011.3	3011.3	TPD
CAPEX	1066.94	1126.82	MM €
FOM	38.65	40.53	MM €/yr
VOM	10.62	10.62	MM €/yr
Scale Factors	0.67	0.67	-
Liftime	25	25	yr

KBR. The base data for KBR are based on the work of Del Pozo & Cloete who modelled the KBR "Purifier" design with computer software and provided flow streams as well as extensive performance indicators [13]. They furthermore thoroughly calculated the CAPEX and OPEX of the different steps of the plant. The plant takes in NG as its input and produces ammonia and some electricity as its output. Conventional ammonia plants are typically inflexible, operating strictly at design specifications to achieve optimal efficiency. Startup and shutdown procedures in these plants can be time-consuming, lasting for hours or even days. Moreover, there is a minimum capacity below which they cannot operate [8]. To minimize computation time, if such plants are deployed, they are permitted to operate within a range of 30%-100% of their nominal capacity but are not allowed to shut down. Moreover, no ramp-up/down times are considered. Finally, these plants capture most of produced CO_2 during the hydrogen purification stage and utilize a portion of it locally for urea production, while typically venting the remaining CO_2. In this study, no such considerations have been taken into account as the focus is solely on the production of ammonia, and what occurs afterward is outside the scope of the research. Besides, this captured CO_2 is eventually released after urea is applied in the fields.

KBRCCS. The data used for KBRCCS is also based on the work of Del Pozo & Cloete. Capturing the CO_2 produced from the feedstock is elementary. The only difference from KBR is that instead of venting the CO_2 coming out of the MDEA stripper column, pressurization is required with the addition of an intercooled compressor and a supercritical pump [13]. Practically this means that the CAPEX and FOM of KBRCCS is slightly increased in comparison to KBR. The plant now generates a stream of pressurized CO_2 along with ammonia and instead of producing, a minor input of electricity is also required. The flexibility of KBRCCS is simulated like the KBR. The data used both for KBR and KBRCCS are shown in Table 5.

At this point it is noted that a correction giving slightly more conservative results has been made to the KBR and KBRCCS direct emissions and capture rates. Although these values are provided in the work of Del Pozo & Cloete, the ones used in this research have been calculated stoichiometrically according to the flows and NG composition provided by Del Pozo & Cloete. To illustrate, although the capture rate is provided as 82.8% in their work, it has been calculated as 81.3% [13]. The NG specifications can be seen in Table 33 in the Appendix.

HABER. The data used for HABER are based on the "Green Ammonia" plant described by DEA [32]. DEA estimates from publicly available data that the cost of HABER with ammonia storage is given by the Equation 17 below [32]. The storage included amounts to 6% of the total CAPEX of an ammonia plant with the SMR setup and has typically the capacity to hold 20 days of production [32], [75]. Beyond the CAPEX consideration, ammonia storage dynamics have not been modelled. The CAPEX used does not include an ASU. The FOM costs are given as 3% of investment costs. The VOM costs are regarded as the costs of catalyst replacement and other minor consumables at 0.02 €/MWh_{NH3} output.

$$C_{HBplant} = 2.051 \times Q_{HB}{}^{-0.29} \tag{17}$$

where:

$C_{HBplant}$ = the cost of a HB plant (€$_{2021}$)
Q_{HB} = the capacity of the plant (TPD)

The plant is supplied with high-purity hydrogen and nitrogen, and requires a certain amount

of electricity. The plant produces ammonia as well as two separate heat streams. A High Temperature (HT) heat output of high value and a low temperature heat ouput that could be used as a reservoir for district heating heat pumps [32]. Although these heat outputs have been modelled and are calculated, they have no influence in the optimization since they are ignored. Techno-economic data provided by DEA and used for modelling the HABER technology are summarized in Table 6. The actual loop pressure and temperature is not precisely specified but assumed in this study as 200 bar and 450 °C respectively.

Table 6: Techno-economic for the HABER plant [32]. It is noted that the subcript "TIN" means "total inputs".

N2 Input	0.839	ton/ton_{NH3}
H2 Input	0.18	$ton/ton_{N}H_3$
H2 Input	0.947	MWh/MWh_{TIN}
Electricity Input	0.053	MWh/MWh_{TIN}
NH3 Output	0.823	MWh/MWh_{TIN}
High Value Heat Output	0.108	MWh/MWh_{TIN}
District Heat Output	0.038	MWh/MWh_{TIN}
Loop Pressure	200 (150-250)	bar
Loop Temperature	450 (350-550)	°C
Lifetime	30	years
operation_capacity	30-100%	-
FOM	47.6	k€/MWNH3/year
VOM	0.025	€/MWhNH3

It is noted that the lower operation capacity of the plant has been modelled as 30% instead of the 20% given by DEA, since it is deemed too optimistic [13]. Like the KBR and KBRCCS, HABER cannot be turned off if the technology is deployed. Although efficiency penalties should be considered when a HABER plant is operating at lower capacities but these are not included [8], [13]. Flexibility parameters and efficiency penalties are nevertheless shown in Table 7.

Table 7: Flexibility data for the HB plant [13], [76].

Additonal H_2 Demand	188	$kW/MW_{output,cut}$
Additonal Elec. Demand	83	$kW/MW_{output,cut}$
Catalyst Heat Rate	38	°C/hr (up to 400 °C)
Catalyst Heat Rate	19	°C/hr (from 400 °C to 510 °C)

ASU. According to DEA, nitrogen demand from the ammonia synthesis loop is 0.839 ton_{N2}/ton_{NH3}. This is the stoichiometric quantity required by the reaction plus the amount of nitrogen that is purged from the loop [32]. The work of Pozo and Cloete, from which techno-economic data for the KBR plants are extracted, includes the LAC plant [13]. This plant requires an ASU which has been extensively modelled. The technoeconomic data found for the ASU are given in Table 8.

Table 8: Techno-economic data considered for the ASU [13], [77].

Base Capacity	2519 (3003)	TPD_{N2} (TPD_{NH3})
CAPEX	142.6	MM €
FOM	2	%
Electricity Input	17.6	MW
Scale Factor	0.67	–
Lifetime	25	yr
Output Temperature	25	°C
Output Pressure	28.7	bar
Purity	99.94	%

The energy for the separation of nitrogen from the air is calculated from these techno-economic data to be about 168 kWh/ton_{N2}, close to the lower end of the 175-280 kWh/ton_{N2} range given by Osman et al. [56]. The ASU is producing nitrogen at an output pressure of 28.7 bar. The energy required to compress it to the Haber Bosch plant should be roughly 48.5 kWh/ton_{N2}, however this compression energy requirement was omitted.

The process is characterized by a high degree of nonlinearity and complexity, and entails multiple fluid flows and components [55]. Cryogenic separation is not very flexible, but since it is following the also inflexible HABER, flexibility was ignored to simplify modelling. Theoretically, flexibility could be increased with nitrogen tanks. Since the maximum capacity of cryogenic air separation systems is unclear but large, in the range of 70000 to 400000Nm^3 N_2/h (2500-14000 TPD_{NH3}), a maximum size is ignored [55], [56]. Finally, oxygen and argon are also produced by the ASU but are ignored although those could be sold if demand in close proximity exists.

eSMRCCS. The data used for the eSMRCCS plant are based on the "Low-Carbon Hydrogen from Natural Gas:Global Roadmap" report by IEAGHG which was acquired via email correspodence [46]. Since eSMRCCS is an emerging technology with data gaps and uncertainties, their assessment builds on their previous report on SMR plants, modified according to the lab work of Wismann et al. and guidance by Haldor Topsoe [16], [46], [78]. Therefore, IEAGHG considers the data they provide as "less reliable" [46]. However, this could rapidly change with the completion of the demonstration project reported as "soon to be tested".

The VOM of the plant are associated with water intake and chemicals for water treatment [79]. A scaling factor of 0.7 is assumed. The high capture rate of 98.6% for eSMRCCS is considered achievable due to the ease of capturing carbon from an eSMR unit at an earlier stage in the process with higher purity CO_2 and no other flue stream existing [46]. Finally, eSMR is assumed capable of operating with high flexibility as the heat reaction is eliminated from the reactor in the process [16], [46]. Therefore, no flexibility constraints were assumed in this study, either in terms of operating range or ramp up/down times. The data used are summarized in Table 9.

Table 9: Techno-economic for the eSMRCCS plant [46], [79]. [a] The actual electricity input used is decreased due to compression considerations that are explained later.

Base Capacity	216.44	ton_{H2}/day
CAPEX	241.32	MM €
FOM	3.85	%
VOM	13.38	€/ton_{H2}
NG input	35.95	kWh_{NG}/kg
Electricity Input	9.43[a] (9.78)	kWh_e/kg
H2 Purity	99.50	%
H2 Export Pressure	200.00	bar
Capture Rate	98.62	%
Specific Emissions	2.78	ton_{CO2}/MWh_{NG}
CO_2 Export Pressure	110.00	bar
Lifetime	25.00	yr
Scaling Factor	0.70	–

The outcome of all the scalings and linear approximations are shown in Figure 18. Table 10 summarizes the cost functions.

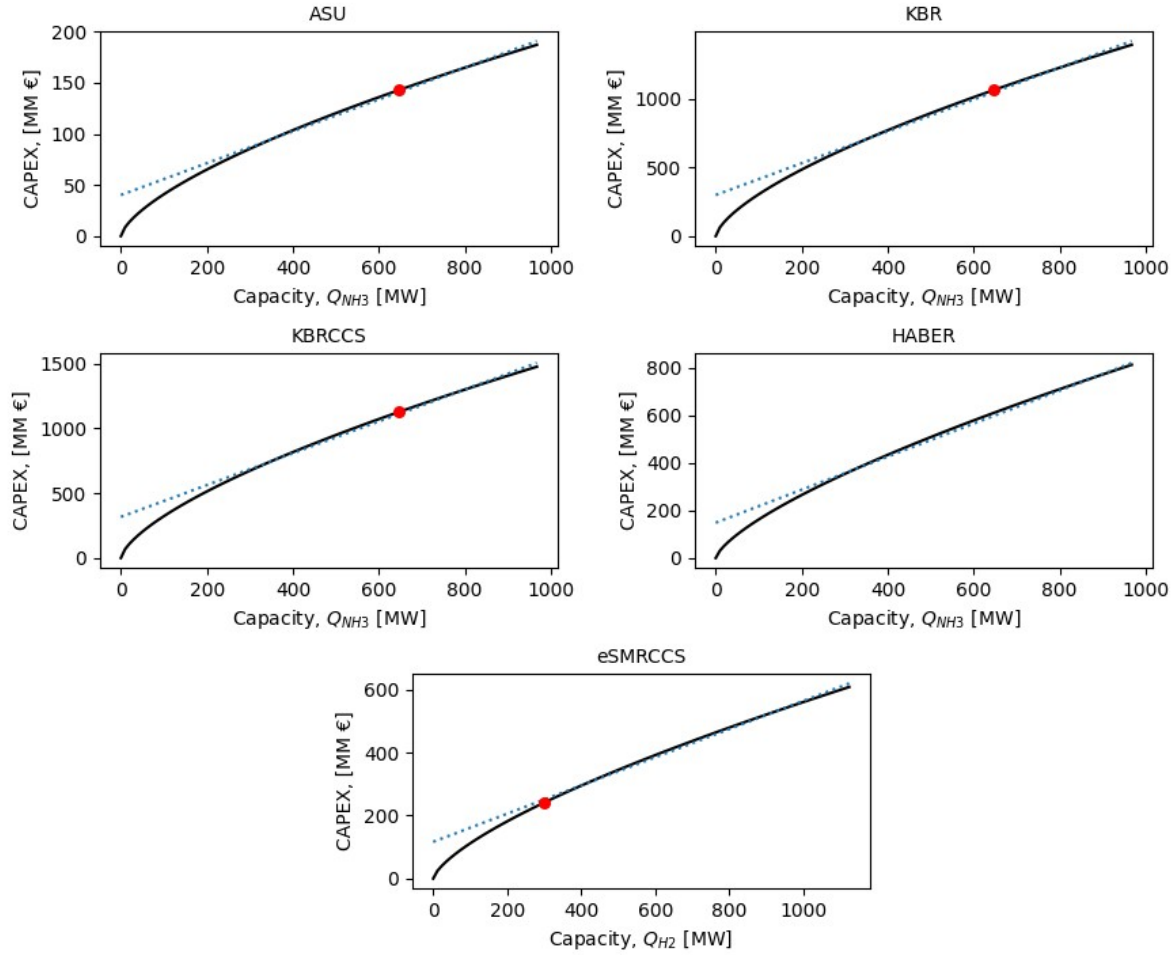

Figure 18: CAPEX scaling and linear approximation along with the base data for the KBR, KBRCCS, HABER, ASU and eSMRCCS technologies. As shown, with the way the linearization was performed, very small plants are discouraged.

Table 10: Cost functions, both power function and linear approximation, for the technologies modelled.

Technology	Coefficient	Exponent	Slope	Intercept
KBR	136341	0.67	1162	3.00×10^8
KBRCCS	143992	0.67	1227	3.17×10^8
HABER	45285	0.711	694	1.48×10^8
ASU	18260	0.67	156	4.01×10^7
eSMRCCS	35317	0.7	447	1.16×10^8

4.5 Other Technologies

This section presents the various supplementary technologies modelled used in conjunction with the primary ones. No limitation of maximum deployable capacities and no scaling has been considered for these technologies. Moreover, they are considered fully flexible except if otherwise stated.

PEME. The techno-economic data used for PEME are shown in Table 11 and are based on data by IEA, DEA and Siemens [32], [49], [80].

Table 11: PEM electrolyzer system techno-economic data used for PEME. [a]The decreased efficiency is due to hydrogen compression considerations as explained later.

CAPEX	1340	€/kWh$_e$
FOM	7	%
Lifetime	20	yr
Plant Efficiency	74.5[a] (75.5)	%
Footprint	20	m^2/MW$_e$

HOS. Storing hydrogen in large quantities for the industry is currently seen in the form of pressurized hydrogen tanks [81]. Salt caverns is also a good alternative, however, since there are no places with such geology in the vicinity of the nodes, this technology was not further explored. Hydrogen is stored in tanks as a gas in a variety of pressures or as liquid in more sophisticated tanks. The choice of materials for the hydrogen tanks depends on factors such as their intended use, the complexity of the tank and its cost. Generally, the cost of the tank increases with the nominal working pressure [81].

Figure 19: Type I hydrogen storage (500 kg$_{H2}$) [81].

Regarding tanks, a cheap solution for stationary applications are usually the large and weighty "Type I" tanks made of seamless steel or aluminium [81]. They are designed for lower pressures up to 250 bar which is adequate for the purpose of this study. At this pressure, hydrogen can be stored for years and the operational as well as standby losses of gas are considered negligible [81]. Technology improvements in the future are not expected [81]. Techno-economic data on Type I hydrogen storage systems are given in Table 12 below based on DEA data [81]. A compressor and related energy requirements are not included as those have been considered in hydrogen production as also discussed later. Finally, the charging and discharging rate is assumed as three times the nominal storage capacity.

Table 12: Type I hydrogen storage data used for HOS.

Unit Capacity	16700	kWh
CAPEX	34.3	€/kWh
–Tank	22.9	€/kWh
–Installation	11.4	€/kWh
FOM	2.22	%
Lifetime	25	yr
Footprint	29.5	m^2

BAT. Techno-economic data for the batteries considered are given in Table 13 below and are based on DEA and NREL [82]. The charging and discharging rate is assumed as three times the nominal storage capacity.

Table 13: Lithium-ion battery techno-economic data used for BAT.

CAPEX	507	€/kWh
FOM	2.5	%
Lifetime	15	yr
Charge Efficiency	96	%
Discharge Efficiency	96	%
Self-discharge	0.1	%/day
Footprint	6.25	m^2/MWh

OSW. Offshore wind energy has been modelled based on the work of Weimann et al. [74]. The model takes into consideration wake loss of wind farms. Techno-economic data used for the wind turbines of OSW are given in Table 14 below. The average depth at the OSW site is considered as 17.4m and the distance from the shore as 27.1km [74]. The hub height of the turbines was assumed as 100m.

Table 14: Wind turbine techno-economic data used for modelling OSW.

P_{rated}	9500	kW
V_{cutin}	3	m/s
V_{rated}	13	m/s
Wake loss	3	%
Hub height	100	%
CAPEX	1394	€/kW
FOM	2.2	%
Lifetime	25	yr

PV. The investment costs of PV are considered as 119.36 €/m^2, based on data for utility PV systems in the Netherlands by IEA [83]. The peak power of these systems is assumed as 176 W/m^2. The lifetime of the systems are taken for 20 years. The system efficiency is calculated hourly with Equation 18 based on hourly irradiation and air temperature data. The average efficiency for the 2019 weather data was 15.55%.

$$\begin{aligned} n_{PV} = {} & 1.618 \cdot 10^{-1} + 5.615 \cdot 10^{-5} \cdot Irr - 7.34 \cdot 10^{-4} \cdot T_{air} - 1.257 \cdot 10^{-7} \cdot Irr^2 \\ & + 1.596 \cdot 10^{-7} \cdot Irr \cdot T_{air} - 4.24 \cdot 10^{-7} \cdot T_{air}^2 + 6.315 \cdot 10^{-10} \cdot Irr^3 \\ & - 1.073 \cdot 10^{-10} \cdot Irr^2 \cdot T_{air} + 9.506 \cdot 10^{-11} \cdot Irr \cdot T_{air}^2 + 1.122 \cdot 10^{-9} \cdot T_{air}^3 \end{aligned} \tag{18}$$

where:

Irr = the solar irradiation (J/cm^2)
T_{air} = the air Temperature (°C)
n_{PV} = the system efficiency (–)

ELON and **ELOFF.** The cost of transmitting electricity onshore is assumed as 1.326 €/kW/km based on a 500 kV single line line rated at 1500 MW [84]. For the offshore transmission, the cost is assumed as 2.763 €/kW/km [85]. The techno-economic data used are given in Table 15 below.

Table 15: Electricity transmission techno-economic data [84], [85].

	Onshore	Offshore	Unit
CAPEX	1.326	2.763	€/kW/km
OPEX	1	1	%
Lifetime	40	40	yr
Loss	0.00014	0.00014	%/km

4.6 Hydrogen Compression

A modern ammonia synthesis loop has an operating pressure between 150 and 250 bar and thus it is assumed in this study as 200 bar [8], [32]. DEA does not specify a hydrogen input pressure among the techno-economic data provided for the synthesis loop but assumes a "higher pressure electrolysis available in the future". Moreover, they give an output pressure for PEM and SOEC electrolyzers of 35 bar with a potential of 100 bar in the future. Therefore, it is assumed that the hydrogen input pressure of the synthesis loop is 100 bar. Finally, the output pressure of eSMRCCS is provided by IEAGHG as 200 bar [46].

The work for hydrogen compression can calculated with Formula 19 which is based on Cengel et al. and is corrected for the non-ideality of the gas [86].

$$w_{comp} = \frac{ZRT_i \cdot \frac{Nk}{k-1} \cdot [(\frac{P_2}{P_1})^{(\frac{k-1}{Nk})} - 1]}{\eta_{is}\eta_{mech}} \tag{19}$$

where:

w_{comp} = compression work ($J \cdot mol^{-1}$)
Z = compressibility factor for non-ideality correction (1.05)
R = gas constant (8.3145 $J \cdot mol^{-1} \cdot K^{-1}$)
T_i = inlet temperature (K)
k = specific heat ratio C_p/C_v (1.41)
P_1 = inlet pressure (bar)
P_2 = outlet pressure (bar)
η_{is} = isoentropic efficiency (0.80)
η_{mech} = mechanical efficiency (0.99)
N = number of stages such that pressure ration is not more than 4

Therefore, an electricity addition of 0.60 kWh/ kg_{H2} for PEME and a reduction of 0.35 kWh/kg_{H2} for eSMRCCS is taken into account in the optimization. Possible investment costs changes due to compression step changes are ignored as are not expected to be significant if any at all.

4.7 CO_2 Transmission and Storage

To reduce computation time and since CO_2 management after the plant is beyond the scope of this study, it was decided to use a simple specific transmission and storage fee for every ammonia production node. The amount of CO_2 that will need to be stored if CCS technologies are used is in the range of 3 and 2 $Mton_{CO2}/yr$ for the Sluiskil and Chemelot demand nodes respectively [23]. Sites that can store such large amounts of CO_2 for decades exist both onshore as well as offshore and are economically and technically feasible [87], [88]. However, due to the failure of onshore CCS projects in the Netherlands in the past, among other due to societal and political reasons, there is currently a shift towards offshore CCS [89].

One of the leading CCS development initiatives in Europe is the Porthos project, which envisions a network of pipelines passing through the port of Rotterdam area [89]. According to the H-vision project that considers the Porthos project for CO_2 storage, the "tariff" of transporting CO_2 from Maasvlakte in Rotterdam and storing it into depleted gas fields under the North Sea seabed is about 23.31 €/ton_{CO2} for the ambitious "reference" scenario which is able to accept the flows required by the ammonia industry [90].

DEA asserts that pipeline transmission may be the most desirable option for point sources of more than 1Mt of CO_2 [91]. For an onshore pipeline with capacity of 300 ton_{CO2}/h (2.6 $Mton_{CO2}/yr$), DEA gives an investment cost of 2.73 €/ton_{CO2}/m of, a fixed O&M cost of 23.75 €/ton_{CO2}/yr/km and a technical lifetime of 50 years [91].

For long distances, CO_2 is transferred in the dense phase with a minimum pressure of 80 bar. DEA considers 12" pipes with a pressure drop of roughly 0.5 bar/km. However it is possible, and desirable when relatively longer distances are considered, to have lower pressure drop with larger pipes [92]. Since the outlet pressure of CO_2 from eSMRCCS is 110 bar and the distances in the Netherlands relatively short, it makes sense to use slightly larger pipes to avoid compression stations and their energy demand [78]. Using the following equations 20 and 21, pipe sizes can be calculated to limit output pressure of the pipeline at minimum 80 bar for the three nodes [86], [93].

The CO_2 output pressure and temperature for KBRCCS is 150 bar and 25°C respectively. Therefore, to account for the pressure difference with eSMRCCS, a correction of roughly -5.7 kWh_e/ton_{CO2} is calculated with Formula 19 above by using CO_2 parameters k = 1.294 and Z = 0.89. Although a compression stage could possible be removed from the KBRCCS, saving some costs, it is ignored.

$$\frac{1}{f'} = -1.8 \log_{10} \left(\frac{\varepsilon}{3.7D}\right)^{1.11} + \left(\frac{6.9\alpha}{\rho D \nu}\right)^{2} \tag{20}$$

$$\Delta p = \frac{L}{2D} \rho \nu^2 f' \tag{21}$$

where:

ν = flow velocity of the gas ($m \cdot s^{-1}$)
Δp = pressure drop (Pa)
D = pipe diameter (m)
L = pipe length (m)
ρ = density of the gas (kg $\cdot m^{-3}$) (820 kg $\cdot m^{-3}$ at 10-11 MPa)
ε = roughness height (about 50 $\cdot_{10}{}^{-6}$m)
α = dynamic viscosity (83.9 $\cdot_{10}{}^{-6}$Pa $\cdot$s)
f' = Darcy friction coefficient (Pa)

According to these calculations, and rounding up to readily available pipe diameters, for the pressure drop of less than 30 bar, Sluiskil's pipe diameter remains at 12" but Chemelot's requires a larger pipe at 14". DEA gives costs for CO_2 pipelines as shown in Table 16.

Table 16: Pipeline techno-economic data [91].

Average Capacity (ton/h)	Diameter (inch)	Cost (k€/km)
20	4	356.3
75	8	712.5
300	12	819.4

From these data the following Equation 22 is extracted with a R^2 equal to 0.989 showing a good fit. The corrected costs for the pipelines are shown in Table 17 below.

$$Cost_{corrected} = 453697 \ln D - 261439 \tag{22}$$

where

D = pipe diameter (inch)

Table 17: Corrected cost for CO_2 pipeline.

Node	Pipe (inch)	Cost (k€/km)
Sluiskil	12	819.4
Chemelot	14	912.2

The levelized cost of CO_2 transmission (onshore) is calculated using a discount rate of 8% with the following Equation 23 and are given in Table 18.

$$LCOT_{CO_2} = \frac{\sum_{n=1}^{n} \frac{I_t + OM_t}{(1+t)^t}}{\sum_{n=1}^{n} \frac{M_{CO_2}}{(1+t)^t}} \tag{23}$$

where:

I_t = investment expenditures in the year t
OM_t = operations and maintenance expenditures in the year t
r = discount rate
n = expected lifetime of system or power station
M_{CO_2} = mass of CO_2 in the year t

Table 18: Corrected cost for CO_2 pipeline, cost for storing CO_2 offshore and total fee for management of CO_2 for the two nodes considered in the optimization.

Node	Onshore Cost €/ton	Offshore & Storage Cost €/ton	Total Cost €/ton
sluiskil	2.37	23.31	25.68
chemelot	5.55	23.31	28.86

The onshore CO_2 transportation values calculated are in very close agreement with values given by Equation 22 reported by Knoope and Ramirez [94]. Offshore transport and storage costs as of 2015 were estimated to be between 17 and 49€/$tonne_{CO2}$ [95]. It is noted that these calculations are a conservative correction. The plants have in the proximity other industrial sites that will also require pipelines for CO_2 transmission. It will make sense to install larger pipelines and therefore have reduced costs due to economies of scales.

5 Results

This chapter presents the results of the conducted optimizations and discusses their implications. Emission reductions for all cases are compared to a new KBR plant, as economic data for current ammonia producing plants was unavailable. Consequently, the reduction potential is actually higher than the results indicate, as current ammonia production is less efficient than the newer KBR plants. For detailed result data, please refer to the supplementary material.

5.1 Case 1 - Base Grid Profile without RES

As shown in Figure 20 below, the cost-minimization algorithm selects the KBR plant as the sole source for meeting ammonia demand due to its lower production cost of approximately 252 €/ton$_{NH3}$. However, constraining the total emissions results in the optimization incorporating the KBRCCS technology, leading in an 81.2% reduction in annual emissions at a cost of approximately 292 €/ton$_{NH3}$. This finding highlights the effectiveness of the KBRCCS plant in largely reducing emissions while still meeting ammonia demand and is slightly more optimistic than the ISPT results [29]. The trade-off between emissions reduction and ammonia price is reflected in a 16.1% increase in price and an abatement cost of 30.3 €/ton$_{CO2}$. The price-emission Pareto front for Case 1 is presented in Figure 21.

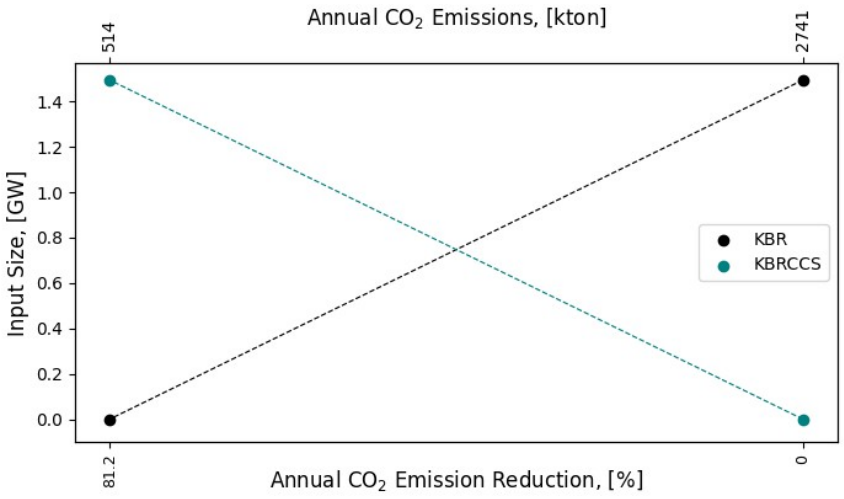

Figure 20: Pareto front for the technologies deployed in case 1.

The Pareto front analysis reveals that the optimal production mix includes only KBR and KBRCCS technologies, while other technologies, although allowed, are not cost-effective and therefore not installed. The high CO_2 rate of the electricity mix in the Netherlands makes electricity-demanding technologies like eSMR and PEME less viable due to their higher emissions. This result is consistent with previous findings in the literature [3], [46]. The emissions reductions in Case 1 are therefore limited by the installed technology, specifically by its capture rate, meaning that further reducing emissions is not possible beyond this point. Important result data for Case 1 are given in Table 19.

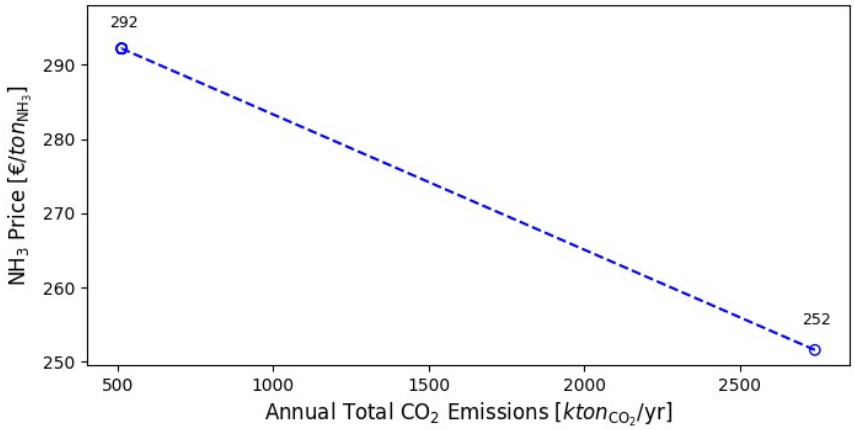

Figure 21: Price-emission Pareto front for the Case 1.

Table 19: Optimization results for Case 1.

Pareto Point	1	2	
Emissions	2741	514	$kton_{CO2}$/yr
Ems. Reduction	–	81.2%	–
Annual Cost	418.2	485.6	MM €
Ammonia Price	251.6	292.2	€/ton_{NH3}
Price Change	–	16.1%	–
Abatement Cost	–	30.3	€/ton_{CO2}
Gas Imports	13094	13094	GWh/yr
Electricity Imports	-180.7	5.2	GWh/yr

5.2 Case 2 - Test Grid Profile without RES

Similar to the previous case, the optimization model utilizes the KBRCCS plant to remove 81.3% of emissions, which is negligibly higher due to the lower carbon intensity of the imported test profile grid electricity. The important difference now is that emissions can be further reduced and potentially eliminated completely, since CO_2-free electricity can be stored in BAT or hydrogen produced with it can be stored in HOS. Further reductions are realized by installing the standalone HB plant (always followed by the ASU) and feeding it with hydrogen produced by the eSMRCCS technology. Only when it is necessary to completely eliminate emissions is PEME is deployed, since eSMRCCS can only remove up to roughly 98.6% of direct emissions.

Energy storage is heavily utilized in this scenario, and as emissions reduction targets become more stringent, the amount of HOS and BAT installed increases. It is noteworthy that with higher reductions, the model installs two eSMRCCS plants, operating them at a lower capacity factor, and continues to increase the size of the second one as it becomes optimal to produce more and more hydrogen than needed at each time-slice, with the excess hydrogen being stored and used at times with higher electricity prices. This result is also attributed to the assumption that eSMRCCS is more flexible compared to KBRCCS. Figure 22 presents the Pareto front for the technologies deployed in Case 2.

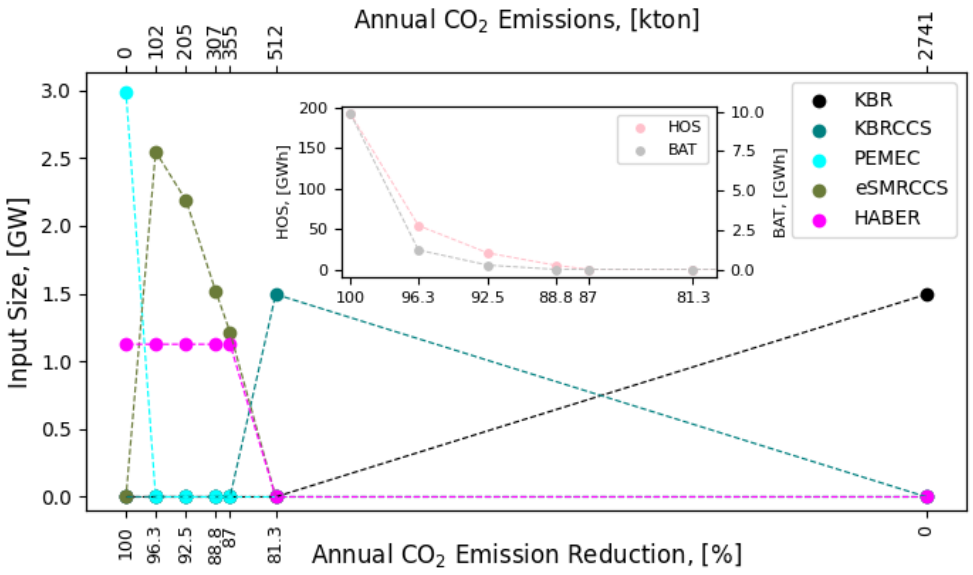

Figure 22: Pareto front for the technologies deployed in Case 2.

As emissions reductions become more stringent, the system requires an increasing amount of electricity imports, eventually reaching 14.7 TWh/yr for complete decarbonization. The amount of electricity required is substantial, equivalent to the output of two nuclear power plants, which emphasizes the importance of careful considerations for both the production and transmission of electricity. Moreover, this scenario requires large amounts of energy storage, including both HOS and BAT. Table 20 provides more information on Case 2.

Table 20: Optimization results for Case 2.

Pareto Point	1	2	3	4	5	6	7	
Emissions	2741	512	355	307	205	102	0	$kton_{CO2}/yr$
Ems. Reduction	0.0%	81.3%	87.0%	88.8%	92.5%	96.3%	100.0%	–
Gas Imports	13094	13094	10643	10643	10643	10643	0	GWh/yr
Elec Imports	-181	5	3579	3579	3594	3634	14681	GWh/yr

Figure 23 below displays the inputs and outputs for BAT and HOS over a 10-day period at the Pareto point of full decarbonization. Predictably, BAT generally charges during electricity price minimums and when grid carbon intensity is zero. Discharging occurs during electricity high peaks and at the beginning of carbon intensity hikes. Additionally, a small amount of electricity is supplied by BAT during high grid carbon intensity and high electricity prices to maintain the HB plant and ASU in constant operation. HOS operates similarly to BAT, charging when the grid carbon intensity is zero and as long as the batteries hold enough energy to power the electrolyzers. Discharging occurs during electricity price peaks, but primarily when grid carbon intensity is high. As a result, the installed storage capacity is related to the duration of consecutive days during which grid carbon intensity is high. The same principle applies to Pareto points that involve lower emissions reductions, albeit on a smaller scale.

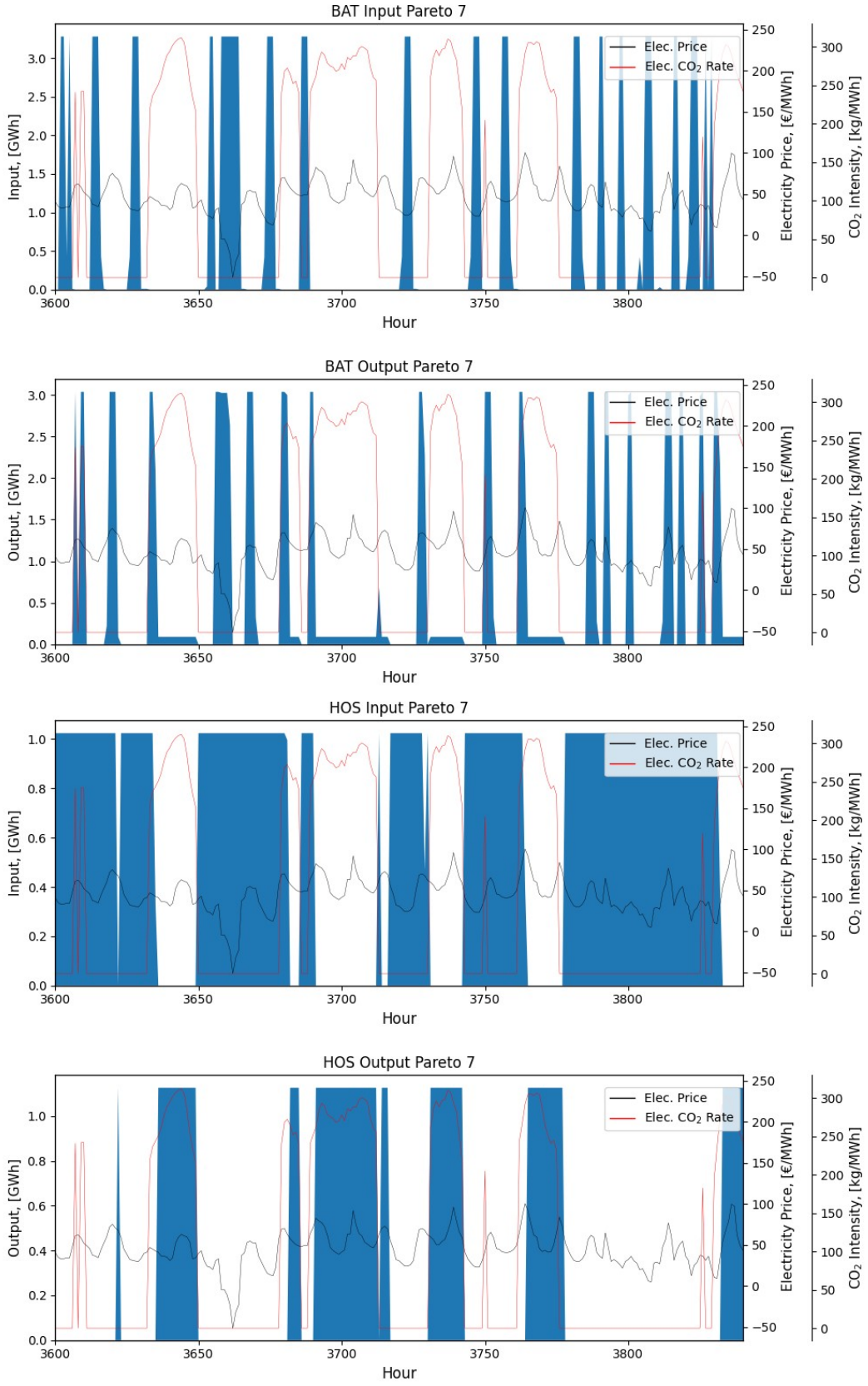

Figure 23: Energy storage input and output for 10 concecutive days of the year in Case 2. Electricity price and carbon intensity used in this optimization are also plotted. It is noted that Pareto 7 is at 100% decarbonization.

5.3 Case 3 - Including RES

Allowing for different types of storage systems can lead to notable differences in the price-emission Pareto front. Figure 24 illustrates the differences among the three systems. Although all three simulations start similarly, their results diverge as emissions reductions become more demanding. Notably, a system that relies solely on HOS is not able to achieve emissions reductions beyond a certain point and is more expensive than the system that uses both storage technologies. A system using only BAT can eventually achieve full decarbonization, but is consistently more expensive than the system using both storage technologies.

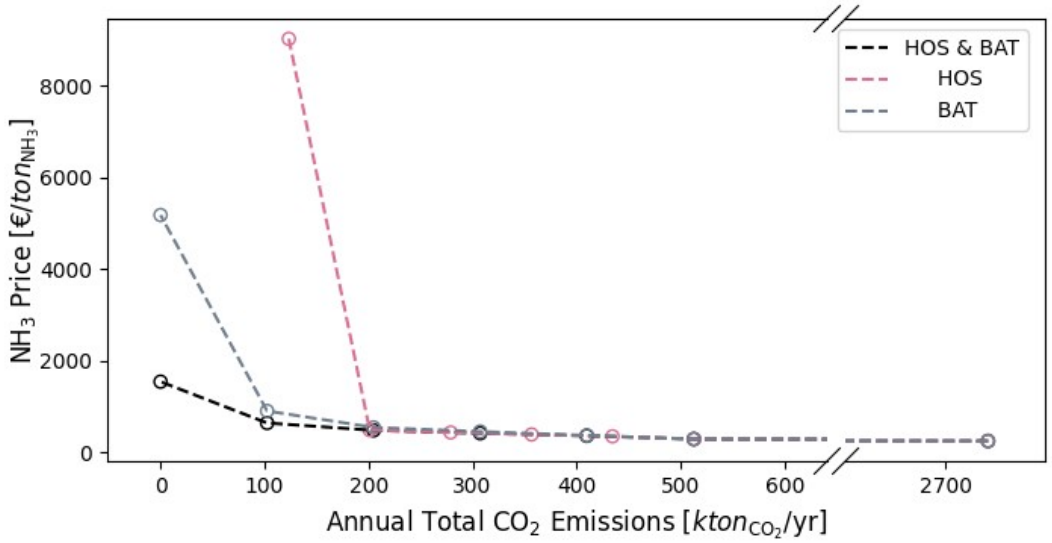

Figure 24: Price-emission Pareto front for all three systems of Case 3. It is clear that a combination of both BAT and HOS is optimal.

Decarbonization using only HOS cannot proceed beyond 95.5%, as HABER and ASU require electricity from the carbon-intensive grid to meet their power needs. The optimization tries to exploit as much CO2-free RES potential as is available but it cannot proceed further due to a maximum system cost constraint. However, there are also physical limitations, since there are 11 hours throughout the year when neither PV nor OSW generate electricity. At maximum decarbonization, this system has built enormous capacities of PV and OSW, as well as HOS.

The system using only BAT typically relies on KBRCCS to achieve an 81.3% reduction in emissions and then uses eSMR to achieve a 96.3% reduction. However, achieving full decarbonization requires the deployment of 1.5 GW of PEME and a significant increase in costs, primarily due to the installation of 30 GW of PV, 9.3 GW of OSW, and 62.2 GWh of BAT. As both the HOS-only and BAT-only systems are deemed inadequate, the optimization process continues by utilizing both storage types in the system.

The Pareto front for the system utilizing both HOS and BAT is displayed in Figure 25 below. Typically, the system achieves 81.3% reductions through KBRCCS, but in this case, PV and BAT are already installed to satisfy the plant's minimal electricity demand. Over time, the system gradually replaces KBRCCS with eSMRCCS while simultaneously increasing the installation of OSW, PV, BAT and HOS. Once again, the optimization deploys 2.6 GW of PEME only for 100%

reduction in emissions and it is only at this point where KBRCCS is not deployed. At this point, the system builds also 3.9 GW of PV, 4.8 GW of OSW, 1.6 GWh of BAT and 163 GWh of HOS.

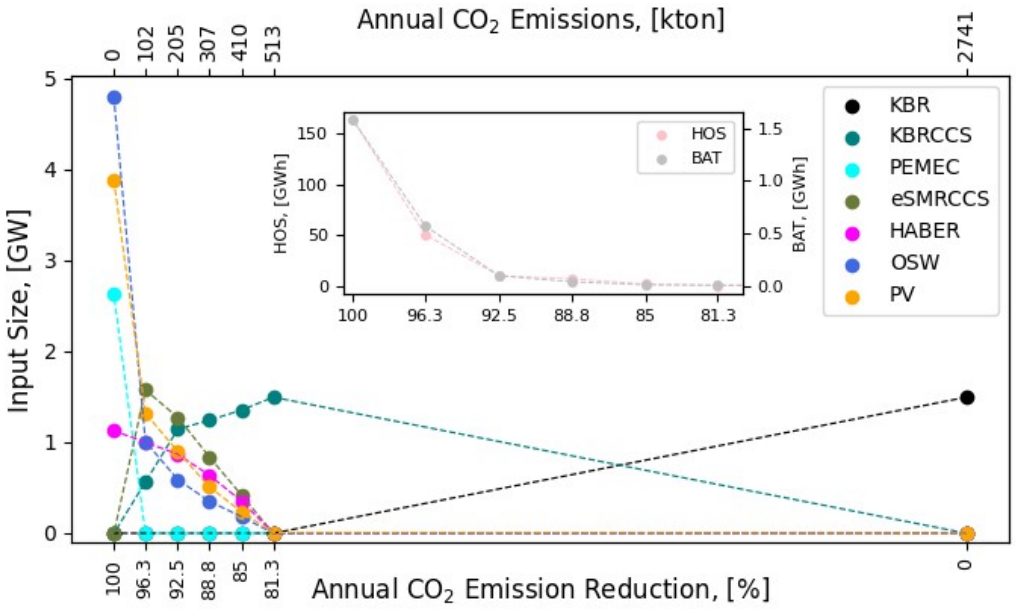

Figure 25: Pareto front for the technologies deployed in the system utilizing both HOS and BAT in Case 3.

Achieving 81.3% of reductions with KBRCCS comes with an abatement cost of 30.8 €/ton$_{CO2}$. Utilizing more and more eSMRCCS in place of KBRCCS increases gradually the costs, reaching a price of ammonia at 644 €/ton$_{NH3}$ and CO_2 abatement cost of 247 €/ton$_{CO2}$ for 96.3% emission reductions. Removing the last few percentages of emissions comes with an exponential increase in RES capacities deployed. Naturally, ammonia prices and abatement costs also exponentially increase to 1545 €/ ton$_{NH3}$ and 784.5 €/ ton$_{CO2}$. To provide context, according to Yara, ammonia prices averaged at 214 €, 415 €and 1020 €per ton$_{NH3}$ in 2019, 2021 and 2022, respectively, following the changes in the price of NG [85]. It is noteworthy that the system produces significant amount of excess electricity and HT heat which are not taken into account. Table 21 presents the results of the system utilizing both storage technologies, which will serve as the reference system for the upcoming sensitivity analysis.

Table 21: Optimization results for system with both storage technologies in Case 3.

Pareto Point	1	2	3	4	5	6	7	
Emissions	2740.5	512.7	409.8	307.3	204.9	102.4	0.0	kton$_{CO2}$/yr
Ems. Reduction	0.0%	81.3%	85.0%	88.8%	92.5%	96.3%	100.0%	–
System Cost	418.2	486.9	606.6	699.5	803.4	1070.6	2568.2	MM €/yr
Ammonia Price	251.6	292.9	365.0	420.9	483.4	644.1	1545.2	€/ton$_{NH3}$
Price Change	0.0%	16.4%	45.1%	67.3%	92.1%	156.0%	514.1%	–
Abatement Cost	–	30.8	80.8	115.6	151.9	247.3	784.5	€/ton$_{CO2}$
Elec. Imports	-181	0	-66	-89	-386	-682	-1575	GWh/yr
Gas. Imports	13094	13094	12553	12036	11521	10995	0	GWh/yr
HT Heat	0	0	248	485	722	964	1125	GWh/yr

5.4 Case 4 - Including Networks

The inclusion of onshore and offshore electricity transmission costs and energy losses results, as expected, in a small but significant increase in ammonia prices at the Pareto points where electricity demand is increased, as illustrated in Figure 26. At full decarbonization, the increase in ammonia price reaches 5.3%, primarily due to higher total investment costs. Although not great, notable differences in deployed capacities are a 16.2% increase in the capacity of PV, an increase of 8.2% in the capacity of HOS, and a decrease of 5.8% in the capacity of PEME. These changes happen mostly due to the system compensating for energy losses. PV is preferred over OSW due to the higher ELOFF costs.

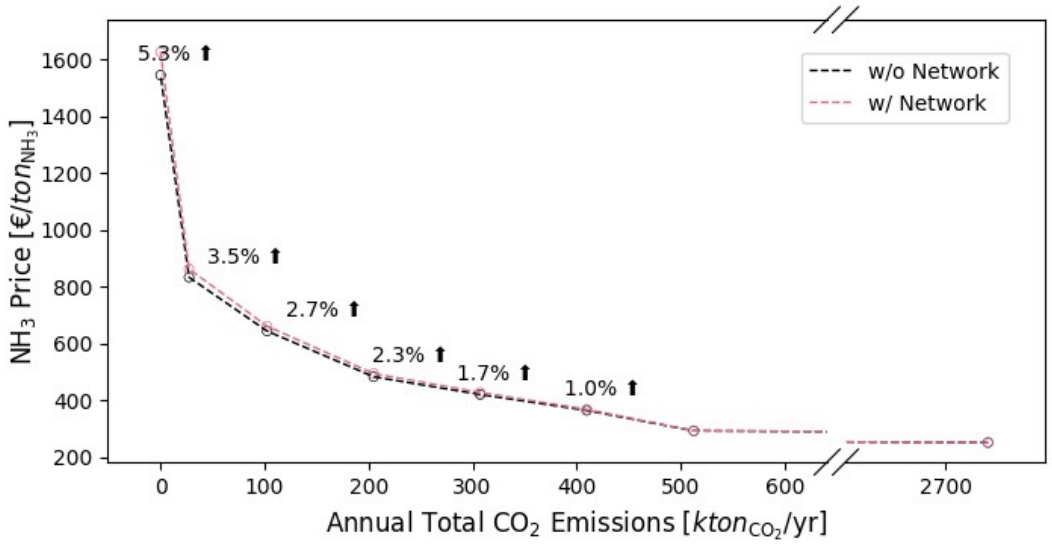

Figure 26: Price-emission Pareto front for the systems with and without electricity networks.

A result was also produced with a constraint of 99% emissions reduction and was included in the Pareto front. It is seen that while costs increase with more emission reductions, the abrupt exponential increase in costs happen at the last 1% of reductions. This is the result of RES intermittency and the system compensating by building more and more of PV and OSW. This indicates that it might be optimal to simply stop producing ammonia at certain timeslices and use ammonia storage. The results of this simulation are presented in Table 22.

Table 22: Optimization results for the Sluiskil demand node in Case 4, after the addition of electricity networks in the simulation.

Pareto Point	1	2	3	4	5	6	7	8	
Emissions	2740.5	512.7	409.8	307.3	204.9	102.4	27.4	0.0	$kton_{CO2}$/yr
Ems. Reduction	0.0%	81.3%	85.0%	88.8%	92.5%	96.3%	99.0%	100.0%	–
System Cost	418.2	486.9	612.5	711.6	822.0	1099.3	1434.1	2703.1	MM €/yr
Ammonia Price	251.6	292.9	368.6	428.1	494.6	661.4	862.9	1626.4	€/ton_{NH3}
Abatement Cost	–	30.8	83.4	120.6	159.3	258.2	374.4	833.8	€/ton_{CO2}
Elec. Imports	-181	0	-33	-99	-235	-638	-655	-1012	GWh/yr
Gas. Imports	13094	13094	12553	12036	11521	10995	9204	0	GWh/yr
HT Heat	0	0	248	485	722	963	1125	1125	GWh/yr

Figure 27 presents the cost breakdown of the system at different emission reduction levels. At no reductions, the costs are primarily divided between the CAPEX of KBR and gas imports.

At 81.3% reductions, the transmission and storing of capturedCO_2 becomes a significant portion of the total cost at 11.8% of the total. As emissions reductions increase further, the costs become primarily related to the CAPEX and FOM of the various technologies, with imports becoming less and less significant. It is noteworthy that at 99% emission reductions, the optimization imports very expensive electricity, evidently having tapped most of the available RES potential. At 100% CO2 reductions, the cost breakdown shows that HOS-related expenses account for 25.9% of the total cost, with OSW, PEME and PV accounting for 30.1%, 21.1%, and 11.5% respectively. The pareto front for the technologies deployed is shown in Figure 28. Networks installed at full decarbonization are 2.9 GW of ELOFF and 2.7 GW of ELON.

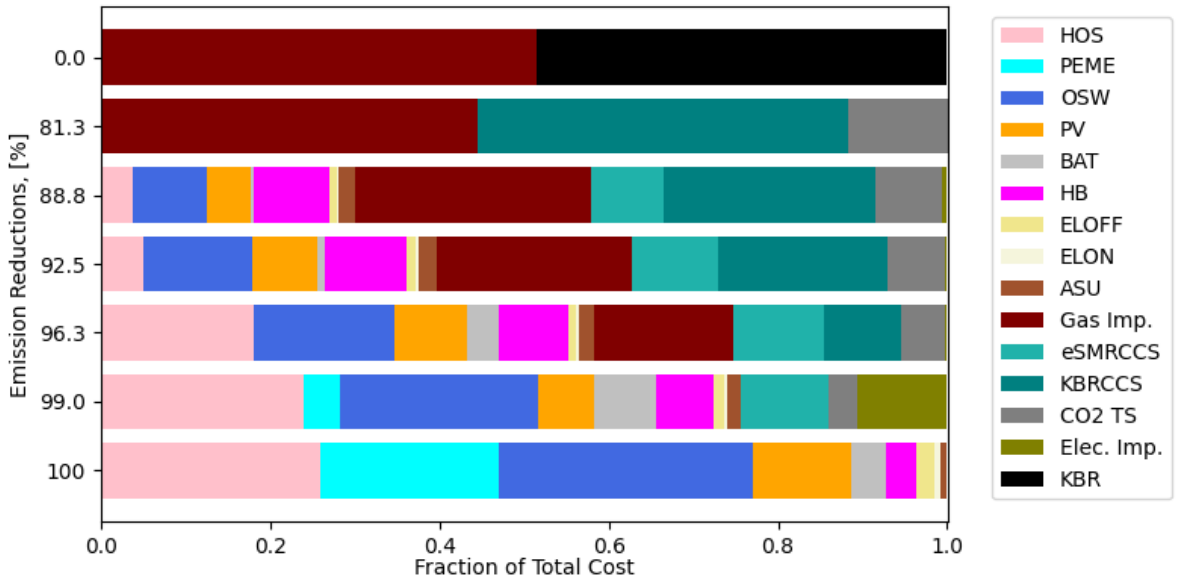

Figure 27: Cost breakdown for different Pareto points in Case 4. CAPEX, VOM and FOM for each technology are aggregated together. Contributions of more than 0.01% are shown.

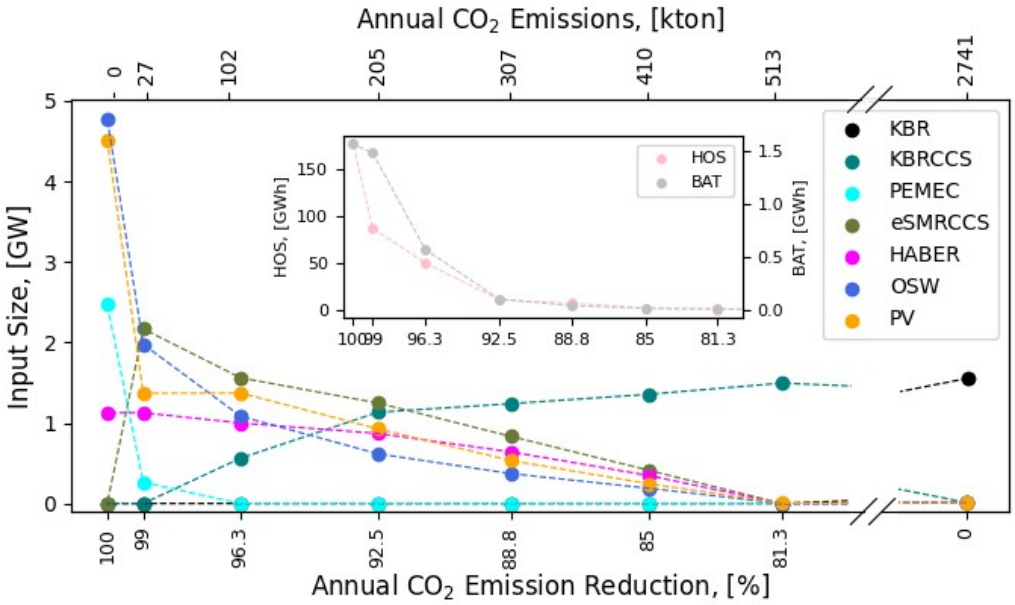

Figure 28: Pareto front for the technologies deployed for Chemelot node with the addition of electricity transmission in the model.

The same optimization was run for the Chemelot node and ammonia demand, and the results are shown in Figure 29 and Table 23 below. Beyond the differences in capacities deployed and small differences in ammonia prices and abatement costs no other changes were found. The technologies deployed are identical and the differenes are the result of scaling and electricity transmission and CO_2 transportation differences.

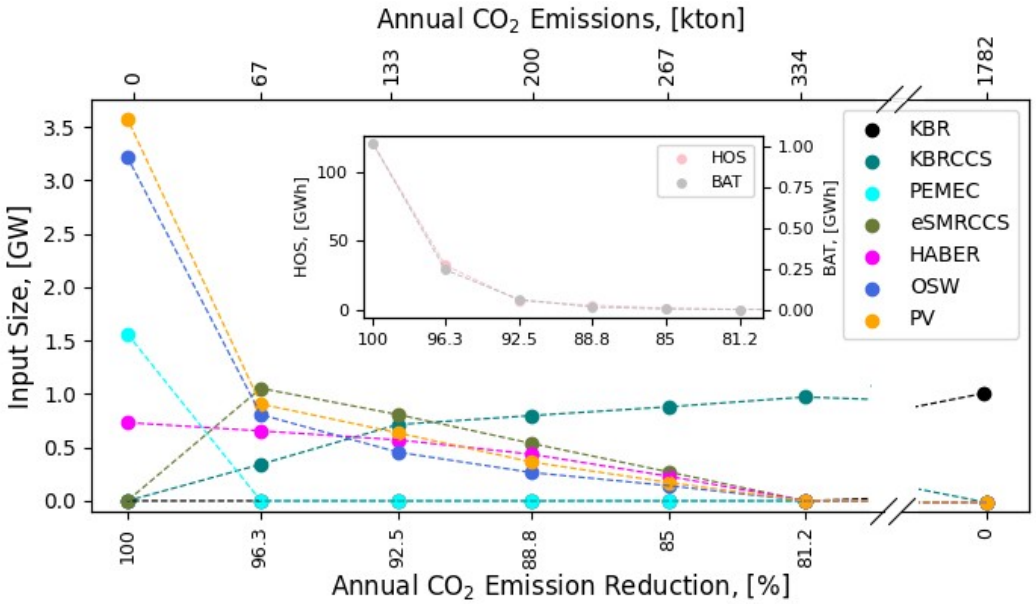

Figure 29: Pareto front for the technologies deployed for Chemelot node with the addition of electricity transmission in the model.

Table 23: Optimization results for the Chemelot demand node in Case 4, after the addition of electricity networks in the simulation.

Pareto Point	1	2	3	4	5	6	7	
Emissions	1782.5	334.2	266.5	199.9	133.3	66.6	0.0	$kton_{CO2}/yr$
Ems. Reduction	0.0%	81.2%	85.0%	88.8%	92.5%	96.3%	100.0%	–
System Cost	285.6	336.1	436.7	500.8	581.7	756.2	1880.4	MM €/yr
Ammonia Price	264.2	310.9	404.0	463.3	538.1	699.5	1739.5	$€/ton_{NH3}$
Abatement Cost	–	34.8	99.7	136.0	179.5	274.3	894.7	$€/ton_{CO2}$

5.4.1 Geographic Influence

Assuming same level of ammonia demand as Sluiskil at the location of Chemelot results in a substantial increase in the cost of ammonia due to the higher investment costs associated with transmission lines and the slightly higher cost of transporting captured CO_2. The magnitude of these increases is depicted in Figure 30 and data are summarized in Table 24. The substantial increase in ammonia price and abatement costs indicates that Sluiskil's location may have a comparative advantage over Chemelot's, especially if Chemelot is unable to access potential RES nearby.

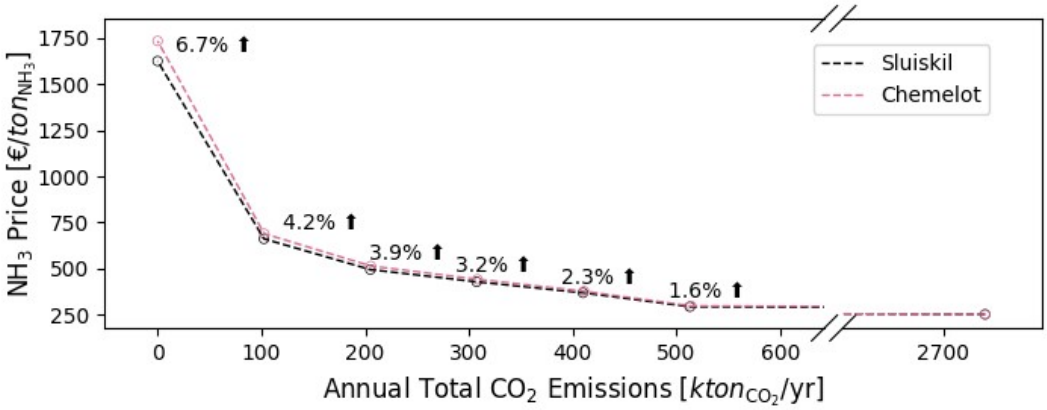

Figure 30: Pareto front for the technologies deployed for the Chemelot node.

Table 24: Optimization results for the Chemelot demand node.

Pareto Point	1	2	3	4	5	6	7	–
Emissions	2740.5	512.7	409.8	307.3	204.9	102.4	0.0	$kton_{CO2}$/yr
Ems. Reduction	0.0%	81.3%	85.0%	88.8%	92.5%	96.3%	100.0%	–
Sluiskil NH3 Price	251.6	292.9	368.6	428.1	494.6	661.4	1626.4	€/ton_{NH3}
Chemelot NH3 Price	251.6	297.6	377.0	441.9	513.8	689.3	1735.2	€/ton_{NH3}
Price Increase	0.0%	1.6%	2.3%	3.2%	3.9%	4.2%	6.7%	–
Sluiskil Ab. Cost	–	30.8	83.4	120.6	159.3	258.2	833.8	€/ton_{CO2}
Chemelot Ab. Cost	–	34.3	89.4	130.0	171.9	275.8	899.7	€/ton_{CO2}
Ab. Cost Increase	–	11.3%	7.2%	7.8%	7.9%	6.8%	7.9%	–

A price-emission Pareto front comparison for different technology sets without networks for the Sluiskil demand node is given in Figure 31 below.

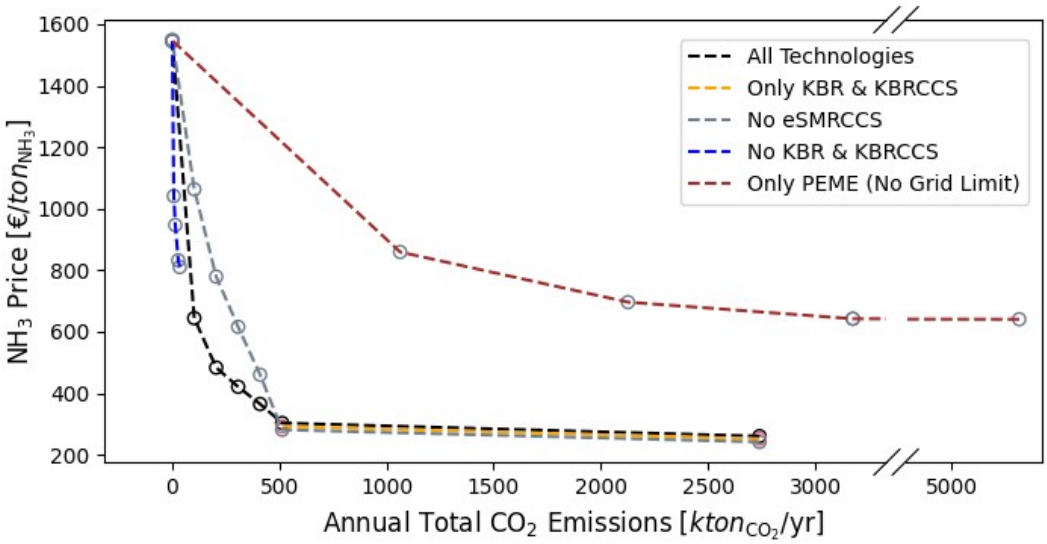

Figure 31: Price-emission Pareto front comparison between different set of technologies. There is no grid constraint for the "Only PEME" case.

6 Discussion

This section examines the limitations of the results presented in the previous chapter and discusses their implications for decarbonizing ammonia production in the Netherlands. To maintain reasonable computation times, the sensitivity analysis in this chapter was performed to the copperplate system of Case 3, which does not include networks.

6.1 Limitations

Although the findings of this study offer valuable insights into decarbonizing ammonia production, there are limitations that must be taken into account when interpreting the results.

6.1.1 Techno-Economic Data

Assessing the quality of data gathered can be a significant limitation in this study, particularly as sources may not always agree on economic data. For example, there has been disagreement over the ASU CAPEX, as already mentioned, and similar issues arise for other technology data such as the HABER plant [13], [56]–[59]. Even the KBR and KBRCCS data are based on software simulations and not the real, notoriously hard to find industry data. It is mentioned here for example that while this study has taken the capture rate of KBRCCS as 81.3%, another study estimates this specific value for such technology as 73% [96]. In addition, the captured CO_2 transmission and storage values used might prove too optimistic and this could also be the case for electricity transmission [46], [97]. In any case, variations in certain parameters are expected and acceptable because they are plant- and location-specific.

Rapid changes in techno-economic data, particularly for emerging and developing technologies like PEME, further complicate the analysis. To account for these uncertainties, a sensitivity analysis was performed to assess the potential impact of variations of their CAPEX on the overall system. The potential for reducing CAPEX by 25% and 50% is being explored for PEME technology, as high technological learning rates and increased cumulative capacity suggest that these reductions could be achievable in the near future [98], [99].

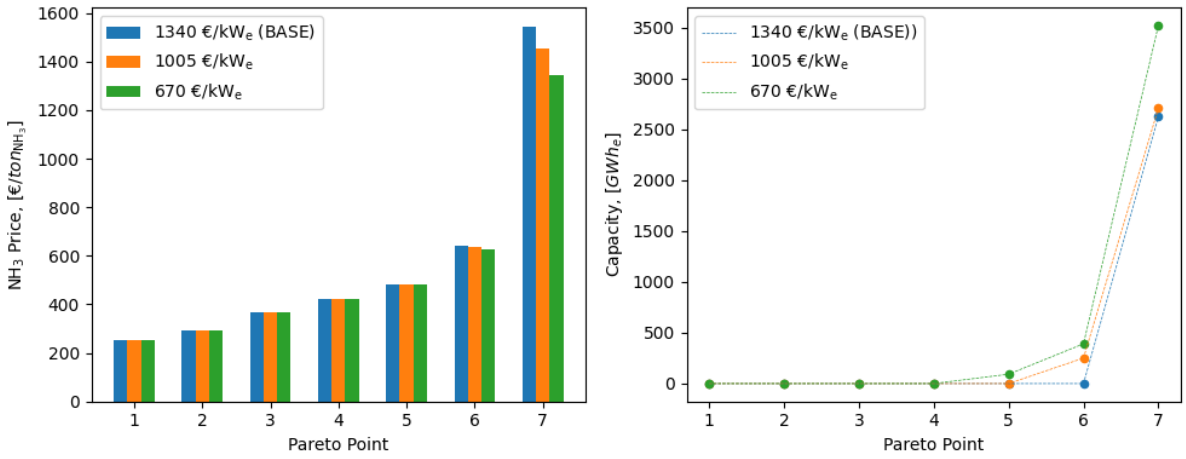

Figure 32: Ammonia price and and PEME deployed capacities for different PEME CAPEX values.

Figure 32 illustrates that a reduction in PEME's CAPEX could result in a meaningful decrease

(6% and 12.9% for 25% and 50% CAPEX reduction) in ammonia prices at full decarbonization. However, the system does not change substantially, except for an expected small increase in the deployment of PEME capacity and a small amount installed earlier in the Pareto front. This is also followed by a substantial 24.6% decrease in HOS capacity deployment at full decarbonization for the very optimistic CAPEX scenario.

Battery technologies that have been widely adopted and have a significant combined installed capacity, such as nickel-metal hydride, large-scale lithium-ion, and sodium-sulfur systems, are currently priced at approximately 200 to 600 €/KWh and are becoming more affordable [99]. The system installs large amounts of HOS, and differences in the CAPEX of battery technologies could potentially shift deployment towards this storage technology. Tests of a 30% increase and decreases of 30% and 75% in BAT's CAPEX did not significantly impact the overall system or prices, and thus were not reported. This is due to the strong preference for HOS over BAT, which has negligible energy losses [81].

As previously explained, eSMRCCS is a nascent technology with a low TRL, which means that it has not yet been fully developed and may not be feasible on an industrial scale. Although a demonstration plant was expected to have been developed by now, no recent news on its progress can be found, and Haldor Topsoe, the company developing the technology, has not responded to inquiries regarding its status. Even if the technology is feasible, it might not be able to scale with the factor of 0.7 assumed in this study. In any case, a pessimistic scaling factor or a failure for the technology to develop at an industrial scale would result in increased costs, with the upper bound being the prices given by not including the technology in the simulation, as depicted in Figure 33 and the results given in Table 25 below.

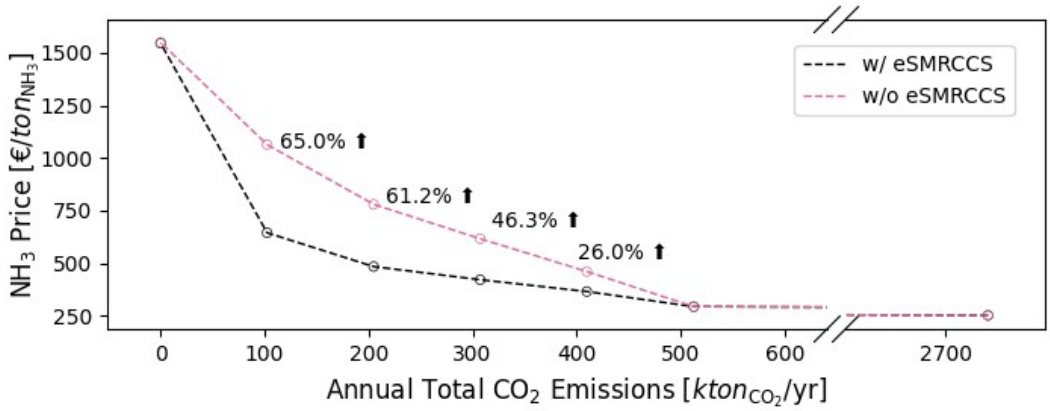

Figure 33: Price-emission Pareto front comparison between the reference system and one without eSMRCCS.

Table 25: Results for the run that does not include the eSMRCCS technology.

Pareto Point	1	2	3	4	5	6	7	
Emissions	2740.5	512.7	409.8	307.3	204.9	102.4	0.0	$kton_{CO2}/yr$
Ems. Reduction	0.0%	81.3%	85.0%	88.8%	92.5%	96.3%	100.0%	–
Ammonia Price	251.6	292.9	389.2	477.0	589.0	739.0	1545.3	€/ton_{NH3}
Abatement Cost	–	30.82764	98.12849	153.922	221.1537	307.0382	784.575	€/ton_{CO2}

6.1.2 Natural Gas

There are a number of limitations that must be taken into account when evaluating the use of NG in ammonia production. Firstly, it cannot be assumed that gas infrastructure is readily available, and additional investments may be necessary to ensure that it is. Additionally, the composition of the NG can have a significant impact on the efficiency of the process [8]. However, the most significant limitation is the unknown actual price paid for NG by the ammonia industry, which is assumed to be constant at a generally low but can actually be highly volatile over time and cost more. To address this limitation, a sensitivity analysis was performed to assess the effect of gas prices on the results. The average gas prices for the Netherlands for the years 2018, 2019, 2021, and 2022 were 22.45 €/MWh, 16.45 €/MWh, 32.05 €/MWh, and 70.2 €/MWh, respectively [70].

Figure 34 shows that, as expected, the cost of ammonia increases with higher gas prices. Interestingly, for the average gas prices developed during the troubled period for the European energy system in 2021 and 2022, it is possible to eliminate most emissions at a cost that is at or below the market price of ammonia. However, the overall system does not change even with the extreme gas prices, but naturally, higher gas prices lead to faster deployment of PEME in the Pareto front, along with greater deployment of RES. The full data can be found in the supplementary material, while ammonia prices and abatement costs are provided in Table 26. The results show that increasing gas prices leads to a substantial decrease in abatement costs.

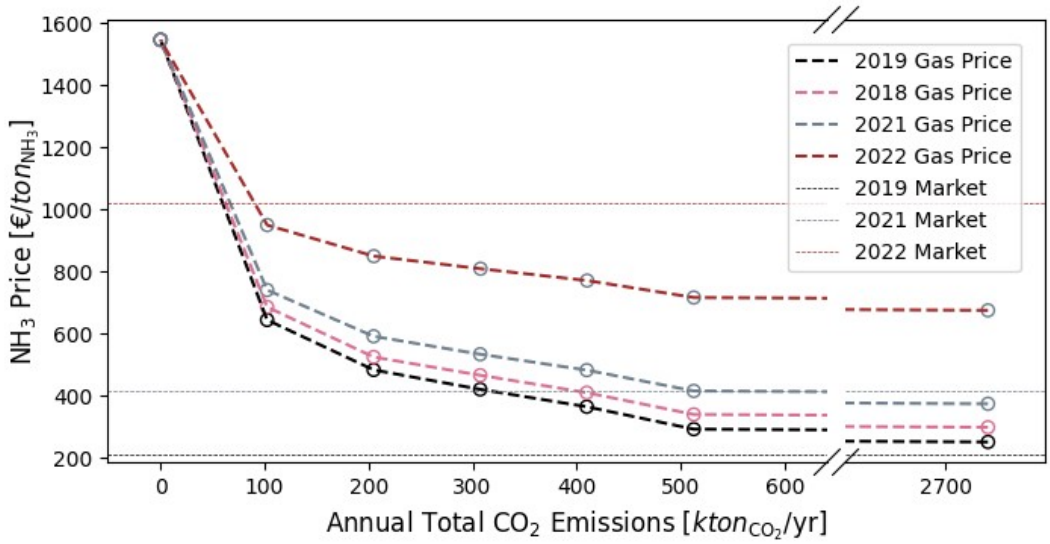

Figure 34: Price-emission Pareto front for different average gas prices. Plotted are also average market prices for these years calculated by averaged quarter prices reported by Yara [100].

Table 26: Ammonia prices and abatement costs for the different gas prices tested.

	Em. Reductions	0.0%	81.3%	85.0%	88.8%	92.5%	96.3%	100.0%	
2019	Ammonia Price	251.6	292.9	365.0	420.9	483.4	644.1	1545.2	€/ton_{NH3}
	Abatement Cost	–	30.8	80.8	115.6	151.9	247.3	784.5	€/ton_{CO2}
2018	Ammonia Price	298.9	340.2	421.5	503.4	589.5	944.7	2128.7	€/ton_{NH3}
	Abatement Cost	–	30.8	79.4	114.4	148.2	243.8	755.8	€/ton_{CO2}
2021	Ammonia Price	374.5	415.8	494.0	570.7	656.7	1000.1	2128.7	€/ton_{NH3}
	Abatement Cost	–	30.8	77.2	108.9	142.3	230.6	710.0	€/ton_{CO2}
2022	Ammonia Price	675.1	716.4	781.1	849.8	913.6	1154.7	2131.0	€/ton_{NH3}
	Abatement Cost	–	30.8	68.3	91.5	114.3	172.8	527.7	€/ton_{CO2}

Additionally, the substantial indirect emissions from the production and transmission of NG, estimated at 0.035 kg_{CO2}/kWh_{NG}, are not accounted for [46]. An optimization run was performed including these indirect emissions and the results of an optimization run are shown in Figure 35 and Table 27 below. It is evident that the Pareto front radically changes. First of all, producing ammonia with the KBR technology now emits 3199 $kton_{CO2}$/yr, an increase of 16.7% in comparison to the reference case, while with the KBRCCS, 971 $kton_{CO2}$/yr are emitted, an increase of 89.4% compared to the reference case. As for the technologies deployed, although the general picture remains the same, KBRCCS and eSMR are utilized less while PEME, HOS, BAT and HABER and utilized in greater capacities and earlier. This test emphasizes the importance of establishing a natural gas supply chain that prioritizes emissions reduction, while ensuring reliable accounting of methane leakage as concluded by Romano et al. [101].

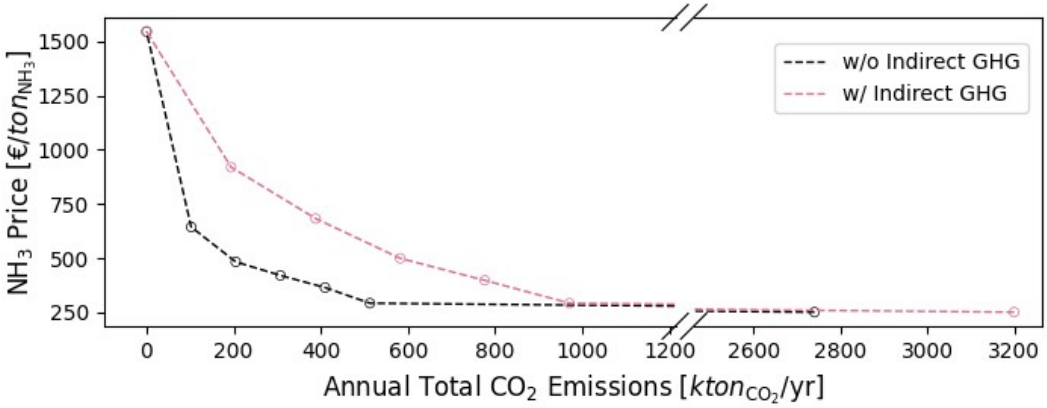

Figure 35: Price-emission Pareto front comparison between the reference and the optimization with the CO_2 emissions of producing and transporting NG.

Table 27: Result of the optimization when taking into account the CO_2 emissions of producing and transporting NG.

Pareto Point	1	2	3	4	5	6	7	
Emissions	3198.8	971.0	776.4	582.3	388.2	194.1	0.0	$kton_{CO2}$/yr
Ammonia Price	251.6	292.9	398.4	499.8	683.1	920.1	1545.2	€/ton_{NH3}
Abatement Cost	–	30.8	100.7	157.6	255.1	369.8	672.1	€/ton_{CO2}

6.1.3 Flexibility

Perhaps, the most significant limitation of the model developed is the assumed flexibility of the KBRCCS, HABER and ASU technologies, as it may have had a substantial impact on the accuracy and reliability of the findings. Such inflexible plants operate solely at their nameplate capacity and experience efficiency losses when operating outside of strict conditions, limiting their adaptability to changes in energy demand or unexpected operational issues. This limitation is particularly evident in the results showing emissions reductions between 85% and 96.3% since they operate at full capacity otherwise. To test how flexibility affects the results, an optimization run was performed with KBRCCS and HABER being able to operate if built, with a minimum capacity of 80% instead of the reference 30%. Figure 36 shows the output of KBRCCS for both the reference and a stricter operation range. The fast ramps ups and ramp downs shown above are simply impossible for the actual plants.

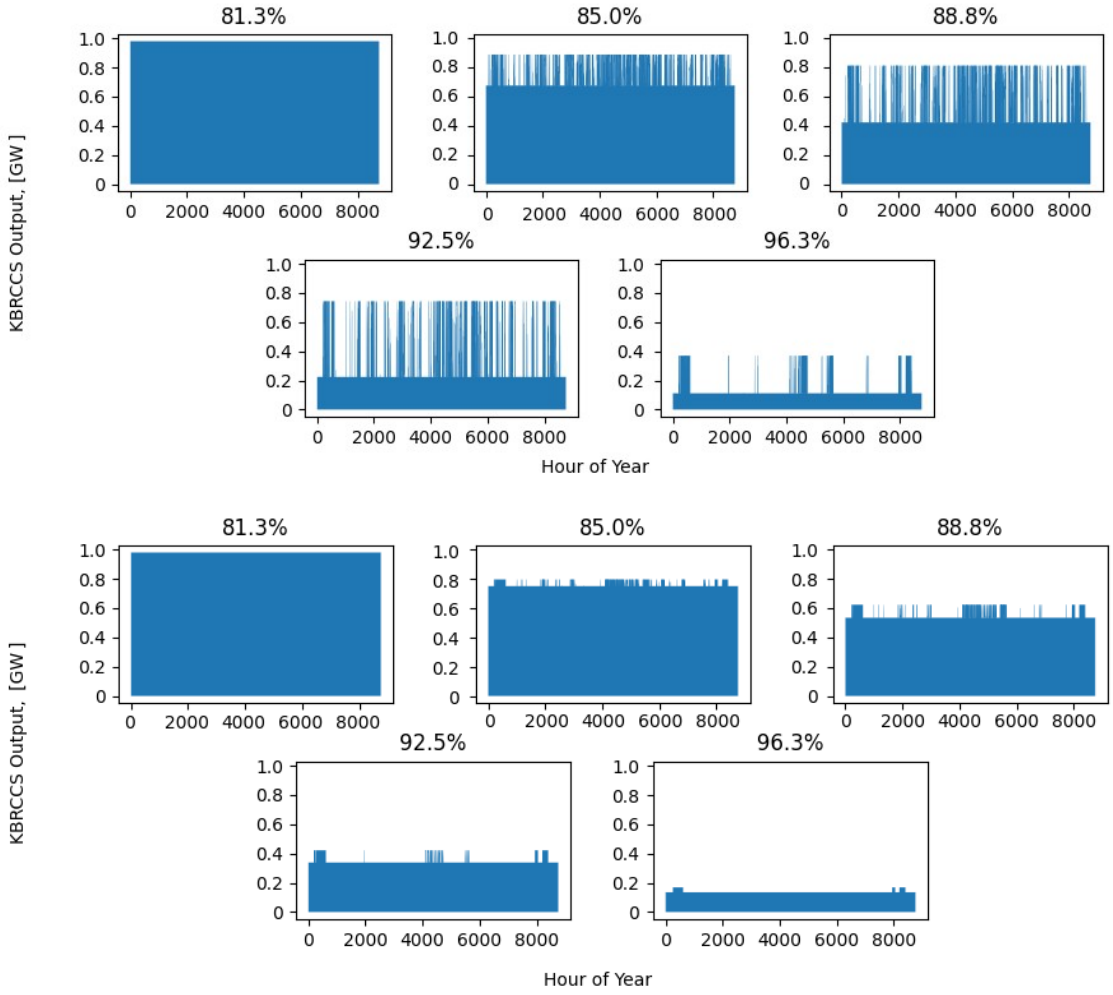

Figure 36: Comparison of KBRCCS ammonia output throughout the year for the Pareto points that the plant is deployed for both the reference 30%-100% (above) and a more strict 30%-100% (down) operation range.

The results indicate that there will be a substantial increase in costs to ammonia price and abatement costs at different points of the Pareto front as shown in Figure 37. Figure 38 illustrates the deployment of the technologies across the Pareto front. While the same technologies are

utilized, there are significant differences in the capacities deployed. The model deploys smaller capacities of KBRCCS (in the range of 10% to 54% depending on the Pareto point) and HABER (in the range of 25% to 3%) when forced to operate them closer to maximum capacity. In contrast, the model deploys larger capacities of BAT (in the range of 623% to 99%) and HOS (in the range of 609% to 44%). There is also a shift in the deployment of RES, with a decrease in PV and an opposite deployment of OSW due to the later's ability to produce electricity throughout the day. Table 28 gives more information on ammonia prices and abatement costs.

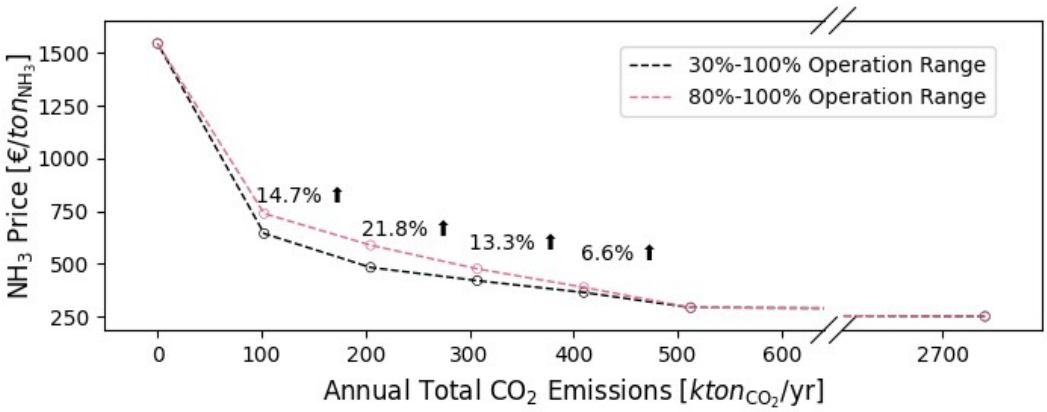

Figure 37: Price-emission Pareto front comparison between the reference and the more inflexible optimization.

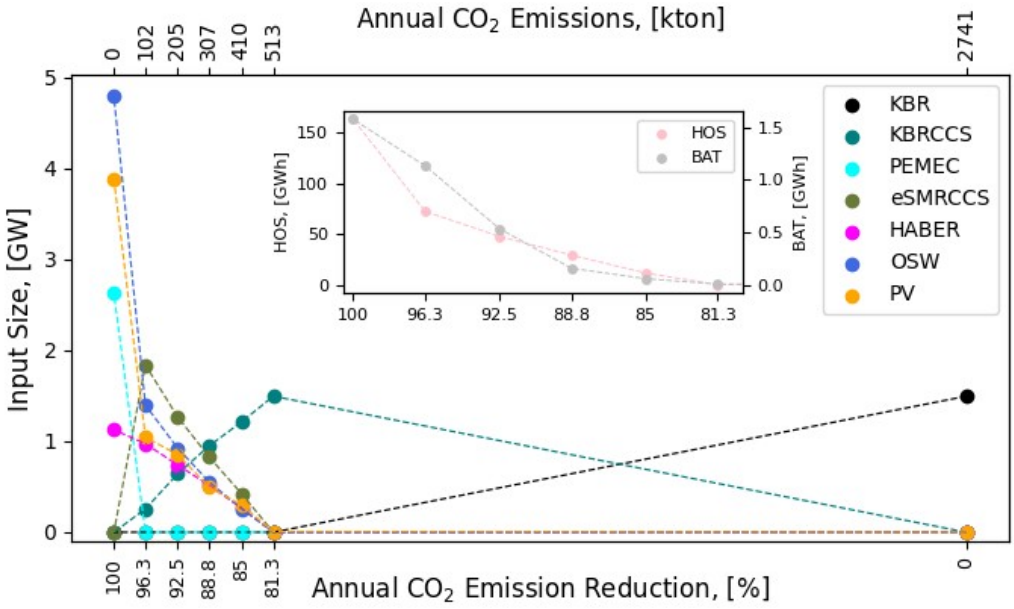

Figure 38: Pareto front for the technologies deployed in the less flexible run.

This analysis highlights the importance of considering the flexibility and dynamics of the plants. Moreover, it draws attention to the lack of ammonia storage in the model since it assists inflexible technologies. Although this study takes into account ammonia storage CAPEX and FOM, the system cannot currently store ammonia. Attempts to model ammonia storage were unsuccessful due to technical limitations and time constraints. However, incorporating the ability

to turn off and on the plants, store ammonia and account for efficiency losses during ramp-ups and ramp-downs would provide a much more accurate representation of a real system. The flexibility of eSMRCCS was not tested as these plants are expected to be flexible, and it is reasonable to assume that there will be always available demand and perhaps a grid to export excess hydrogen, allowing the plants to operate at maximum capacity.

Table 28: Result of the optimization with less flexible operation range for KBRCCS and HABER.

Pareto Point	1	2	3	4	5	6	7	
Emissions	2740.5	512.7	409.8	307.3	204.9	102.4	0.0	kton_CO2/yr
Ems. Reduction	0.0%	81.3%	85.0%	88.8%	92.5%	96.3%	100.0%	–
System Cost	418.2	486.9	646.9	792.7	978.9	1228.2	2568.3	MM $kton_{CO2}$/yr
Ammonia Price	251.6	292.9	389.2	477.0	589.0	739.0	1545.3	€/ton_{NH3}
Abatement Cost	–	30.8	98.1	153.9	221.2	307.0	784.6	€/ton_{CO2}

6.1.4 Discount Rate

The choice of discount rate can have a large impact on the final ammonia price and abatement cost, as shown in Table 29. In terms of the technologies deployed, there is no significant difference. A higher discount rate marginally favors deployment of PV and HOS and consequently removes some PEME.

Table 29: Effect of discount rate on ammonia price and abatement costs.

	Ems. Reduction	0.0%	81.3%	85.0%	88.8%	92.5%	96.3%	100.0%	
8%	Ammonia Price	251.6	292.9	365.0	420.9	483.4	644.1	1545.2	€/ton_{NH3}
	Abatement Cost	–	30.8	80.8	115.6	151.9	247.3	784.5	€/ton_{CO2}
10%	Ammonia Price	271.4	313.8	400.2	466.9	541.5	731.0	1806.8	€/ton_{NH3}
	Abatement Cost	–	31.7	91.9	133.5	177.0	289.6	931.2	€/ton_{CO2}
6%	Ammonia Price	233.1	273.3	332.3	377.8	429.6	563.8	1303.5	€/ton_{NH3}
	Abatement Cost	–	30.0	70.8	98.8	128.8	208.4	649.2	€/ton_{CO2}

6.1.5 Other Limitations

Area Requirements. The model has no constraints on the available area for deploying the technologies. As shown in Table 30 just for Sluiskil, there is a need of 10.3km^2 and 30.9 km^2 for 99% and 100% decarbonization respectively. There is also the need for 208 and 503 offshore turbines respectively. To put it into perspective, large KBR plants are advertised as requiring a plot of 0.025 km^2 [39]. Although technically feasible, the requirements of area (and material needs), put into question an industrial decarbonized ammonia production with current PEME and RES technologies.

Table 30: Area requirements for 99% and 100% decarbonizing of the Sluiskil site.

Em. Reductions	99.0%	100.0%	
BAT	0.009	0.010	km2
PEME	0.005	0.049	km2
HOS	2.55	5.20	km2
PV	7.78	25.63	km2
Total	10.3	30.9	km3

Exporting Excess Resources. RES are optimally deployed to meet the electricity demand throughout the year. Due to mostly seasonal weather variation, this results in excess electricity production. Although this excess electricity is not accounted for in the results, it could potentially be sold to the grid leading to lower production costs but also increasing risk of grid congestion. Similarly, the HABER plant generates a significant amount of HT heat that has significant value but is not accounted for in the study. This excess heat could potentially be exported to meet demand in the vicinity of the plant. Additionally, the ASU may produce and export oxygen and argon as valuable by-products.

Future Electricity Grid Profile. The future price and emission profiles used in Case 2 are highly uncertain and not directly related. It is probable that in a decarbonized grid of the future, low-cost periods can coincide with high renewable energy supply, which would lead to lower costs of production for the eSMRCCS and PEME technologies.

MILP Gap. The MILP model used in this study is set to have a relative gap of 1%, therefore it is possible that more optimal solutions exist. Nevertheless, when the optimization was run with a 0.1% gap, the results shown no significant change to mention.

Conventional Plant High Capture Rate. The model notably lacks a conventional plant with a higher CCS that would also capture most of the flue gases in it's set of technology. This technology will have a worse NG conversion efficiency but will probably demand less electricity than eSMRCCS.

Indirect Emissions. Production and deploying of the technologies have assosiated emissions that are not accounted for.

While more limitations could be discussed, in the end, it is important to remind that the results presented in this study are based on a simplified model that reflects just one interpretation of the real world.

6.2 Implications and Future Research

The results of Case 1, which assumes unlimited imports of grid electricity, show that the cheapest technology that can meet ammonia demand at Sluiskil and Chemelot is the conventional KBR technology, at an ammonia price of 251.6 €/ ton_{NH3} and 264.2 €/ ton_{NH3} for the two sites, respectively. These plants would produce 2740 ton_{CO2}/yr and 1782.5 ton_{CO2}/yr, respectively, essentially reducing current emissions of ammonia production by roughly 14% and 19% respectively just due to better efficiency. Furthermore, the study finds that roughly 81% of these emissions (84% compared to current emissions) can be further reduced with the use of the KBRCCS technology, which is essentially the conventional ammonia production with the pressurization, transportation, and offshore storage of CO_2. For this to happen, ammonia price increases to 292.9 €/ ton_{NH3} and 310.9 €/ ton_{NH3} with an abatement cost of 30.8 €/ ton_{CO2} and 34.8 €/ ton_{CO2} for the two sites, respectively. To put this into perspective, the EU carbon price in May 2023 was above 100 €/ ton_{CO2} and was expected to average at 81.4 €/ ton_{CO2} in 2023, indicating a strong incetive for using this technology [102], [103].

The outcomes of Case 1, moreover, reveal that further decarbonization of ammonia production in The Netherlands cannot proceed due to the high carbon intensity of the current grid electricity. This is in agreement with other works [3], [46]. Therefore, the decarbonization of Dutch

ammonia production will benefit from policies seeking to reduce the carbon footprint of the electricity grid. For example, IEA states that in order for electrolysis-based ammonia to have lower emissions than the SMR-based ammonia, electricity carbon intensity must be lower than 0.18 kg_{CO2}/kWh.

In light of the results of Case 1, Case 2 assumes a futuristic grid with frequent availability of CO2-free electricity due to an abundance of renewable energy. The results suggest that emissions can indeed be further reduced by gradually shifting from KBRCCS-based ammonia production to the cleaner eSMRCCS-based production. However, for this to happen, large capacities of hydrogen storage should also be utilized. Full decarbonization, proceeds by using only PEME-based ammonia production. The results also show that how electricity is produced and its transmission should also be taken into account due to the sheer scale of electricity requirements, especially at full decarbonization.

The findings of Case 3, which includes both RES as well as grid import constraints in the analysis, demonstrate that a combination of both BAT and HOS is optimal when considering ammonia production. Furthermore, they make it clear that further emission reductions by shifting towards eSMRCCS-based and/or PEME-based ammonia production come with a significant increase of ammonia price as well as abatement costs. This increase happens not only due to the higher CAPEX and FOM of the cleaner technologies, but mostly due to their large electricity demand which forces the system to increasingly deploy more of OSW, PV and energy storage technologies. In general, with more emission reductions, the cost of ammonia is affected less and less by gas imports and increasingly by the CAPEX and FOM of the technologies used.

Data from Case 4 suggests that electricity networks have substantial impact on the decarbonization costs. Despite using arguably optimistic CAPEX for both ELON and ELOFF, there was a significant increase in the system costs. This not only occurs due to transmission line costs but it is also attributed to the electricity losses during transmission, which require more PV and HOS to compensate. Data from this case also underscore the importance of production location. Specifically they indicate that if RES are not available closer to Chemelot, except at the discussed locations, and since CO_2 storage will likely proceed offshore as already explained, then the location of Sluiskil has a significant advantage compared to the location of Chemelot.

Full decarbonization of ammonia production requires an ammonia price of 1626.4 €/ton_{NH3} and 1739.5 €/ton_{NH3}, with an abatement cost of 833.8 €/ton_{CO2} and 894.7 €/ton_{CO2} for Sluiskil and Chemelot, respectively. Nevertheless, the data reveal that the last 1% of emissions is the most difficult to decarbonize due to limited availability of RES during specific times of the year with an ammonia price of 862.9 €/ton_{NH3} an abatement cost of 374.4 €/ton_{CO2} at 99% emission reductions for the Sluiskil node. This 88% increase in ammonia price, with an associated 123% increase in abatement costs for the last 1% of reductions suggests that it may be optimal for some emissions to be released while simultaneously compensating with a negative emissions technology such as BG with CCUS.

It is crucial for future research to address the limitations of the study and expand on the model created to obtain more accurate and in-depth insights. First of all, expanding the model should begin with taking into account ammonia storage dynamics and see how this affects the results as it is expected to have meaningful impact during periods of low RES potential. This will also require the introduction of flexibility parameters and perhaps efficiency losses considerations to the inflexible plants. By doing so, more accurate results of the prices and abatement costs may

be obtained but it is not expected that the technologies deployed will see significant changes. Then, the addition of a conventional ammonia producing plant that has a high capture rate by also capturing the flue gasses should be added. Such plants may prove competitive to the novel eSMRCCS technology while their TRLs are higher [3]. It would also be useful to investigate ATR plants, particularly with CCS, since these plants might prove competitive to two-step reforming plants. There might also exist potential synergies of ATR with SOEC technologies. Additionally, it could be beneficial to determine whether the system leads to lower costs by deploying BG with CCS and utilizing associated negative emissions.

Future research should also seek to find the optimal location of ammonia plants which should be where CO_2 and hydrogen storage as well as high RES potential exists, probably somewhere in the North. Some studies go so far as to propose ammonia production offshore like the OFFSET project funded by the Dutch government [104], [105]. By producing the carriers at optimal locations and shipping them on demand, the system could be radically improved. Decarbonizing ammonia is linked to energy networks and therefore, current and future energy infrastructure should be taken into account. Furthermore, the addition of hydrogen and ammonia pipelines should be considered as a replacement to transmission lines. Finally, it is recommended to gather updated data on all technologies used in the study. Ideally, this data should be obtained through direct communication with the industry.

6.3 Policy Implications

Based on the results of this study, it is evident that most of ammonia emissions can be affordably eliminated by employing technologies with CCUS. Therefore, it is recommended to:

- Establish supportive policies that facilitate the development of infrastructure for CO_2 transport and offshore storage. The absence of such infrastructure currently leads to a significant portion of Dutch emissions being released, which can be effectively mitigated. The TRL of both CO_2 transport and offshore storage is already quite high, with operational industrial capacities. This infrastructure not only benefits other industries but even taking into account that PEME might be able to affordably fully decarbonize ammonia production by 2050, this target exceeds the lifetimes assumed for KBRCCS plants, thus avoiding technological lock-in concerns
- Prioritize funding for eSMRCCS related research and development projects like ”EReTech” [106]. The eSMRCCS technology shows great promise not only for ammonia production but also for the hydrogen sector at large but its industrial-scale viability is yet to be proven.
- Continue policy support for PV and OSW since this work highlights the crucial role of renewable electricity in enabling ammonia decarbonization.
- Condition NG imports on reducing associated production and transportation emissions.
- Assist on deploying a hydrogen grid, particularly one connected to cheap hydrogen storage such as salt caverns.
- Enable policies promoting open energy models and data since they are crucial for enhancing the quality of scientific research, achieving effective policy outcomes and increasing productivity if not simply ethical when research has been publicly funded [107].

7 Conclusion

The decarbonization of the ammonia industry is a critical step towards achieving global climate goals and reducing GHG emissions. This study aimed to identify the "cost-optimal production route to decarbonize the Dutch ammonia industry, taking into account site limitations". To address this objective, the following sub-questions were formulated:

I What alternative ammonia production routes with low CO_2 emissions are available?

The research examined the existing ammonia production processes and various alternative routes, identifying KBRCCS, eSMRCCS and PEME as the most promising technologies for decarbonizing the Dutch ammonia sector. Extensive techno-economic data for these technologies and supporting systems were gathered.

II What is the potential for decarbonizing ammonia production using alternative routes and what are the associated costs assuming no constraints in electricity and gas imports?

A MES model was created in MATLAB, and a MILP algorithm was utilized to assess the potential for decarbonization under the current Dutch grid electricity profile. The results revealed that emissions in the sector can be reduced by 16%, resulting in 877 $kton_{CO2}$ less annually, by simply replacing the current older production plants with newer, more efficient ones, at an average ammonia price of 256.6 €/ton_{NH3}. Moreover, it was found that emissions can be cost-effectively reduced by 84%, equivalent to 4553$kton_{CO2}$ annualy, by utilizing the readily available KBRCCS technology, with an average ammonia price of 300.0 €/ton_{NH3} and an average abatement cost of 32.4 €/ton_{CO2}. This relies on infrastructure related to offshore CO_2 transport and storage, for which policies should assist in its development. Finally, the optimization determined that without lowering the carbon intensity of the Dutch grid, further reductions in emissions are not achievable with the examined technology set.

III What is the impact of solar and offshore wind availability on the overall decarbonization process?

By incorporating RES in the optimization, it was discovered that additional emission reductions can be achieved by gradually shifting some of KBRCCS-based production to eSMRCCS-based production, although at progressively higher ammonia costs. The results determined that the industry can achieve complete elimination of emissions through PEME-based production, but this would require simultaneous deployment of large capacities of OSW, PV and HOS.

IV How does the geographical location of ammonia production sites impact the industry's decarbonization?

By introducing electricity networks into the model, the optimization results revealed that their contribution to the total cost of ammonia is significant and should be considered in the analysis. Moreover, the impact of the geographic location of the production sites at Sluiskil and Chemelot was examined, and it was determined that ammonia produced at Chemelot would be 1.6% to 6.7% more expensive than Sluiskil (assuming the same demand), depending on the level of decarbonization. Finally, it was determined that achieving full decarbonization of Dutch ammonia production would necessitate an ammonia price of 1671 €/ton$_{NH3}$, with an abatement cost of 858 €/ton$_{CO2}$. That being said, it was also discovered that at a 99% emissions reduction, the cost of ammonia production is nearly halved. This finding highlights both the challenge of achieving full decarbonization due to the intermittency of RES and the limitations of the model, such as the absence of ammonia storage dynamics.

Overall, the optimization consistently favors the deployment of KBRCCS technology due to its affordability and its ability to significantly reduce emissions. When renewable electricity is available, KBRCCS remains the preferred option until achieving very high emission reductions of approximately 96%, but it is also complemented by eSMRCCS. For complete decarbonization, PEME is employed. Despite conducting numerous scenarios in the sensitivity analysis, the overall outcome remains unchanged.

8 Acknowledgements

I would like to thank my supervisor and mentor, Julia Tiggeloven, for her valuable input, patience, advice and support throughout my thesis. Her guidance and feedback were essential in shaping my ideas and navigating the research process. I am grateful for her expertise and generosity in guiding me. I am also deeply grateful to Professor Matteo Gazzani for providing me with the opportunity to work on such an engaging topic as well as his advice and insightful comments, which were instrumental in this work. I would like to extend my thanks to Jan Wiegner for his valuable comments, assistance, and willingness to provide support whenever needed throughout my thesis. Last but not least, a huge shoutout to my partner, Maria Sofia Skaltsa, for putting up with my endless ramblings about this thesis and for keeping me sane throughout this journey. Without her love, support, and occasional nagging, this work would have probably never seen the light of day!

Bibliography

[1] K. H. Rouwenhorst and G. Castellanos, *Innovation Outlook: Renewable Ammonia*, en. Irena, May 2022, OCLC: 9517959936, ISBN : 978-92-9260-423-3.

[2] G. V. Duinen, "How a century of ammonia synthesis changed the world," en, *nature geoscience*, vol. 1, p. 4, 2008.

[3] International Energy Agency, *Ammonia Technology Roadmap: Towards more sustainable nitrogen fertiliser production*, en. OECD, Oct. 2021, ISBN : 978-92-64-96568-3. DOI : 10.1787/f6daa4a0-en. [Online]. Available: https://www.oecd-ilibrary.org/energy/ammonia-technology-roadmap_f6daa4a0-en (visited on 11/27/2022).

[4] O. Elishav, B. Mosevitzky Lis, E. M. Miller, *et al.*, "Progress and Prospective of Nitrogen-Based Alternative Fuels," en, *Chemical Reviews*, vol. 120, no. 12, pp. 5352–5436, Jun. 2020, ISSN : 0009-2665, 1520-6890. DOI : 10.1021/acs.chemrev.9b00538. [Online]. Available: https://pubs.acs.org/doi/10.1021/acs.chemrev.9b00538 (visited on 11/28/2022).

[5] Y. Robiou du Pont and M. Meinshausen, "Warming assessment of the bottom-up Paris Agreement emissions pledges," en, *Nature Communications*, vol. 9, no. 1, p. 4810, Dec. 2018, ISSN : 2041-1723. DOI : 10.1038/s41467-018-07223-9. [Online]. Available: http://www.nature.com/articles/s41467-018-07223-9 (visited on 11/27/2022).

[6] Y. Bicer, I. Dincer, C. Zamfirescu, G. Vezina, and F. Raso, "Comparative life cycle assessment of various ammonia production methods," en, *Journal of Cleaner Production*, vol. 135, pp. 1379–1395, Nov. 2016, ISSN : 09596526. DOI : 10.1016/j.jclepro.2016.07.023. [Online]. Available: https://linkinghub.elsevier.com/retrieve/pii/S0959652616309118 (visited on 11/29/2022).

[7] A. E. Yüzbaşıoğlu, A. H. Tatarhan, and A. O. Gezerman, "Decarbonization in ammonia production, new technological methods in industrial scale ammonia production and critical evaluations," en, *Heliyon*, vol. 7, no. 10, e08257, Oct. 2021, ISSN : 24058440. DOI : 10.1016/j.heliyon.2021.e08257. [Online]. Available: https://linkinghub.elsevier.com/retrieve/pii/S2405844021023604 (visited on 11/29/2022).

[8] M. Appl, "Ammonia, 2. Production Processes," en, in *Ullmann's Encyclopedia of Industrial Chemistry*, Wiley-VCH Verlag GmbH & Co. KGaA, Ed., Weinheim, Germany: Wiley-VCH Verlag GmbH & Co. KGaA, Oct. 2011, o02_o11, ISBN : 978-3-527-30673-2. DOI : 10.1002/14356007.o02_o11. [Online]. Available: https://onlinelibrary.wiley.com/doi/10.1002/14356007.o02_o11 (visited on 11/29/2022).

[9] Wiley-VCH Verlag GmbH & Co. KGaA and M. Appl, "Ammonia, 3. Production Plants," en, in *Ullmann's Encyclopedia of Industrial Chemistry*, Weinheim, Germany: Wiley-VCH Verlag GmbH & Co. KGaA, Oct. 2011, o02_o12, ISBN : 978-3-527-30673-2. DOI : 10.1002/14356007.o02_o12. [Online]. Available: https://onlinelibrary.wiley.com/doi/10.1002/14356007.o02_o12 (visited on 12/16/2022).

[10] M. Appl, *Ammonia: principles and industrial practice*, en. Weinheim ; New York: Wiley-VCH, 1999, ISBN : 978-3-527-29593-7.

[11] Rahimpour, M. R., Makarem, M. A., and Meshksar, M., *Advances in Synthesis Gas: Methods, Technologies and Applications, Volume 4, Syngas Process Modelling and Apparatus Simulation*, 2022.

[12] Rahimpour, M. R., Makarem, M. A., and Meshksar, M., *Advances in Synthesis Gas: Methods, Technologies and Applications, Voume 3, Syngas Products and Usages*, 2022.

[13] C. Arnaiz del Pozo and S. Cloete, "Techno-economic assessment of blue and green ammonia as energy carriers in a low-carbon future," en, *Energy Conversion and Management*, vol. 255, p. 115 312, Mar. 2022, ISSN: 01968904. DOI: 10.1016/j.enconman.2022.115312 [Online]. Available: https://linkinghub.elsevier.com/retrieve/pii/S019689042200108X (visited on 03/23/2023).

[14] P. Arora, A. F. Hoadley, S. M. Mahajani, and A. Ganesh, "Small-Scale Ammonia Production from Biomass: A Techno-Enviro-Economic Perspective," en, *Industrial & Engineering Chemistry Research*, vol. 55, no. 22, pp. 6422–6434, Jun. 2016, ISSN: 0888-5885, 1520-5045. DOI: 10.1021/acs.iecr.5b04937. [Online]. Available: https://pubs.acs.org/doi/10.1021/acs.iecr.5b04937 (visited on 12/02/2022).

[15] J. Andersson and J. Lundgren, "Techno-economic analysis of ammonia production via integrated biomass gasification," en, *Applied Energy*, vol. 130, pp. 484–490, Oct. 2014, ISSN: 03062619. DOI: 10.1016/j.apenergy.2014.02.029 [Online]. Available: https://linkinghub.elsevier.com/retrieve/pii/S0306261914001652 (visited on 12/02/2022).

[16] S. T. Wismann, J. S. Engbæk, S. B. Vendelbo, *et al.*, "Electrified methane reforming: A compact approach to greener industrial hydrogen production," en, *Science*, vol. 364, no. 6442, pp. 756–759, May 2019, ISSN: 0036-8075, 1095-9203. DOI: 10.1126/science.aaw7775 [Online]. Available: https://www.science.org/doi/10.1126/science.aaw7775 (visited on 12/11/2022).

[17] R. Zhao, H. Xie, L. Chang, *et al.*, "Recent progress in the electrochemical ammonia synthesis under ambient conditions," en, *EnergyChem*, vol. 1, no. 2, p. 100 011, Sep. 2019, ISSN: 25897780. DOI: 10.1016/j.enchem.2019.100011 [Online]. Available: https://linkinghub.elsevier.com/retrieve/pii/S2589778019300144 (visited on 12/02/2022).

[18] M. Byun, D. Lim, B. Lee, *et al.*, "Economically feasible decarbonization of the Haber-Bosch process through supercritical CO2 Allam cycle integration," en, *Applied Energy*, vol. 307, p. 118 183, Feb. 2022, ISSN: 03062619. DOI: 10.1016/j.apenergy.2021.118183 [Online]. Available: https://linkinghub.elsevier.com/retrieve/pii/S0306261921014549 (visited on 12/02/2022).

[19] A. Oni, K. Anaya, T. Giwa, G. Di Lullo, and A. Kumar, "Comparative assessment of blue hydrogen from steam methane reforming, autothermal reforming, and natural gas decomposition technologies for natural gas-producing regions," en, *Energy Conversion and Management*, vol. 254, p. 115 245, Feb. 2022, ISSN: 01968904. DOI: 10.1016/j.enconman.2022.115245 [Online]. Available: https://linkinghub.elsevier.com/retrieve/pii/S0196890422000413 (visited on 12/02/2022).

[20] H. Zhang, L. Wang, J. Van herle, F. Maréchal, and U. Desideri, "Techno-economic comparison of green ammonia production processes," en, *Applied Energy*, vol. 259, p. 114 135, Feb. 2020, ISSN: 03062619. DOI: 10.1016/j.apenergy.2019.114135 [Online]. Available: https://linkinghub.elsevier.com/retrieve/pii/S0306261919318227 (visited on 12/02/2022).

[21] P. Tunå, C. Hulteberg, and S. Ahlgren, "Techno-economic assessment of nonfossil ammonia production," en, *Environmental Progress & Sustainable Energy*, vol. 33, no. 4, pp. 1290–1297, Dec. 2014, ISSN: 19447442. DOI: 10.1002/ep.11886. [Online]. Available: https://onlinelibrary.wiley.com/doi/10.1002/ep.11886 (visited on 12/02/2022).

[22] K. Rouwenhorst, P. Krzywda, N. Benes, G. Mul, and L. Lefferts, "Ammonia Production Technologies," en, in *Techno-Economic Challenges of Green Ammonia as an Energy Vector*, Elsevier, 2021, pp. 41–83, ISBN: 978-0-12-820560-0. DOI: 10.1016/B978-0-12-820560-0.00004-7. [Online]. Available: https://linkinghub.elsevier.com/retrieve/pii/B9780128205600000047 (visited on 11/30/2022).

[23] M. Batool and W. Wetzels, "Decarbonisation options for the Dutch fertiliser industry," en, p. 39,

[24] P. Mancarella, "MES (multi-energy systems): An overview of concepts and evaluation models," en, *Energy*, vol. 65, pp. 1–17, Feb. 2014, ISSN: 03605442. DOI: 10.1016/j.energy.2013.10.041. [Online]. Available: https://linkinghub.elsevier.com/retrieve/pii/S0360544213008931 (visited on 12/01/2022).

[25] P. Gabrielli, M. Gazzani, and M. Mazzotti, "Electrochemical conversion technologies for optimal design of decentralized multi-energy systems: Modeling framework and technology assessment," en, *Applied Energy*, vol. 221, pp. 557–575, Jul. 2018, ISSN: 03062619. DOI: 10.1016/j.apenergy.2018.03.149. [Online]. Available: https://linkinghub.elsevier.com/retrieve/pii/S0306261918304872 (visited on 11/11/2022).

[26] M. J. Palys and P. Daoutidis, "Using hydrogen and ammonia for renewable energy storage: A geographically comprehensive techno-economic study," en, *Computers & Chemical Engineering*, vol. 136, p. 106 785, May 2020, ISSN: 00981354. DOI: 10.1016/j.compchemeng.2020.106785. [Online]. Available: https://linkinghub.elsevier.com/retrieve/pii/S0098135419313055 (visited on 12/02/2022).

[27] N. Lazouski, A. Limaye, A. Bose, M. L. Gala, and D. S. Mallapragada, "Cost and performance targets for fully electrochemical ammonia production under flexible operation," en,

[28] Edse Dantuma, *Dutch industry goes from top gear into reverse*, 2023. [Online]. Available: https://archive.is/NbbYE .

[29] Institute for Sustainable Process Technology, Amersfoort, *ISPT DR-20-09-Power-to-Ammonia-2017-publication.pdf*, 2017. [Online]. Available: https://library.wur.nl/WebQuery/titel/2204556.

[30] S. Chatterjee, R. K. Parsapur, and K. -W. Huang, "Limitations of Ammonia as a Hydrogen Energy Carrier for the Transportation Sector," en, *ACS Energy Letters*, vol. 6, no. 12, pp. 4390–4394, Dec. 2021, ISSN: 2380-8195, 2380-8195. DOI: 10.1021/acsenergylett.1c02189. [Online]. Available: https://pubs.acs.org/doi/10.1021/acsenergylett.1c02189 (visited on 11/29/2022).

[31] A. I. Amhamed, S. Shuibul Qarnain, S. Hewlett, *et al.*, "Ammonia Production Plants—A Review," en, *Fuels*, vol. 3, no. 3, pp. 408–435, Jul. 2022, ISSN: 2673-3994. DOI: 10.3390/fuels3030026. [Online]. Available: https://www.mdpi.com/2673-3994/3/3/26 (visited on 01/23/2023).

[32] DEA, *Technology_data_for_renewable_fuels.pdf*, 2017. [Online]. Available: https://ens.dk/sites/ens.dk/files/Analyser/technology_data_for_renewable_fuels.pdf .

[33] V. Pattabathula and J. Richardson, "Introduction to Ammonia Production," en, *Back to Basics*, 2016.

[34] K. Aasberg-Petersen, I. Dybkjær, C. Ovesen, N. Schjødt, J. Sehested, and S. Thomsen, "Natural gas to synthesis gas – Catalysts and catalytic processes," en, *Journal of Natural Gas Science and Engineering*, vol. 3, no. 2, pp. 423–459, May 2011, ISSN: 18755100. DOI: 10.1016/j.jngse.2011.03.004 [Online]. Available: https://linkinghub.elsevier.com/retrieve/pii/S1875510011000242 (visited on 04/16/2023).

[35] L. G. Pinaeva and A. S. Noskov, "Modern Level of Catalysts and Technologies for the Conversion of Natural Gas into Syngas," en, *Catalysis in Industry*, vol. 14, no. 1, pp. 66–85, Mar. 2022, ISSN: 2070-0504, 2070-0555. DOI: 10.1134/S2070050422010081 [Online]. Available: https://link.springer.com/10.1134/S2070050422010081 (visited on 04/16/2023).

[36] E. Worrell and K. Blok, "Energy savings in the nitrogen fertilizer industry in the Netherlands," en, *Energy*, vol. 19, no. 2, pp. 195–209, Feb. 1994, ISSN: 03605442. DOI: 10.1016/0360-5442(94)90060-4 [Online]. Available: https://linkinghub.elsevier.com/retrieve/pii/0360544294900604 (visited on 04/16/2023).

[37] J. Brightling, "Ammonia and the Fertiliser Industry: The Development of Ammonia at Billingham," en, *Johnson Matthey Technology Review*, vol. 62, no. 1, pp. 32–47, Jan. 2018, ISSN: 2056-5135. DOI: 10.1595/205651318X696341 [Online]. Available: http://www.ingentaconnect.com/content/10.1595/205651318X696341 (visited on 04/16/2023).

[38] Ruther, Joachim and Larsen, John and Lippmann, Dennis and Claes, and Detlev, *4000 mtpd Ammonia plant based on proven technology*, 2005.

[39] KBR, *AMMONIA 6000 - Single Stream 6,000 MTPD Ammonia Plant*, 2022. [Online]. Available: https://www.google.com/url?sa=t&rct=j&q=&esrc=s&source=web&cd=&cad=rja&uact=8&ved=2ahUKEwie-JCugJf-AhXmgv0HHcQSDG8QFnoECBAQAQ&url=https%3A%2F%2Fwww.kbr.com%2Fsites%2Fdefault%2Ffiles%2F2009%2FAmmonia-6000-Brochure.pdf&usg=AOvVaw1hgdZRYrikF-wXzeJo-fyJ

[40] P. J. Dahl, C. Speth, A. E. K. Jensen, *et al.*, "New SynCOR Ammonia™ process," en,

[41] L. Ramos and S. Zeppieri, "Feasibility study for mega plant construction of synthesis gas to produce ammonia and methanol," en, *Fuel*, vol. 110, pp. 141–152, Aug. 2013, ISSN: 00162361. DOI: 10.1016/j.fuel.2012.12.045. [Online]. Available: https://linkinghub.elsevier.com/retrieve/pii/S0016236112010691 (visited on 04/16/2023).

[42] Klaus Noelker and Joachim Johanning, "Autothermal reforming: A flexible syngas route with future potential," en, *UHDE*, 2010.

[43] R. Carapellucci and L. Giordano, "Steam, dry and autothermal methane reforming for hydrogen production: A thermodynamic equilibrium analysis," en, *Journal of Power Sources*, vol. 469, p. 228 391, Sep. 2020, ISSN: 03787753. DOI: 10.1016/j.jpowsour.2020.228391 [Online]. Available: https://linkinghub.elsevier.com/retrieve/pii/S0378775320306959 (visited on 12/17/2022).

[44] M. Ambrosetti, A. Beretta, G. Groppi, and E. Tronconi, "A Numerical Investigation of Electrically-Heated Methane Steam Reforming Over Structured Catalysts," en, *Frontiers in Chemical Engineering*, vol. 3, p. 747 636, Oct. 2021, ISSN: 2673-2718. DOI: 10.3389/fceng.2021.747636 [Online]. Available: https://www.frontiersin.org/articles/10.3389/fceng.2021.747636/full (visited on 12/16/2022).

[45] S. Renda, M. Cortese, G. Iervolino, M. Martino, E. Meloni, and V. Palma, "Electrically driven SiC-based structured catalysts for intensified reforming processes," en, *Catalysis Today*, vol. 383, pp. 31–43, Jan. 2022, ISSN: 09205861. DOI: 10.1016/j.cattod.2020.11.020 [Online]. Available: https://linkinghub.elsevier.com/retrieve/pii/S0920586120307860 (visited on 12/16/2022).

[46] IEAGHG, *'Low-Carbon hydrogen from Natural Gas: Global Roadmap*, Jul. 2022.

[47] Svend Ravn, *Topsoe to Build Demonstration Plant to Produce Cost-Competitive CO2-Neutral Methanol from Biogas and Green Electricity*, 2019. [Online]. Available: https://archive.is/VIMGM.

[48] A. T. Mayyas, M. F. Ruth, B. S. Pivovar, G. Bender, and K. B. Wipke, "Manufacturing Cost Analysis for Proton Exchange Membrane Water Electrolyzers," en, Tech. Rep. NREL/TP-6A20-72740, 1557965, Aug. 2019, NREL/TP–6A20–72 740, 1 557 965 DOI: 10.2172/1557965 [Online]. Available: http://www.osti.gov/servlets/purl/1557965/ (visited on 12/16/2022).

[49] IEA, "Energy Technology Perspectives 2023," en, *Energy Technology Perspectives*, 2023. [Online]. Available: https://www.iea.org/reports/energy-technology-perspectives-2023

[50] *Global installed electrolysis capacity by technology, 2015-2020 – Charts – Data & Statistics*, en-GB. [Online]. Available: https://www.iea.org/data-and-statistics/charts/global- installed- electrolysis- capacity- by- technology- 2015-2020 (visited on 04/18/2023).

[51] L. Klaas, D. Guban, M. Roeb, and C. Sattler, "Recent progress towards solar energy integration into low-pressure green ammonia production technologies," en, *International Journal of Hydrogen Energy*, vol. 46, no. 49, pp. 25 121–25 136, Jul. 2021, ISSN: 03603199. DOI: 10.1016/j.ijhydene.2021.05.063. [Online]. Available: https://linkinghub.elsevier.com/retrieve/pii/S0360319921017833 (visited on 12/10/2022).

[52] Garagounis, Vourros, Stoukides, Dasopoulos, and Stoukides, "Electrochemical Synthesis of Ammonia: Recent Efforts and Future Outlook," en, *Membranes*, vol. 9, no. 9, p. 112, Aug. 2019, ISSN: 2077-0375. DOI: 10.3390/membranes9090112 [Online]. Available: https://www.mdpi.com/2077-0375/9/9/112 (visited on 12/10/2022).

[53] S. Giddey, S. Badwal, and A. Kulkarni, "Review of electrochemical ammonia production technologies and materials," en, *International Journal of Hydrogen Energy*, vol. 38, no. 34, pp. 14 576–14 594, Nov. 2013, ISSN: 03603199. DOI: 10.1016/j.ijhydene.2013.09.054. [Online]. Available: https://linkinghub.elsevier.com/retrieve/pii/S0360319913022775 (visited on 12/09/2022).

[54] F. Jiao and B. Xu, "Electrochemical Ammonia Synthesis and Ammonia Fuel Cells," en, *Advanced Materials*, vol. 31, no. 31, p. 1 805 173, Aug. 2019, ISSN: 0935-9648, 1521-4095. DOI: 10.1002/adma.201805173 [Online]. Available: https://onlinelibrary.wiley.com/doi/10.1002/adma.201805173 (visited on 12/10/2022).

[55] E. R. Morgan, "Techno-Economic Feasibility Study of Ammonia Plants Powered by Offshore Wind," en, Publisher: University of Massachusetts Amherst. DOI: 10.7275/11KT-3F59. [Online]. Available: https://scholarworks.umass.edu/cgi/viewcontent.cgi?article=1704&context=open_access_dissertations (visited on 01/31/2023).

[56] O. Osman, S. Sgouridis, and A. Sleptchenko, "Scaling the production of renewable ammonia: A techno-economic optimization applied in regions with high insolation," en, *Journal of Cleaner Production*, vol. 271, p. 121 627, Oct. 2020, ISSN: 09596526. DOI: 10.1016/j.jclepro.2020.121627. [Online]. Available: https://linkinghub.elsevier.com/retrieve/pii/S0959652620316747 (visited on 01/30/2023).

[57] S. A. Nosherwani and R. C. Neto, "Techno-economic assessment of commercial ammonia synthesis methods in coastal areas of Germany," en, *Journal of Energy Storage*, vol. 34, p. 102 201, Feb. 2021, ISSN: 2352152X. DOI: 10.1016/j.est.2020.102201. [Online]. Available: https://linkinghub.elsevier.com/retrieve/pii/S2352152X20320247 (visited on 01/30/2023).

[58] M. Fasihi, R. Weiss, J. Savolainen, and C. Breyer, "Global potential of green ammonia based on hybrid PV-wind power plants," en, *Applied Energy*, vol. 294, p. 116 170, Jul. 2021, ISSN: 03062619. DOI: 10.1016/j.apenergy.2020.116170. [Online]. Available: https://linkinghub.elsevier.com/retrieve/pii/S0306261920315750 (visited on 04/18/2023).

[59] A. Kakavand, S. Sayadi, G. Tsatsaronis, and A. Behbahaninia, "Techno-economic assessment of green hydrogen and ammonia production from wind and solar energy in Iran," en, *International Journal of Hydrogen Energy*, vol. 48, no. 38, pp. 14 170–14 191, May 2023, ISSN: 03603199. DOI: 10.1016/j.ijhydene.2022.12.285. [Online]. Available: https://linkinghub.elsevier.com/retrieve/pii/S0360319922061481 (visited on 04/18/2023).

[60] M. Palys, A. McCormick, E. Cussler, and P. Daoutidis, "Modeling and Optimal Design of Absorbent Enhanced Ammonia Synthesis," en, *Processes*, vol. 6, no. 7, p. 91, Jul. 2018, ISSN: 2227-9717. DOI: 10.3390/pr6070091. [Online]. Available: http://www.mdpi.com/2227-9717/6/7/91 (visited on 01/31/2023).

[61] K. H. R. Rouwenhorst and L. Lefferts, "Feasibility Study of Plasma-Catalytic Ammonia Synthesis for Energy Storage Applications," en, *Catalysts*, vol. 10, no. 9, p. 999, Sep. 2020, ISSN: 2073-4344. DOI: 10.3390/catal10090999. [Online]. Available: https://www.mdpi.com/2073-4344/10/9/999 (visited on 01/31/2023).

[62] K. H. R. Rouwenhorst, Y. Engelmann, K. van 't Veer, R. S. Postma, A. Bogaerts, and L. Lefferts, "Plasma-driven catalysis: Green ammonia synthesis with intermittent electricity," en, *Green Chemistry*, vol. 22, no. 19, pp. 6258–6287, 2020, ISSN: 1463-9262, 1463-9270. DOI: 10.1039/D0GC02058C. [Online]. Available: http://xlink.rsc.org/?DOI=D0GC02058C (visited on 04/18/2023).

[63] B. King, D. Patel, J. Zhu Chen, *et al.*, "Comprehensive process and environmental impact analysis of integrated DBD plasma steam methane reforming," en, *Fuel*, vol. 304, p. 121 328, Nov. 2021, ISSN: 00162361. DOI: 10.1016/j.fuel.2021.121328. [Online]. Available: https://linkinghub.elsevier.com/retrieve/pii/S0016236121012072 (visited on 02/01/2023).

[64] Weeda M. and Segers R. C., *The-dutch-hydrogen-balance-and-current-and-future-representation-of-hydrogen-in-energy-statistics.pdf*, 2020.

[65] J. S. Larsen and D. Lippmann, "The Uhde Dual Pressure Process – Reliability Issues and Scale Up Considerations," en, 2002.

[66] KNMI, *Dutch climate data*. [Online]. Available: https://daggegevens.knmi.nl/klimatologie/uurgegevens

[67] Hersbach, H., Bell, B., Berrisford, P., Biavati, G., Horányi, A., Muñoz Sabater, J., Nicolas, J., Peubey, C., Radu, R., Rozum, I., Schepers, D., Simmons, A., Soci, C., Dee, D., Thépaut, J-N., *ERA5 hourly data on single levels from 1940 to present*, Copernicus Climate Change Service (C3S) Climate Data Store (CDS), 2023. [Online]. Available: https://doi.org/10.24381/cds.adbb2d47

[68] ENTSO-E, *Day-ahead Prices*. [Online]. Available: https://transparency.entsoe.eu/dashboard/show

[69] L. van Cappellen, L. Wielders, and T. Scholten, "Emissiefactor elektriciteit uit fossiele bronnen," nl, 2021.

[70] EUROSTAT, *Gas prices for non-household consumers - bi-annual data (from 2007 onwards) [NRG_pc_203__custom_4835168]*. [Online]. Available: https://ec.europa.eu/eurostat/databrowser/view/NRG_PC_203__custom_5656415/default/table?lang=en (visited on 04/02/2023).

[71] P. Gabrielli, M. Gazzani, E. Martelli, and M. Mazzotti, "Optimal design of multi-energy systems with seasonal storage," en, *Applied Energy*, vol. 219, pp. 408–424, Jun. 2018, ISSN: 03062619. DOI: 10.1016/j.apenergy.2017.07.142. [Online]. Available: https://linkinghub.elsevier.com/retrieve/pii/S0306261917310139 (visited on 11/11/2022).

[72] M. Geidl and G. Andersson, "Optimal Power Flow of Multiple Energy Carriers," en, *IEEE Transactions on Power Systems*, vol. 22, no. 1, pp. 145–155, Feb. 2007, ISSN: 0885-8950, 1558-0679. DOI: 10.1109/TPWRS.2006.888988. [Online]. Available: https://ieeexplore.ieee.org/document/4077107/ (visited on 12/05/2022).

[73] L. Weimann and M. Gazzani, "A novel time discretization method for solving complex multi-energy system design and operation problems with high penetration of renewable energy," en, *Computers & Chemical Engineering*, vol. 163, p. 107 816, Jul. 2022, ISSN: 00981354. DOI: 10.1016/j.compchemeng.2022.107816. [Online]. Available: https://linkinghub.elsevier.com/retrieve/pii/S0098135422001545 (visited on 05/02/2023).

[74] L. Weimann, P. Gabrielli, A. Boldrini, G. J. Kramer, and M. Gazzani, "Optimal hydrogen production in a wind-dominated zero-emission energy system," en, *Advances in Applied Energy*, vol. 3, p. 100 032, Aug. 2021, ISSN: 26667924. DOI: 10.1016/j.adapen.2021.100032. [Online]. Available: https://linkinghub.elsevier.com/retrieve/pii/S2666792421000251 (visited on 12/02/2022).

[75] M. Appl, "Ammonia, 1. Introduction," en, in *Ullmann's Encyclopedia of Industrial Chemistry*, 1st ed., Wiley, Oct. 2011, ISBN: 978-3-527-30385-4 978-3-527-30673-2. DOI: 10.1002/14356007.a02_143.pub3. [Online]. Available: https://onlinelibrary.wiley.com/doi/10.1002/14356007.a02_143.pub3 (visited on 01/31/2023).

[76] ARENHA consortium, *ADVANCED MATERIALS AND REACTORS FOR ENERGY STORAGE THROUGH AMMONIA (ARENHA)*, 2020. [Online]. Available: https://arenha.eu/sites/arenha.drupal.pulsartecnalia.com/files/documents/ARENHA-WP7-D721-DLR-CNH2-22112021-final.pdf

[77] J. Ikäheimo, J. Kiviluoma, R. Weiss, and H. Holttinen, "Power-to-ammonia in future North European 100 % renewable power and heat system," en, *International Journal of Hydrogen Energy*, vol. 43, no. 36, pp. 17 295–17 308, Sep. 2018, ISSN: 03603199. DOI: 10.1016/j.ijhydene.2018.06.121. [Online]. Available: https://linkinghub.elsevier.com/retrieve/pii/S0360319918319931 (visited on 01/30/2023).

[78] Collodi, G., Azzaro, G., Ferrari, N., *et al.*, *IEAGHG 2017-02-unlocked.pdf*, 2017.

[79] Ida Synnøve Bukkholm, *Electric steam methane reforming*, Jun. 2021.

[80] Siemens, *Silyzer 300 Datasheet*. [Online]. Available: https://assets.siemens-energy.com/siemens/assets/api/uuid:a193b68f-7ab4-4536-abe2-c23e01d0b526/datasheet-silyzer300.pdf.

[81] DEA, *Technolofy Data Energy Storage*, 2018. [Online]. Available: https://ens.dk/en/our-services/projections-and-models/technology-data/technology-data-energy-storage

[82] W. Cole, A. W. Frazier, and C. Augustine, "Cost Projections for Utility-Scale Battery Storage: 2021 Update," en, *Renewable Energy*, 2021.

[83] IEA, *Projected Costs of Generating Electricity 2020 Edition*, 2020. [Online]. Available: https://iea.blob.core.windows.net/assets/ae17da3d-e8a5-4163-a3ec-2e6fb0b5677d/Projected-Costs-of-Generating-Electricity-2020.pdf

[84] F. H. Saadi, N. S. Lewis, and E. W. McFarland, "Relative costs of transporting electrical and chemical energy," en, *Energy & Environmental Science*, vol. 11, no. 3, pp. 469–475, 2018, ISSN: 1754-5692, 1754-5706. DOI: 10.1039/C7EE01987D. [Online]. Available: http://xlink.rsc.org/?DOI=C7EE01987D (visited on 04/23/2023).

[85] Y. Yan, H. Zhang, Q. Liao, Y. Liang, and J. Yan, "Roadmap to hybrid offshore system with hydrogen and power co-generation," en, *Energy Conversion and Management*, vol. 247, p. 114 690, Nov. 2021, ISSN: 01968904. DOI: 10.1016/j.enconman.2021.114690. [Online]. Available: https://linkinghub.elsevier.com/retrieve/pii/S0196890421008669 (visited on 04/23/2023).

[86] Çengel, Y. A., Boles, M. A., and Kanoğlu, M., *Energy Analysis for a systems. Thermodynamics: An Engineering approach*, 2019.

[87] A. Ramírez, S. Hagedoorn, L. Kramers, T. Wildenborg, and C. Hendriks, "Screening CO2 storage options in The Netherlands," en, *International Journal of Greenhouse Gas Control*, vol. 4, no. 2, pp. 367–380, Mar. 2010, ISSN: 17505836. DOI: 10.1016/j.ijggc.2009.10.015. [Online]. Available: https://linkinghub.elsevier.com/retrieve/pii/S1750583609001364 (visited on 02/07/2023).

[88] T. Wildenborg, D. Loeve, and F. Neele, "Large-scale CO2 transport and storage infrastructure development and cost estimation in the Netherlands offshore," en, *International Journal of Greenhouse Gas Control*, vol. 118, p. 103 649, Jul. 2022, ISSN: 17505836. DOI: 10.1016/j.ijggc.2022.103649. [Online]. Available: https://linkinghub.elsevier.com/retrieve/pii/S1750583622000688 (visited on 02/07/2023).

[89] S. Akerboom, S. Waldmann, A. Mukherjee, C. Agaton, M. Sanders, and G. J. Kramer, "Different This Time? The Prospects of CCS in the Netherlands in the 2020s," en, *Frontiers in Energy Research*, vol. 9, p. 644 796, May 2021, ISSN: 2296-598X. DOI: 10.3389/fenrg.2021.644796. [Online]. Available: https://www.frontiersin.org/articles/10.3389/fenrg.2021.644796/full (visited on 02/07/2023).

[90] TNO, *Blue hydrogen as accelerator and pioneer for energy transition in the industry*, 2019. [Online]. Available: http://resolver.tudelft.nl/uuid:65c255a9-1006-4992-8dbf-21c411e64663

[91] DEA, *Technology Data - Energy transport*, 2017. [Online]. Available: https://ens.dk/en/our-services/projections-and-models/technology-data/technology-catalogue-transport-energy.

[92] EBN and GASUNIE, *Transport en Opslag van CO2 in Nederland*, 2018. [Online]. Available: https://www.ebn.nl/wp-content/uploads/2022/10/Studie-Transport-en-opslag-van-CO2-in-Nederland-EBN-en-Gasunie-1.pdf.

[93] J. Twidell and T. Weir, *Renewable energy resources*, en, Third edition. London ; New York: Routledge, Taylor & Francis Group, 2015, ISBN: 978-0-415-58437-1 978-0-415-58438-8.

[94] M. Knoope, A. Ramírez, and A. Faaij, "A state-of-the-art review of techno-economic models predicting the costs of CO2 pipeline transport," en, *International Journal of Greenhouse Gas Control*, vol. 16, pp. 241–270, Aug. 2013, ISSN: 17505836. DOI: 10.1016/j.ijggc.2013.01.005. [Online]. Available: https://linkinghub.elsevier.com/retrieve/pii/S175058361300011X (visited on 02/10/2023).

[95] Lawrence Irlam, *GLOBAL COSTS OF CARBON CAPTURE AND STORAGE*, 2017.

[96] R. J. Lee Pereira, P. A. Argyris, and V. Spallina, "A comparative study on clean ammonia production using chemical looping based technology," en, *Applied Energy*, vol. 280, p. 115 874, Dec. 2020, ISSN: 0306-2619. DOI: 10.1016/j.apenergy.2020.115874. [Online]. Available: https://www.sciencedirect.com/science/article/pii/S0306261920313453 (visited on 04/08/2023).

[97] Buljan A., *Borssele Beta Cable Work to Cost TenneT EUR 50 Million More*, Jun. 2020. [Online]. Available: https://archive.is/wvmsD.

[98] A. H. Reksten, M. S. Thomassen, S. Møller-Holst, and K. Sundseth, "Projecting the future cost of PEM and alkaline water electrolysers; a CAPEX model including electrolyser plant size and technology development," en, *International Journal of Hydrogen Energy*, vol. 47, no. 90, pp. 38 106–38 113, Nov. 2022, ISSN: 03603199. DOI: 10.1016/j.ijhydene.2022.08.306. [Online]. Available: https://linkinghub.elsevier.com/retrieve/pii/S0360319922040253 (visited on 05/08/2023).

[99] Junginger, M. and Louwen, A., *Technological learning in the transition to a low-carbon energy system: Conceptual issues, empirical findings, and use, in energy modeling*. en. Academic Press, 2019, ISBN: 978-0-12-818762-3. DOI: 10.1016/C2018-0-04547-8. [Online]. Available: https://linkinghub.elsevier.com/retrieve/pii/C2018004547-8 (visited on 04/24/2023).

[100] Y. I. Asa, "Key Market prices 3Q 2022," en, [Online]. Available: https://www.yara.com/siteassets/investors/057-reports-and-presentations/other/2022/key-market-prices-3q-2022.pdf/.

[101] M. C. Romano, C. Antonini, A. Bardow, *et al.*, "Comment on "How green is blue hydrogen?"" en, *Energy Science & Engineering*, vol. 10, no. 7, pp. 1944–1954, Jul. 2022, ISSN: 2050-0505, 2050-0505. DOI: 10.1002/ese3.1126. [Online]. Available: https://onlinelibrary.wiley.com/doi/10.1002/ese3.1126 (visited on 05/11/2023).

[102] Hodgson C. and Sheppard D., *EU carbon price tops €100 a tonne for first time*. [Online]. Available: https://archive.is/jdkj5 .

[103] Susanna Twidale, *Analyst EU carbon price forecasts edge higher but risks remain*, Jan. 2023. [Online]. Available: https://archive.is/Sj4C3 .

[104] Unknown, *Three Million Euro Grant for Dutch Industrial Scale Floating Green Hydrogen and Ammonia Project*, Apr. 2023. [Online]. Available: https://archive.is/w1G0Q.

[105] H. Wang, P. Daoutidis, and Q. Zhang, "Harnessing the Wind Power of the Ocean with Green Offshore Ammonia," en, *ACS Sustainable Chemistry & Engineering*, vol. 9, no. 43, pp. 14 605–14 617, Nov. 2021, ISSN: 2168-0485, 2168-0485. DOI: 10.1021/acssuschemeng.1c06030 [Online]. Available: https://pubs.acs.org/doi/10.1021/acssuschemeng.1c06030 (visited on 12/05/2022).

[106] TECHNISCHE UNIVERSITAET MUENCHEN, *Electrified Reactor Technology - EReTech Project*, Aug. 2022. [Online]. Available: https://cordis.europa.eu/project/id/101058608 (visited on 05/11/2023).

[107] S. Pfenninger, J. DeCarolis, L. Hirth, S. Quoilin, and I. Staffell, "The importance of open data and software: Is energy research lagging behind?" en, *Energy Policy*, vol. 101, pp. 211–215, Feb. 2017, ISSN: 03014215. DOI: 10.1016/j.enpol.2016.11.046 [Online]. Available: https://linkinghub.elsevier.com/retrieve/pii/S0301421516306516 (visited on 05/11/2023).

[108] Charles Maxwell, *CEPCI Values*, 2023. [Online]. Available: https://toweringskills.com/financial-analysis/cost-indices/ .

Appendix

Table 31: CEPCI values list [108].

Year	CEPCI	Year	CEPCI
2021	708.0	2011	585.7
2020	596.2	2010	550.8
2019	607.5	2009	521.9
2018	603.1	2008	575.4
2017	567.5	2007	525.4
2016	541.7	2006	499.6
2015	556.8	2005	468.2
2014	576.1	2004	444.2
2013	567.3	2003	402.0
2012	584.6	2002	395.6

Table 32: Distances between the nodes used in this work. All values are in km.

Distance Matrix	sluiskil	chemelot	antwerp	bowf	solar
sluiskil	–	154.0	33.0	73.6	63.8
chemelot	154.0	–	126.5	–	155.1
antwerp	33.0	126.5	–	–	48.4
bowf	73.6	–	–	–	–
solar	63.8	155.1	48.4	–	–

Table 33: NG specifications used for the KBR and KBRCCS.

N_2	0.89	%
CO_2	2	%
C_1	89	%
C_2	7	%
C_3	1	%
C_4	0.05	%
C_5	0.05	%
C_6	0.005	%
Other	0.005	%
LHV	46.5	MJ/kg_{NG}
Sp. Emissions	2.69969	kg_{CO2}/kg_{NG}